UNIVERSIDADE ESTADUAL PAULISTA
"JÚLIO DE MESQUITA FILHO"
Campus de Botucatu

FCA
FACULDADE DE CIÊNCIAS AGRONÔMICAS
UNESP | BOTUCATU

MATHEUS MEREB NEGRISOLI

MONITORAMENTO E DETECÇÃO DA FERRUGEM ASIÁTICA DA SOJA POR ESPECTRORADIOMETRIA E CRIAÇÃO DE MODELO DE PREDIÇÃO PARA TOMADA DE DECISÃO DO CONTROLE

Botucatu

2022

MATHEUS MEREB NEGRISOLI

MONITORAMENTO E DETECÇÃO DA FERRUGEM ASIÁTICA DA SOJA POR ESPECTRORADIOMETRIA E CRIAÇÃO DE MODELO DE PREDIÇÃO PARA TOMADA DE DECISÃO DO CONTROLE

Tese apresentada à Faculdade de Ciências Agronômicas da Unesp Campus de Botucatu, para obtenção do título de Doutor em Agronomia (Proteção de Plantas)

Orientador: Prof. Dr. Carlos Gilberto Raetano

Botucatu

2022

N392m

Negrisoli, Matheus Mereb
Monitoramento e detecção da ferrugem asiática da soja por espectroradiometria e criação de modelo de predição para tomada de decisão do controle / Matheus Mereb Negrisoli. -- Botucatu, 2022
132 p. : il., tabs., fotos

Tese (doutorado) - Universidade Estadual Paulista (Unesp), Faculdade de Ciências Agronômicas, Botucatu
Orientador: Carlos Gilberto Raetano

1. Tecnologia de aplicação. 2. Sensoriamento remoto. 3. Ferrugem da soja (Doença). 4. Fungicidas. I. Título.

Sistema de geração automática de fichas catalográficas da Unesp. Biblioteca da Faculdade de Ciências Agronômicas, Botucatu. Dados fornecidos pelo autor(a).

Essa ficha não pode ser modificada.

UNIVERSIDADE ESTADUAL PAULISTA

Câmpus de Botucatu

CERTIFICADO DE APROVAÇÃO

TÍTULO DA TESE: MONITORAMENTO E DETECÇÃO DA FERRUGEM ASIÁTICA DA SOJA POR ESPECTRORADIOMETRIA E CRIAÇÃO DE MODELO DE PREDIÇÃO PARA TOMADA DE DECISÃO DO CONTROLE

AUTOR: MATHEUS MEREB NEGRISOLI
ORIENTADOR: CARLOS GILBERTO RAETANO

Aprovado como parte das exigências para obtenção do Título de Doutor em AGRONOMIA (PROTEÇÃO DE PLANTAS), pela Comissão Examinadora:

Prof. Dr. CARLOS GILBERTO RAETANO (Participaçao Presencial)
Protecao Vegetal / Faculdade de Ciencias Agronomicas de Botucatu UNESP

Prof. Dr. MARCELO DA COSTA FERREIRA (Participaçao Virtual)
Departamento de Ciências da Produção Agrícola (Fitossanidade) / FCAV / UNESP - Jaboticabal

Prof. Dr. MARCOS RAFAEL NANNI (Participaçao Virtual)
Agronomia / Universidade Estadual de Maringá

PROFESSORA TITULAR LILIAN AMORIM (Participaçao Virtual)
Departamento de Fitopatologia / ESCOLA SUPERIOR DE AGRICULTURA LUIZ DE QUEIROZ - USP

Prof. Dr. PAULO CEZAR CERESINI (Participaçao Virtual)
Departamento de Fitossanidade, Engenharia Rural e Solos / Faculdade de Engenharia de Ilha Solteira - UNESP

Botucatu, 20 de maio de 2022

À minha família e a Deus,

dedico.

AGRADECIMENTOS

A Deus por todas as oportunidades, bênçãos, conquistas, coragem, força e saúde;

Aos meus pais, Edson e Vanuza, por todo o amor, apoio, compreensão, paciência e suporte, sem eles eu não chegaria onde estou atualmente;

Aos meus irmãos, Raphael e Patrícia, também pelo apoio incondicional e companheirismo que fizeram toda a diferença na minha vida;

À minha esposa Ariani Garcia, por todo o suporte, amor, compreensão e carinho;

À Universidade Estadual Paulista Júlio de Mesquita Filho, Faculdade de Ciências Agronômicas – Campus de Botucatu que abriram as portas para a realização desse projeto e que tanto contribuiu para minha formação;

Ao meu orientador e professor Dr. Carlos Gilberto Raetano, por toda orientação, conselhos, apoio, paciência, suporte e amizade oferecidos nos anos de trabalho juntos;

Aos Docentes do Programa de Pós-Graduação em Agronomia – Proteção de Plantas, funcionários da Fazenda de Ensino, Pesquisa e Extensão (FEPE) e Seção de Pós-Graduação por toda a orientação, ensino, oportunidade e convivência;

À Fundação de Amparo à Pesquisa do Estado de São Paulo (FAPESP), pela concessão da bolsa de estudos de Doutorado (processo nº 2018/26486-0) e Auxílio Regular a Pesquisa (processo nº 2018/24869-0) essenciais para a condução deste trabalho;

Ao Conselho Nacional de Desenvolvimento Científico e Tecnológico (CNPq) pela concessão parcial da bolsa de estudos de Doutorado (142443/2018-2);

Ao Núcleo de Pesquisas Avançadas em Matologia (NUPAM), em especial aos professores Dr. Edivaldo D. Velini e Caio A. Carbonari, pelo suporte com equipamentos, conhecimentos e experiências que foram importantes para a execução dos trabalhos;

Ao professor Dr. Sergio Rodrigues pelo suporte nas análises estatísticas dos dados aqui apresentados;

Aos companheiros de trabalho e amigos do PROTEC, que batalharam da mesma forma para que esse projeto fosse realizado, além de todo apoio, amizade e suporte;

Aos amigos de Botucatu e de República pela amizade e apoio durante esses anos;

Aos companheiros de trabalho da Pentair pelo apoio, suporte e paciência nos momentos decisivos de finalização dessa tese de doutorado;

O presente trabalho foi realizado com apoio da Coordenação de Aperfeiçoamento de Pessoal de Nível Superior - Brasil (CAPES) - Código de Financiamento 001.

RESUMO

O monitoramento da ferrugem asiática da soja (FAS) por sensoriamento remoto pode otimizar a detecção da doença no campo e ser utilizado como base para tomada de decisão do controle, podendo influenciar na qualidade da aplicação e na eficácia do controle. Assim, o objetivo geral desse trabalho foi obter correlação entre o progresso da FAS na cultura da soja com os valores de refletância da cultura sob condições de níveis de severidade da doença e cultivares de soja, de modo a propor um modelo de predição da doença e utilizá-lo como método no monitoramento para tomada de decisão do uso do controle químico. O projeto de pesquisa foi conduzido entre 2018 e 2021 na Faculdade de Ciências Agronômicas (FCA/UNESP), Botucatu, SP, divididos em três capítulos. Inicialmente foi avaliado à campo e em laboratório o efeito da FAS sobre cultivares de soja suscetível e parcialmente resistentes, em termos de severidade da doença, produtividade da cultura, fluorescência da clorofila, trocas gasosas, e a aplicabilidade do sensoriamento remoto para determinação desses efeitos. A seguir foi avaliada a detecção da ferrugem da soja por sensoriamento remoto e criação do modelo de predição e classificação da doença com base na refletância dos folíolos em diferentes níveis de severidade da FAS. Foram avaliadas diferentes técnicas estatísticas para redução da dimensionalidade dos dados e algoritmos de classificação. Posteriormente foi realizada a aplicação do modelo de predição da doença à campo, avaliando a aplicabilidade do modelo de previsão e comparando-o com métodos convencionais de monitoramento como fonte para tomada de decisão de controle (aplicações calendarizadas em um período pré-definido e no início do aparecimento dos sintomas). O efeito dos diferentes momentos de aplicação foram avaliados quanto à deposição de calda, cobertura da pulverização, eficácia de controle da doença e produtividade da cultura. Diferenças significativas no efeito da doença sobre os dois cultivares de soja foram constatadas, com redução dos efeitos negativos do patógeno sobre o cultivar de soja com resistência parcial. Foi possível distinguir plantas sadias e com FAS com base na refletância da cultura em diferentes níveis de severidade com até 93% de acurácia e precisão, e esses dados puderam ser utilizados na criação de um modelo de classificação e predição da doença. Os diferentes momentos de aplicação influenciaram na eficácia de controle e tecnologia de aplicação, no qual os tratamentos com aplicação em momentos de maior índice de área foliar obtiveram

distribuição de calda menos uniforme. A utilização do modelo de predição proposto e as técnicas de sensoriamento remoto são eficazes e promissores para ser integrados a programas de manejo da doença.

Palavras-chave: sensoriamento remoto; tecnologia de aplicação; *Phakopsora pachyrhizi*; fungicidas; manejo integrado de doenças.

ABSTRACT

Monitoring of soybean rust (SBR) by remote sensing can improve disease detection in the field and be used as a decision support system for control, which can influence the quality of application and the effectiveness of control. Thus, the objective of this study was to obtain a correlation between SBR progress and the reflectance values of the crop under different conditions of disease severity levels and soybean cultivars, in order to propose a disease prediction model and use it as a monitoring method to aid in the decision making of chemical control. The research project was conducted between 2018 and 2021 at the School of Agriculture (FCA/UNESP), Botucatu, SP, divided into three phases. Initially, the effects of SBR on susceptible and partially resistant soybean cultivars was evaluated in the field and in the laboratory, in terms of disease severity, crop yield, chlorophyll fluorescence, gas exchange, and the applicability of remote sensing for determination of these effects. After then, we evaluated the detection of soybean rust by remote sensing and the construction of a prediction and classification model based on leaflet reflectance at different levels of SBR severity. Different statistical techniques to reduce data dimensionality and classification algorithms were also evaluated. At the end, the application of the disease prediction model in the field was carried out evaluating the effect of different application timings on the application technology and control effectiveness. The applicability of the prediction model was evaluated, comparing it with conventional monitoring methods as the source for decision making of control (calendarized applications at a pre-defined period and at the first appearance of the symptoms). The effect of different application timings was evaluated in terms of spray deposit, spray coverage, disease control effectiveness and crop yield. Significant differences were observed regarding the effect of the disease on the two soybean cultivars, with a reduction in the negative effects of the pathogen on the soybean cultivar with partial resistance. It was possible to distinguish between healthy and SBR-infected plants based on leaf reflectance at different severity levels with up to 93% accuracy and precision, and these data were successfully used to create a disease classification and prediction model. The different application timings influenced the control effectiveness and application technology, in which treatments with application at times of higher leaf area index obtained less uniform spray distribution. The use of the proposed prediction model and remote sensing

techniques are effective and promising to be integrated into disease management programs.

Keywords: remote sensing; application technology; *Phakopsora pachyrhizi;* fungicides; integrated disease management.

SUMÁRIO

INTRODUÇÃO GERAL

A soja [*Glycine max* (L.) Merrill] é a cultura mais importante cultivada no Brasil, atualmente o maior produtor e exportador do grão (TOLOI et al. 2021). No entanto, apesar de avanços nos sistemas de produção, pragas e doenças continuam a impactar os níveis de produção nacional. O principal exemplo é a ferrugem da soja (FAS) causada por *Phakopsora pachyrhizi* Sydow & Syd. e responsável por perdas de até US$ 15 bilhões de 2000 a 2015 (IEAg/ABAG, 2015). É considerada a principal doença da cultura, com potencial de perdas de até 80% e possui controle baseado na utilização de fungicidas, dos quais existem poucas opções devido à crescente população do fungo resistente (DEISING; REIMANN; PASCHOLATI, 2008; KELLY et al.; 2015; GODOY; BUENO; GAZZIERO, 2015; GODOY et al., 2020). Portanto, torna-se evidente a necessidade de inovações em técnicas a serem integradas no manejo da doença de modo a obter maior eficiência e redução das perdas no controle desses agentes.

Neste contexto, o monitoramento é a base para a integração das diferentes táticas no manejo integrado de doenças (MID), auxiliando na tomada de decisão do controle e promovendo, assim, maior sustentabilidade da produção da cultura da soja (WYLIE; SPEIGHT, 2012). Porém, é considerado um dos procedimentos que mais demandam tempo e que dificilmente é realizado por produtores, os quais preferem a utilização direta do produto fitossanitário de forma calendarizada como garantia da produtividade. Assim, além da perda de insumos, há um estímulo para seleção de fungos resistentes aos fungicidas, maior contaminação ambiental e redução da eficácia de controle (GODOY; BUENO; GAZZIERO, 2015).

Por outro lado, a utilização do sensoriamento remoto no monitoramento de doenças pode reduzir o custo e tempo gasto para a amostragem na área, otimizando tanto a capacidade operacional como financeira, além de fornecer dados e informações que não são visíveis ou aparentes. O sensoriamento remoto é um método indireto e não destrutivo utilizado para obtenção de informações de um objeto sem que exista um contato físico entre o sensor e o objeto à diferentes distâncias (SHIRATSUCHI et al., 2014; AHMED et al., 2016). No campo do sensoriamento remoto, a espectroscopia tem sido uma das técnicas mais utilizadas na detecção de doenças de plantas e monitoramento de campos de produção (KHALED et al., 2018).

Partindo-se do pressuposto que plantas doentes terão diferentes interações com a radiação eletromagnética comparativamente às plantas sadias, é necessário encontrar o espectro da radiação que explicite melhor essa diferença. A condição fitossanitária da cultura é avaliada principalmente com base na identificação do estresse da planta, sendo de grande importância a região do visível ao infravermelho próximo e médio, de 400 a 3000 nm (CUI et al., 2009; MAHLEIN et al., 2013; BAJWA; RUPE; MASON, 2017; KHALED et al., 2018). A identificação parte da "assinatura espectral" dos elementos na área (SHIRATSUCHI et al., 2014; KHALED et al., 2018), sabendo-se que cada patógeno pode afetar a estrutura da planta morfo-fisiologicamente, seja por alteração na pigmentação, concentração química de solutos, estrutura celular, balanço de nutrientes, absorção de água e também as trocas gasosas (HATFIELD; PINTER, 1993).

Diversos estudos já relataram a aplicação do sensoriamento remoto na identificação de estresse e plantas doentes na cultura da soja (CUI et al., 2009; HIKISHIMA et al., 2010; BAJWA; RUPE; MASON, 2017; FURNALETTO et al., 2021). Com o conhecimento dos efeitos da doença na planta, é possível construir uma correlação com os valores espectrais obtidos no monitoramento e posterior construção do modelo de predição da doença. Quanto mais rápido for o monitoramento e detecção, maior a chance de sucesso do MID, tornando o monitoramento por sensoriamento remoto um dos segmentos mais promissores.

No caso da cultura da soja, o monitoramento eficaz da doença é de grande importância, principalmente quanto à otimização da tecnologia de aplicação. Além de evitar o desperdício de fungicidas na pulverização calendarizada, a aplicação em diferentes estádios vegetativos pode influenciar grandemente na penetração e distribuição uniforme da calda de pulverização no dossel da cultura (NEGRISOLI at al., 2019). Existem poucas opções para melhoria da penetração da calda na cultura da soja, representadas por baixa uniformidade de distribuição e controle deficiente (CUNHA et al., 2014). Além da escassez de estudos com sensoriamento remoto e FAS, também há poucos estudos sobre a aplicabilidade de diferentes cultivares de soja com níveis de resistência ao patógeno no manejo da FAS, assim como o efeito dos diferentes tipos de sintomas sobre o monitoramento por sensoriamento remoto.

Portanto, a relevância da cultura e a necessidade de inovações tecnológicas que possibilitem o manejo eficiente dessa doença constituem os motivos que justificaram a realização desse estudo. Para isso, foram conduzidos três trabalhos

divididos em três capítulos, buscando os seguintes objetivos: i) Capítulo 1: avaliar o efeito da doença sobre os cultivares de soja com diferentes níveis de resistência ao patógeno, caracterizando-os e explorando a viabilidade de integração no MID; ii) Capítulo 2: realizar a identificação e classificação da FAS por meio do sensoriamento remoto e criação do modelo de predição da doença; iii) Capítulo 3: realizar a aplicação do modelo de predição proposto para avaliação do efeito de diferentes momentos de aplicação sobre a tecnologia de aplicação, controle da doença e produtividade da cultura.

CHAPTER 1

Impact of soybean rust on susceptible and partially resistant cultivars to *Phakopsora pachyrhizi*[1]

Impacto da ferrugem da soja em cultivares suscetíveis e parcialmente resistentes a *Phakopsora pachyrhizi*

ABSTRACT

Host resistance is one of the key tools in the integrated disease management in several crops. Soybean rust (SBR) can also be managed through resistant cultivars, but little is known and applied in the field. We aimed to assess the responses of soybean cultivars with different levels of resistance to soybean rust, also seeking to explore the effect of *P. pachyrhizi* on soybean photosynthesis. Two field trials and two controlled-environment studies were conducted exploring the response of susceptible and partially resistant soybean cultivars under SBR infection. The treatments in field and laboratory trials consisted of two cultivars (susceptible and partially resistant to SBR) combined with two disease situations: with and without fungicide application. The impact of SBR was evaluated through visual assessment of disease severity, crop yield, chlorophyll fluorescence, gas exchange rates, and vegetation indices (VIs) based on remote sensing. Partially resistant cultivars promoted less severity and disease growth, along with higher crop yield in the field trial. Greater disease impact was observed on chlorophyll fluorescence when compared to infected and healthy plants, with lower values of the variables evaluated. Soybean rust also affected transpiration rate, CO_2 assimilation, and stomatal conductance. The VIs provided good visual observations between treatments with and without SBR infection, highlighting the differences found in the disease severity evaluations. Partially resistant cultivars can promote reduced disease progress and severity with an impact on the yield and, therefore, being considered a valuable tool for the disease management.

[1] Capítulo submetido à *European Journal of Plant Pathology* (1573-8469) e redigido de acordo com as normas da revista.

Keywords: Host resistance, integrated disease management, disease severity, photosynthesis.

RESUMO

A utilização de hospedeiros resistentes é uma das principais ferramentas no manejo integrado de doenças em diversas culturas. A ferrugem da soja (FAS) também pode ser manejada por meio de cultivares resistentes, mas ainda existem poucos estudos sobre o assunto, tampouco com aplicações práticas no campo. Nosso objetivo foi avaliar as respostas diferenciais de cultivares de soja com diferentes níveis de resistência à FAS, buscando também explorar o efeito de *P. pachyrhizi* na fotossíntese da soja. Dois ensaios de campo e dois estudos em ambiente controlado foram conduzidos explorando a resposta de cultivares de soja suscetíveis e parcialmente resistentes à infecção por FAS. Os tratamentos em campo e em laboratório consistiram em dois cultivares (suscetível e parcialmente resistente a FAS), combinadas em duas situações de doença: com e sem aplicação de fungicida. O impacto da FAS foi avaliado através da avaliação visual da severidade da doença, produtividade, fluorescência da clorofila, taxas de trocas gasosas e índices vegetativos (IVs) baseados em sensoriamento remoto. Cultivares parcialmente resistentes promoveram menor severidade e desenvolvimento da doença, além de maior produtividade da cultura no ensaio de campo. Maior impacto da doença foi observado na fluorescência da clorofila na comparação entre plantas infectadas e sadias, com menores valores das variáveis avaliadas. A FAS também afetou a taxa de transpiração, assimilação de CO_2 e condutância estomática. Os IVs proporcionaram boas observações visuais entre os tratamentos com e sem infecção por FAS, destacando as diferenças encontradas nas avaliações da severidade da doença. Cultivares parcialmente resistentes podem promover redução do progresso e severidade da doença com impacto na produtividade e, portanto, sendo considerada uma ferramenta valiosa para o manejo da FAS.

Palavras-chave: Resistência do hospedeiro, manejo integrado da doença, severidade da doença, fotossíntese.

1.1 INTRODUCTION

Soybean is the most important crop cultivated in Brazil, the current biggest producer and exporter of the commodity (Cattelan and Dall'Agnol 2018; Toloi et al. 2021). Despite recent advances in cropping systems, soybean crop faces a wide spectrum of pests that undermine the potential crop yield. In this scenario, soybean rust (SBR), caused by *Phakopsora pachyrhizi* Sydow & Sydow, poses as the most important disease and responsible for significant yield losses (Godoy et al. 2016; Langenback et al. 2016; Lana et al. 2018). The integrated disease management (IDM) of SBR is still heavily dependent on fungicides application, which is critically impaired by resistant population of the fungus frequently present in most of the soybean growing regions (Juliatti et al. 2017).

Along with chemical control, other techniques such as regulatory policies of sowing period restrictions as well as the determination of a specific period without any crop cultivation are also considered effective tools (Godoy et al. 2016). Moreover, host resistance to the pathogen is also an important tool that is under constant development (Childs et al. 2018), although not yet largely applied in the SBR management (Godoy et al. 2016; Juliatti et al. 2021). Resistance genes to *P. pachyrhiz*i (Rpp) have been reported and represented by seven different loci that was mapped in the soybean genome (Godoy et al. 2016; Childs et al. 2018).

Three different reactions are expected in the *P. pachyrhizi* – soybean interaction based on the susceptibility or resistance level of the soybean genotype (Bromfield 1984; Miles et al. 2011; Vittal et al. 2014). A susceptible reaction results in TAN symptoms, represented by tan to light-brown lesions, ample sporulation, and presence of uredinia throughout the leaf. Resistance reaction can be recognized by immune reactions (IM), with no presence of uredinia nor visual symptoms, as well as by RB-reaction type, represented by reddish-brown lesions, lower quantity of uredinia and none to very deficient sporulation (Vittal et al. 2014; Childs et al. 2018). Genotypes that present RB reactions are considered with partial or incomplete resistance and, even though partially resistant genotypes still present SBR symptoms when infected (Miles et al. 2011), great benefits have been reported compared to susceptible cultivars.

Although the differences between susceptible and partial resistance reactions are already known in terms of sporulation and infection processes in the host (Miles et al. 2011; Vittal et al. 2014), little is known regarding its effect on the crop

physiological functions as well as the crop yield, especially in field trials. Furthermore, the wide genetic variability of *P. pachyrhizi* reduce the possibility of introducing a total resistant cultivar to the pathogen populations (Yamanaka et al., 2010; Godoy et al. 2016), which reinforces the use of partial resistance as one of the few options of host resistance against SBR. The application of cultivars with partial resistance has been increasing in Brazil since 2009, when the first cultivars were commercially available (Godoy et al. 2016). Partially resistant cultivars are also known as “slow rusting” due to its effect on epidemic rates by increasing latent period and reducing the production of urediniospores as well as the number and size of SBR lesions (Azevedo et al. 2007; Vittal et al. 2014). Therefore, it acts by reducing the inoculum production and dissemination throughout the fields.

In general, SBR disease affect plant yield by photosynthesis impairment due to necrosis and defoliation (Godoy et al. 2016; Rio et al. 2017). Rio et al. (2017) reported the negative impact of SBR on chlorophyll fluorescence and gas exchange rates, but only few studies have explored the comparison of these parameters between susceptible and resistant cultivars (Kumudini et al. 2008a). Moreover, other studies have also demonstrated the impact of diseases on reducing maximum quantum yield of photosystem II (PSII) (F_v'/F_m'), as well as its effective quantum yield ($\Delta F/F_m'$) and electron transport rate (ETR) (Scholes and Rolfe, 2009; Tatagiba et al. 2015; Rios et al. 2017).

Chlorophyll fluorescence allow a sensitive analysis of the host photosynthetic metabolism as it explores the relationship between absorbed photons that would be used for photosynthesis and those that are reflected as fluorescence energy (Berger et al. 2007). It represents an important parameter of photosynthesis capacity of the plant by demonstrating the effect of the disease on the PSII reaction centers activity (Berger et al. 2007; Rios et al. 2017). Furthermore, when used along with gas exchange rates under disease infection, it has also been helpful to understand the impact of the disease on crop photosynthesis. Remote sensing techniques have also been applied to unveil the effect of diseases through the exploration of morphological and physiological alterations in the plant’s spectrum, such as through the calculation of vegetation indices (VIs) that have been previously studied and correlated to a specific function or structure of the plant (Thenkabail et al. 2000; Behmann et al. 2014).

Despite the commercial availability of partially resistant cultivars for over a few years, its adoption is still low and lacks more research. The comprehension of these impacts and interactions are important to support the use of host resistance in the SBR management and as valuable information for breeding programs. The hypothesis is that partial resistance to SBR promotes lower impact of the disease in terms of severity and yield and that this lower impact reflects on physiological parameters such as chlorophyll fluorescence, gas exchange and leaf reflectance. Therefore, we aimed to assess the responses of soybean cultivars with levels of resistance to soybean rust, seeking to explore the effect of *P. pachyrhizi* on soybean photosynthesis.

1.2 MATERIAL AND METHODS

1.2.1 Field trials

Two experimental fields (replicates) were conducted in Botucatu, SP, Brazil, with geographic coordinates 22° 48' 48"S; 48° 25' 37"W (Field 1) and 22° 49' 38"S; 48º 25' 40"W (Field 2), during the 2019/2020 crop season. In both sites, no-tillage system was adopted and all sowing operations, crop protection management, fertilization, and evaluations were carried out homogeneously. The soybean crop was sown simultaneously in both fields on December 6, 2019, with row spacing of 0.45 m and a population of 299,000 plants ha^{-1} in Field 1 and 288,000 plants ha^{-1} in Field 2.

1.2.1.1 Experimental design

The field trials were carried out in a randomized block design and the treatments were distributed in a 2 x 2 factorial scheme: 2 soybean cultivars (Brevant DS6217 IPRO, susceptible to SBR; TMG IPRO 7063, partially resistant to SBR) and 2 disease situations (with and without chemical control), in five repetitions. Both cultivars are recommended for the region where the study was conducted and have the same indeterminate growth habit (Table 1). The experimental units (plots) of each site was composed by six 3 x 5-m soybean rows (width x length), totaling an area of 15 m^2.

The cultivars choice was based on commercial materials that are commonly used in Brazil, following manufacture's recommendation as SBR susceptibility or resistance level. This is important to assess commercially available cultivars to the

soybean growers, as these results can be used as a reference of its application in the IDM of SBR in the region.

Table 1. Description of the cultivars adopted in the experimental trials

Description	Brevant DS6217 IPRO[1]	TMG 7063[2]
P. pachyrhizi susceptibility	Susceptible	Partially resistant (Inox)
Maturity groups	6.2	6.3
Growth habit	Indeterminate	Indeterminate
Traits	Intacta RR2 PRO®	Intacta RR2 PRO®

[1]BREVANT SEMENTES (2020); [2]TROPICAL MELHORAMENTO GENÉTICO (2020)

Treatments kept with chemical control were conducted under protective and curative fungicides applications. Starting at the vegetative growth stage V6, three applications of the systemic fungicide trifloxystrobin (150.0 g L^{-1}) + prothioconazole (175.0 g L^{-1}) (Fox®) and three applications of the fungicide mancozeb (750 g kg^{-1}) (Unizeb Gold®) were carried out fortnightly. Fox® and Unizeb Gold® were applied at a rate of 0.4 L ha^{-1} and 2.5 kg ha^{-1}, respectively, as recommended by the manufacturers. Sprayings were carried out with a CO_2 pressurized backpack sprayer equipped with a 3-meter boom and six flat fan nozzles XR 11002 (TeeJet). The displacement speed was 5.0 km h^{-1} and pressure of 200 kPa, providing an application rate of 150 L ha^{-1}.

1.2.1.2 *P. pachyrhizi* inoculation

The pathogen was inoculated in both field trials in order to provide greater uniformity of disease incidence throughout the field. Soybean leaves with severe symptoms were collected from plants kept in a greenhouse for this purpose. The leaves were separated into small portions, placed in plastic bags, and 100 mL of distilled water with adhesive spreader Tween 20 (240 µL L^{-1}) were added and manually shaken for 10 minutes to extract urediniospores. The suspension was homogenized for counting and determination of spore concentration in a Neubauer chamber. The number of spores was counted four times in a drop of 10 µL of the suspension. After that, the entire suspension was adjusted to a final concentration of 4 x 10^4 urediniospores mL^{-1} (Zanatta et al. 2012). Finally, the suspension with urediniospores was poured into a backpack sprayer and sprayed evenly in the

central lines of each plot, adjusting the walking speed for better distribution of the suspension. Only one inoculation was performed in the plots without chemical control, when the plants were at the V8 vegetative growth stage (45 days after emergence - DAE). Inoculation was carried out at dusk, in order to keep the spores in the dark as long as possible and with a period of greater humidity and leaf wetness (ZANATTA et al., 2012).

1.2.1.3 Disease severity assessment

Starting at the V6 growth stage, 10 leaflets were collected weekly per plot from the lower region of the soybean canopy and taken to the laboratory for better visualization of fungal structures and symptoms under a stereoscopic microscope. The severity of the disease was estimated through the attribution of notes based on the visual observation of the symptoms using the diagrammatic scale proposed by Godoy et al. (2006). The Area Under the Disease Progress Curve (AUDPC), proposed by Campbell and Madden (1990), was calculated based on the mean values of disease severity obtained in the plots and at the respective evaluation dates.

1.2.1.4 Chlorophyll fluorescence assessment

The effect of SBR on the soybean chlorophyll fluorescence was measured with a pulse modulated fluorometer (Opti-Science, Model SD5p) through the assessment of the parameters: steady-level fluorescence, without biochemical reactions or electron transport (F); maximum fluorescence at light-adapted state (F_{ms}); effective quantum yield of photosystem II (PSII) ($\Delta F/F_m'$ or Y); electron transport rate (ETR); initial fluorescence (F_o); maximum fluorescence (F_m); and maximum quantum yield of PSII (F_v'/F_m'). Only the main variables of this analysis were considered in the statistical tests and discussion, that is Y, ETR, and F_v'/F_m'.

For the variables analyzed in the light-adapted state (F, F_{ms}, $\Delta F/F_m'$ and ETR), two readings were performed per plot, that is two plants at the lower canopy region. For the dark-adapted variables (F_o, F_m and F_v'/F_m'), the same two plants were evaluated at the lower canopy region, dark-adapting it for twenty minutes with subsequently reading by the equipment (Kumudini et al. 2008b). The evaluations were always carried out at the same time range (9:00 – 11:00 am). The first evaluation of both fields were conducted at the same day of pathogen inoculation,

and additionally three other evaluations on Field 1 and two evaluations on Field 2 were also conducted, starting 14 days after the inoculation and spaced at 7 days. The third evaluation of Field 2 was not possible to be conducted due to intense crop defoliation.

1.2.1.5 Crop yield

At the end of the crop season, each plot was harvested to determine the effect of SBR on soybean crop yield of each treatment. On March 26th, 2020 (106 DAE), one meter of the two central lines of each plot was manually harvested, totaling 2.0 meters of cultivated soybean row per plot. The samples were threshed and sieved to remove impurities. The soybean production of each plot was individually weighed on a precision scale and adjusted to a moisture content of 13% (Brasil, 2009), using the Gehaka® AGRI device, model G929. The values obtained were transformed to the final crop yield in kg ha^{-1}. Finally, the thousand seed weight (TSW) of each plot was also evaluated according to Brasil (2009).

1.2.2 Controlled-environment Trials

Due to heterogeneous results between treatments and evaluation dates in the field trials, in addition to the incidence of SBR in treatments without inoculation and with fungicide application, it was decided to replicate the experiment in a greenhouse. Therefore, it would allow the analysis the effects of the disease on physiological aspects of the soybean cultivars in a controlled-environment situation for better comparison of results and interpretation. The figures of the controlled-environment trials conductance and evaluations are shown in the Appendices (Figure A1 – A4).

1.2.2.1 Experimental design

The experiment was carried out in a completely randomized design, following the same treatments and cultivars evaluated in the field trials (Table 1), with 5 repetitions. However, in these trials it was possible to maintain the treatments with completely different disease situations, which consisted of a treatment without inoculation and infection of *P. pachyrhizi*, maintained under application of fungicides; and a treatment with inoculation of SBR and without fungicide application. The whole experiment was replicated. Soybean was sown on July 15, 2020 and July 24, 2020

for the first and second replication, respectively, in 1.8 L pots. Each experimental unit (repetition) consisted of a pot with one plant. The plants were kept in an environment with drip irrigation, temperature (25ºC±5) and relative humidity (50% ±10) control.

The treatments without SBR infection received two fungicide applications (Fox®), at 45 and 65 DAE, at the same dose and application rate described. The treatments with SBR infection were inoculated at 45 DAE. For this, urediniospores of *P. pachyrhizi* were collected in Petri dishes with the aid of a brush from soybean leaves with severe symptoms and high sporulation. Preparation of the spore suspension, counting, and establishment of concentration was conducted as described above for the field trials. The plants were sprayed with the spore suspension (4 x 10^4 urediniospores mL^{-1}) to the point of runoff and immediately placed in a dark environment with high humidity for 18 hours.

1.2.2.2 Disease severity assessment

Disease severity was evaluated as described in the field trials, starting 1 day before inoculation of each experiment. Severity was estimated through the attribution of notes based on the visual observation of the symptoms using the diagrammatic scale of the disease proposed by Godoy et al. (2006). Two leaflets per repetition (plant) were evaluated; one leaflet from the upper region and another one from the lower region of the plant. The AUDPC was also calculated as described above.

1.2.2.3 Chlorophyll fluorescence and leaf gas exchange assessment

Chlorophyll fluorescence was also assessed as fully described in the field trials through two different protocols: i) light-adapted state variables assessment (F, F_{ms}, $\Delta F/F_m'$ and ETR), in which two readings were performed per plant (third and fifth trifoliate leaf); ii) dark-adapted state variables assessment (F_o, F_m and F_v'/F_m'), in which two readings per plant were also performed (third and fifth trifoliate leaf), adapting it to the dark for twenty minutes with subsequent reading by the pulse modulated fluorometer (Opti-Science, Model SD5p).

The evaluation of gas exchange rate was performed with the Infrared Gas Analyzer (IRGA, LCpro-SD, ADC Bioscientific Ltda) in two periods: i) at the beginning of the symptoms of the disease, of which there was mild severity in the inoculated treatments (60 DAE); and ii) 20 days after the first evaluation, with severer disease symptoms (80 DAE). The parameters CO_2 assimilation rate (A), stomatal

conductance (gs), transpiration rate (E), CO_2 internal concentration (Ci), and instantaneous carboxylation efficiency (A/Ci) were analyzed in two leaflets per plant (central third and fifth trifoliolate leaf). The evaluations were conducted under 410 µmol mol^{-1} CO_2 reference and photosynthetic irradiance of 1000 µmol m^{-2} s^{-1} (Rios et al. 2017), using the broad-leaf chamber with a window area of 6.25 cm^2. The evaluations were always carried out at the same time range (9:00 – 11:00 am).

1.2.2.4 Disease severity evaluation by remote sensing

The evaluation of the crop reflectance was performed by the ASD FieldSpec Dual Spectroradiometer (Analytical Spectral Devices, Boulder, CO, USA), with a spectral range from 350 to 1070 nm and 7.5º of field of view. A white panel with approximately 100% reflectance (Spectralon) was used as a reference for calibration. For this evaluation, the plants were placed outside the greenhouse under intense sunlight and without shading, performing a calibration and optimization of the equipment every 10 minutes. All evaluations were performed weekly in all sampling units and in two leaflets per plant (third and fifth trifoliate leaf), keeping the equipment at a uniform distance from the leaves throughout the readings (20 cm).

The spectral curves of each sample were reduced from 350 – 1000 nm to 350 – 900 nm for high noise levels reduction (Abdel-Rahman et al. 2014), and Savitzky-Golay filter was applied using 11 central points and a third-degree polynomial (Savitzky and Golay 1964; Bohnenkamp et al. 2019). The reflectance dataset was used to calculate a list of 19 vegetation indices (VIs) that was representative to the disease effect on the crop and to allow disease severity identification. Vegetation Indices are excellent resources to help interpret this type of data, optimizing the understanding and application of data to identify plant stresses (Shiratsuchi et al., 2014; Bajwa et al., 2017). Besides, it allows other sensors such as multispectral sensors to also be able to obtain enough information to estimate these values, not requiring hyperspectral sensors.

The VIs correlated to physiological or morphological parameters of the plant were divided into two main groups: VIs correlated to pigments and morphological structures of the plant (C420, SIPI, PRI, SG, mRESR, VOG1, RGRI, PSRI, ANTH1, and ANTH2), and VIs correlated to leaf area index and biomass (MSAVI2, NDVI, DVI, RVI, GRVI, SR, EVI, RENDVI, mRENDVI) (Behmann et al. 2014). The whole

VIs descriptions and formulas are described in Table A1, according to Cui et al. (2009) and Behmann et al. (2014).

1.2.2.5 Crop yield

At the end of plant development (100 DAE), each plant was manually harvested to determine the effect of SBR on soybean crop yield of each treatment. Soybean grains were manually extracted from the pods, separated into paper bags corresponding to each treatment, and individually weighed on a precision scale and adjusted to a moisture content of 13% (Brasil 2009), using the Gehaka® AGRI device, model G929.

1.2.3 Data analysis

The data were submitted to analysis of variance (ANOVA) by the F test and, when significant, the means of the treatments were compared by the Tukey test at 5% probability, using the R 3.6 software (R CoreTeam 2019). Chlorophyll fluorescence, gas exchange and the VIs statistical comparisons were performed at each evaluation date. The variables of each field trial were compared separately due to significant differences between Field 1 and 2 ($p<0.01$). On the other hand, since there was no significant interaction between the experimental replications in the controlled-environment trials ($p>0.05$), the variables were here analyzed altogether, except for gas exchange results that differed between replications ($p<0.05$). Data treatment prior to the statistical analysis of reflectance data and VIs were conducted as previously described.

1.3 RESULTS

1.3.1 Field Trials

1.3.1.1 Disease severity assessment

There was no significant difference in the interaction between the factors in the first field trial. However, greater disease severity ($p<0.05$) was observed in the treatment without fungicide application (Figure 1A). Likewise, higher AUDPC was observed in the susceptible soybean cultivar (DS6217) compared to the partially resistant cultivar (TMG 7063) (Figure 1B). No significant difference was found for any of the factors in Field 2.

Soybean rust incidence was firstly found 7 days after inoculation (DAI) at Field 1 and 14 DAI at Field 2, with remarkable development progress after this period (Figure 2). A similar increase in disease progress in both fields was observed, despite the disease severity being higher in Field 1, especially at the end of the evaluations.

Figure 1. Soybean rust severity (AUDPC) according to the disease situation in the field (A) and soybean cultivar (B) in the experimental Field 1.

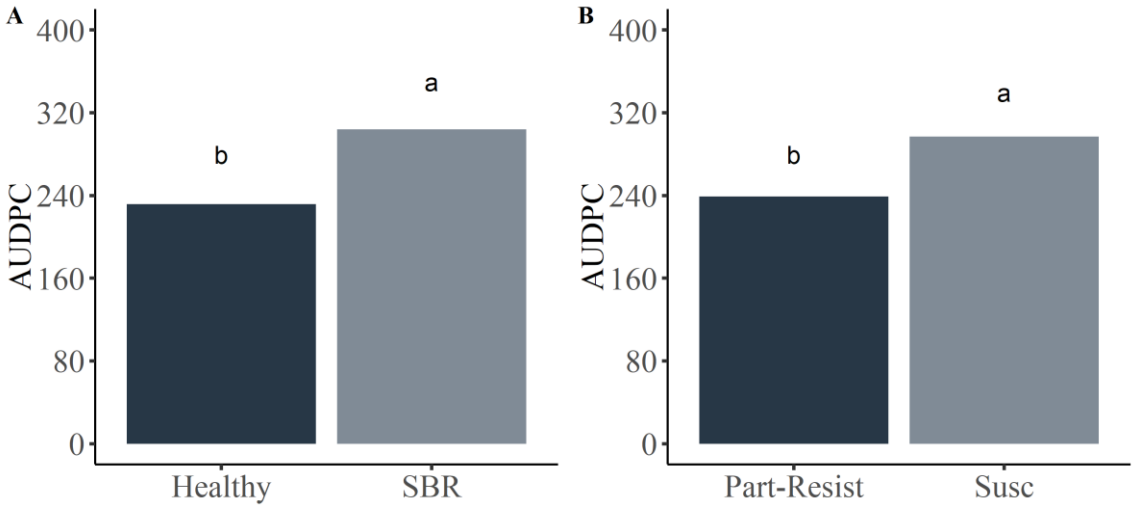

*Healthy: fungicide application; SBR: inoculated with *P. pachyrhizi* and without chemical control. Part-Resist: partially resistant cultivar; Susc: susceptible cultivar. Means followed by the same letter did not differ according to Tukey test at 5% probability ($p<0.05$).

Due to the aggressiveness and dissemination of the disease, there was a high severity level in these treatments even with chemical control, mainly at the end of the crop growth stages, contributing to the severity increase (Figure 2A). Meanwhile, in Field B, the disease remained progressively low for all treatments, without any difference ($p>0.05$) and with distinguished lower severity on the partially resistant cultivar with fungicide application (Figure 2B).

Figure 2. Soybean rust progress curve in the first (A) and second (B) experimental fields according to different cultivars and disease severity levels.

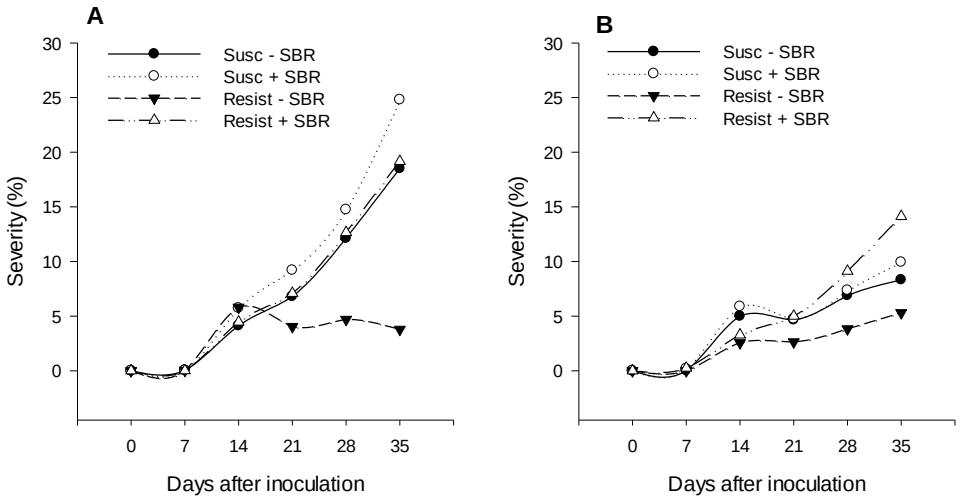

*Susc – SBR: susceptible soybean cultivar (DS6217) with fungicide application; Susc + SBR: susceptible soybean cultivar (DS6217) without fungicide application; Resist – SBR: partially resistant cultivar (TMG7063) with fungicide application; Resist + SBR: partially resistant cultivar (TMG7063) without fungicide application.

1.3.1.2 Chlorophyll fluorescence

In Field 1, significant differences were found only at 21 DAI, when treatments without chemical control presented higher Fv'/Fm' values compared to the treatments with chemical control (Table 2). In the second field trial, differences were found between the cultivars irrespective of disease severity level, in which partially resistant cultivars obtained greater $\Delta F/F_m'$ (Y) and ETR then the susceptible cultivars at 14 DAI (Table 3).

Chlorophyll fluorescence parameters response across the evaluation dates are represented in Figures 3 and 4 for Field 1 and 2, respectively. In general, both cultivars with lower SBR severity obtained higher fluorescence values in most of the parameters assessed. No pattern could be identified in terms of linear or continued progress across the evaluation dates according to the disease progress across this period, in which clearer differences were only found at the last evaluation with higher disease severity.

Table 2. Mean values of maximum quantum yield of PSII (Fv'/Fm') according to different levels of soybean rust severity at 21 days after inoculation (DAI) of Field 1.

Treatments	**F_v'/F_m'**
Healthy	0.558 b
SBR	0.634 a
F	0.376*
CV (%)	11.89

*Healthy: with fungicide application; SBR: inoculated with *P. pachyrhizi* and without chemical control. NS: Not significant; *significant a p ≤ 0.05 by F test. Means followed by the same letter did not differ according to Tukey test at 5% probability (p<0,05).

Table 3. Mean values of effective quantum yield of photosystem II (PSII) ($\Delta F/F_m'$) (Y) and electron transport rate (ETR) of susceptible and partially resistant cultivars to *P. pachyrhizi* under pathogen infection at 14 days after inoculation (DAI) of Field 2.

Treatments	**$\Delta F/F_m'$ (Y)**	**ETR**
Partially resistant	0.724 a	152.18 a
Susceptible	0.690 b	144.89 b
F	5.955*	5.969*
CV (%)	4.43	4.49

*Healthy: with fungicide application; SBR: inoculated with *P. pachyrhizi* and without chemical control. NS: Not significant; *significant a p ≤ 0.05 by F test. Means followed by the same letter did not differ according to Tukey test at 5% probability (p<0,05).

In Field 1, effective quantum yield of PSII (Y) and F_v'/F_m' had either inconsistent behaviour throughout the evaluations or no difference was observed. However, both cultivars with higher soybean severity obtained lower ETR at the last evaluations (14 and 21 DAI), observing greater impact of SBR in the treatments with greater severity (Figure 3). In Field 2, basically same response was found. Electron transport rate values were higher in both cultivars with fungicide protection, especially at 14 DAI. Y and F_v'/F_m' did not show any visual difference between the treatments (Figure 4).

Figure 3. Chlorophyll fluorescence parameters [ΔF/Fm′ (Y) and Fv'/Fm'] and electron transport rate (ETR) of susceptible and partially resistant cultivars to *P. pachyrhizi* under pathogen infection on Field 1, according to the evaluation dates after the pathogen inoculation.

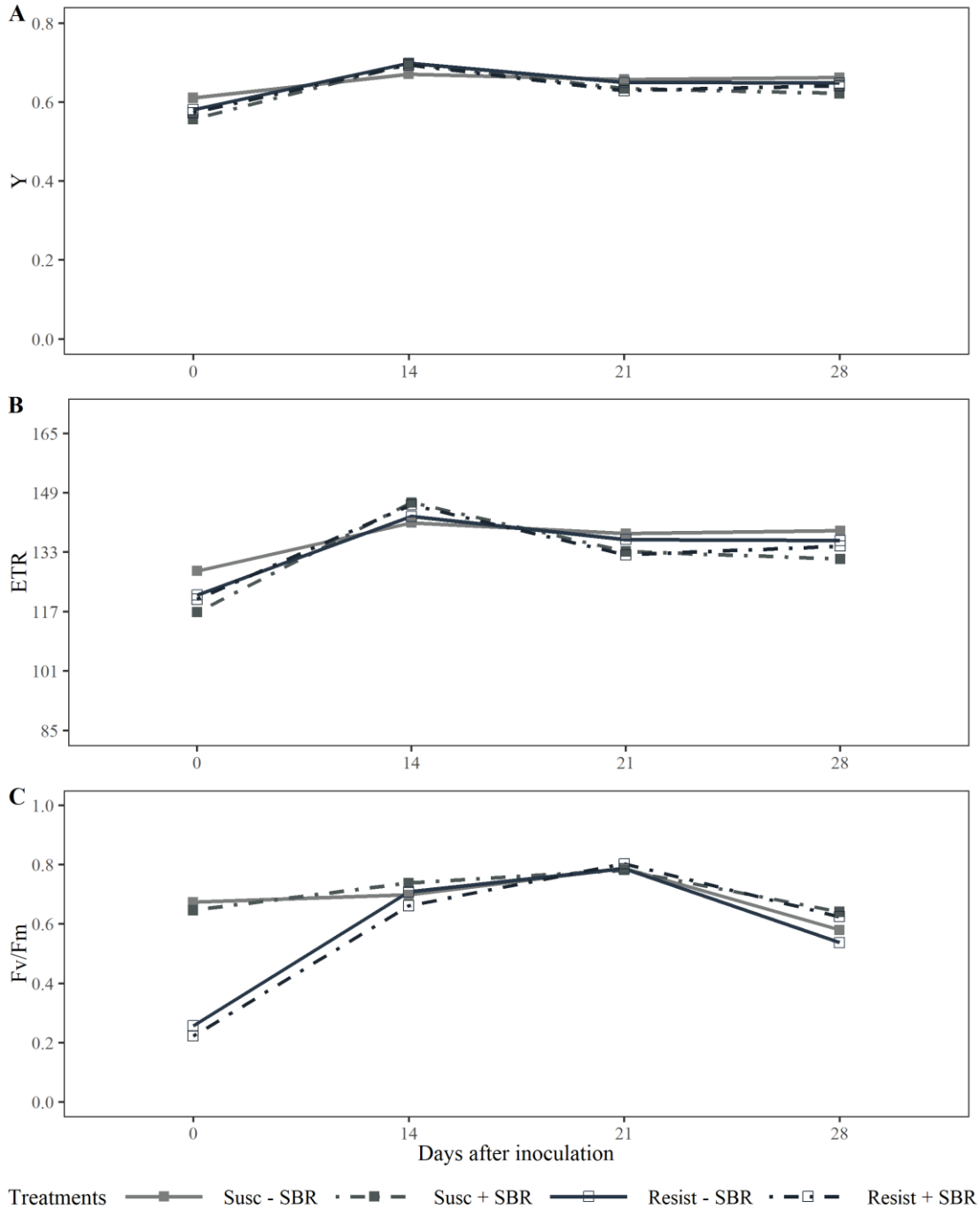

*Susc – SBR: susceptible soybean cultivar (DS6217) with fungicide application; Susc + SBR: susceptible soybean cultivar (DS6217) without fungicide application; Resist – SBR: partially resistant cultivar (TMG7063) with fungicide application; Resist + SBR: partially resistant cultivar (TMG7063) without fungicide application.

**A: effective quantum yield of photosystem II (PSII) (Y = ΔF/Fm′); B: electron transport rate (ETR); C: maximum quantum yield of PSII (Fv'/Fm').

Figure 4. Chlorophyll fluorescence parameters [ΔF/Fm′ (Y) and Fv'/Fm'] and electron transport rate (ETR) of susceptible and partially resistant cultivars to *P. pachyrhizi* under pathogen infection on Field 2, according to the evaluation dates after the pathogen inoculation.

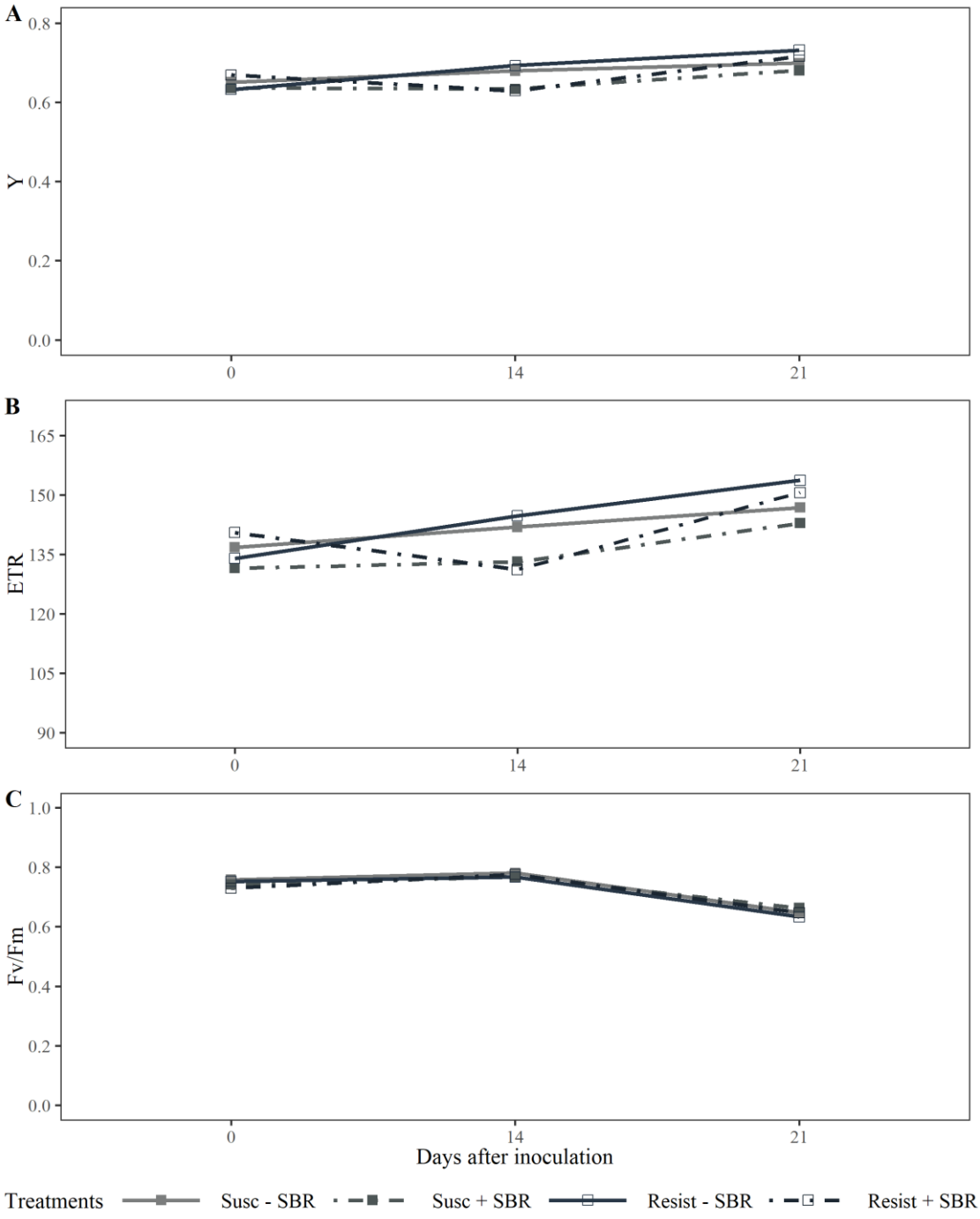

*Susc – SBR: susceptible soybean cultivar (DS6217) with fungicide application; Susc + SBR: susceptible soybean cultivar (DS6217) without fungicide application; Resist – SBR: partially resistant cultivar (TMG7063) with fungicide application; Resist + SBR: partially resistant cultivar (TMG7063) without fungicide application.

**A: effective quantum yield of photosystem II (PSII) (Y = ΔF/Fm′); B: electron transport rate (ETR); C: maximum quantum yield of PSII (Fv'/Fm').

1.3.1.4 Crop yield

As observed for disease severity, there was no significant difference in the interaction of factors for crop yield results of Field 1. However, the treatments with fungicide application presented higher crop yield, producing 1047 kg ha^{-1} more than the treatments where no fungicide was used (Figure 5). No differences were observed between soybean cultivars, nor on any of the factors in Field 2, following same result patterns of disease severity.

Figure 5. Mean values of soybean crop yield (kg ha^{-1}), according to different soybean rust severity level of Field 1.

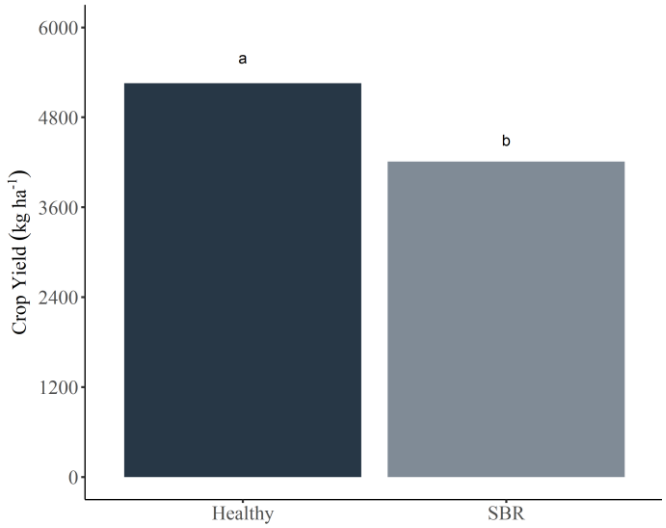

*Healthy: fungicide application; SBR: inoculated with *P. pachyrhizi* and without chemical control. Means followed by the same letter did not differ according to Tukey test at 5% probability ($p<0.05$).

1.3.2 Controlled-environment Trials

1.3.2.1 Disease severity assessment

In the laboratory trials, a similar response was observed regarding disease severity (AUDCP) and crop yield (g) compared to the results obtained in the field experiments, especially Field 1 that presented greater disease severity. There was a significant difference between the factors for the AUDCP variable, with greater severity in the treatments with SBR infection (Table 4). In addition, the susceptible cultivar also presented higher severity compared to the partially resistant cultivar. Clearer distinction between RB and TAN-lesion were also observed (Figure 6).

Table 4. Mean values of disease severity (AUDPC) according to SBR-infected and non-infected susceptible and partially resistant cultivars in the controlled-environment trial.

Cultivar	AUDPC	
	Healthy	**Infected**
Susceptible	0.00 aA	225.37 aA
Partially resistant	0.00 aB	145.22 bA
Cause of Variation	**F**	**P**
Disease (D)	149.789	<0.001***
Cultivar (C)	7.007	0.013*
D x C	7.007	0.013*
CV (%)	51.67	

^{NS}: Not significant; *significant a p ≤ 0.05 by F test. Means followed by the same letter did not differ according to Tukey test at 5% probability (p<0.05). Uppercase letters compare between means of disease level at each cultivar level (columns). Lowercase letters compare between means of cultivars at each disease level (lines).

Figure 6. Tan and reddish-brown (RB) lesions of SBR in susceptible (A) and partially resistant (B) cultivars under SBR infection in the controlled-environment trials.

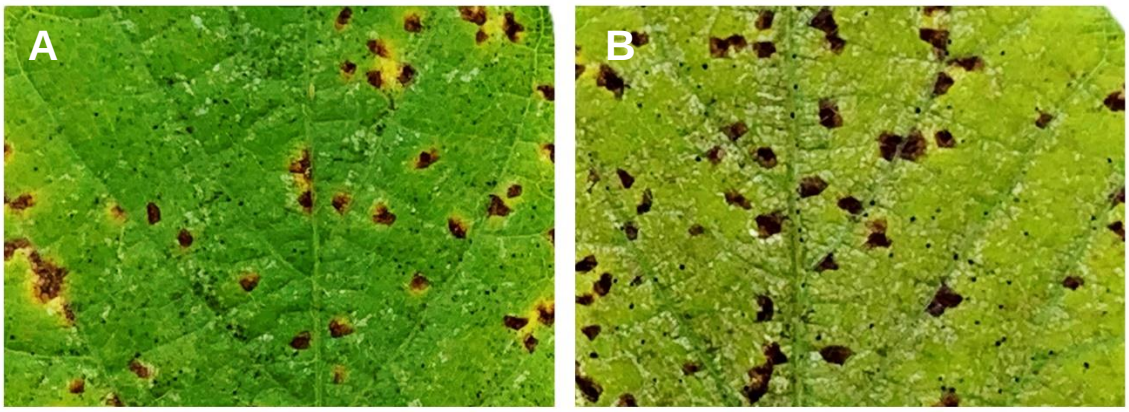

Furthermore, the disease progress curve helps to visualize the difference between cultivars under SBR infection (Figure 7). While the control treatments without inoculation and with fungicide application remained uninfected, differences between soybean cultivars were clear as a function of its resistance level, where the susceptible cultivar presented a greater disease growth compared to the partially resistant. The first symptoms were found 7 DAI in both experimental replications. Soybean crop yield differed only according to the disease levels (p<0.05), in which treatments with fungicide application (healthy) obtained higher yield (Figure 8).

Figure 7. Soybean rust progress curve based on the disease severity (%) of inoculated and non-inoculated soybean cultivars (susceptible and partially resistant to SBR) in the controlled-environment trials.

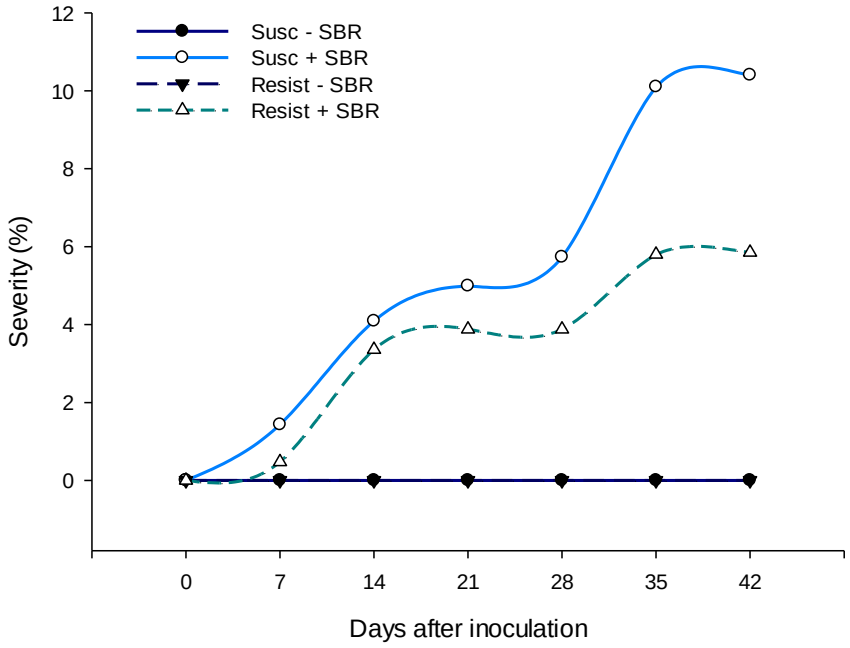

*Susc – SBR: susceptible soybean cultivar (DS6217) non-inoculated with fungicide application; Susc + SBR: susceptible soybean cultivar (DS6217) inoculated without fungicide application; Resist – SBR: partially resistant cultivar (TMG7063) non-inoculated with fungicide application; Resist + SBR: partially resistant cultivar (TMG7063) inoculated without fungicide application.

Figure 8. Mean values of soybean crop yield (kg ha^{-1}), according to different soybean rust severity level on controlled-environment trials.

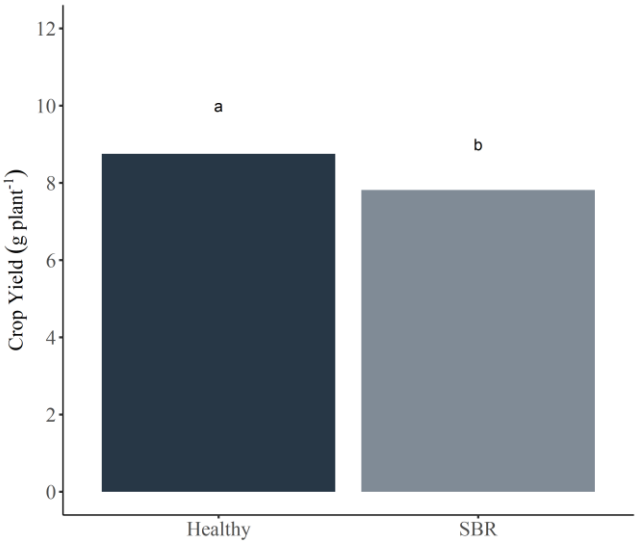

*Healthy: with fungicide application; SBR: inoculated with *P. pachyrhizi* and without chemical control. Means followed by the same letter did not differ according to Tukey test at 5% probability ($p<0.05$).

1.3.2.2 Chlorophyll fluorescence

Significant differences in chlorophyll fluorescence levels were detected only at 35 DAI for the variables analyzed under light and dark-adapted, a moment when the plants presented severer symptoms (Table 5). However, differences were not found for the main variables analysed (ΔF/Fm′, ETR, and F_v'/F_m'). Overall, at this evaluation date, healthy plants showed greater fluorescence values compared to diseased plants (Table 5), demonstrating the pathogen's action on plant physiology, and corroborating the results found in the field. Differences between the treatments are shown in the Figures 9 and 10, where treatments without SBR infection show higher fluorescence values in most of the parameters evaluated (F_s, F_{ms}, ETR, F_m, and F_v'/F_m'). Alternatively to the findings in the field trials, here a subtle pattern was observed across evaluation dates and disease progress, although clearer differences were only found at the last evaluation with higher disease severity. Similar to the field trials, no visual difference was found for Y.

Table 5. Chlorophyll fluorescence (F_s, F_{ms}, ΔF/Fm′, F_o, F_m, Fv'/Fm') and electron transport rate (ETR) of susceptible and partially resistant cultivars to *P. pachyrhizi* under different SBR disease levels at the last evaluation date (35 DAI) of the controlled-environment trials.

Treat.	F_s	F_{ms}	$\Delta F/F_m'$ (Y)	ETR	F_o	F_m	F_v'/F_m'
Healthy	190.45 a	459.93 a	0.582 a	121.92 a	238.55 a	669.25 a	0.632 a
SBR	164.90 b	393.975 b	0.549a	116.22 a	230.00 a	577.55 b	0.578 a
F	13.925^{***}	8.598^{*}	3.725^{NS}	2.936^{NS}	0.113^{NS}	4.523^{*}	3.514^{NS}
CV (%)	12.18	16.65	9.28	8.88	34.36	21.87	15.40

*Healthy: non-inoculated with fungicide application; SBR: inoculated without fungicide application. ^{NS}: Not significant; *significant a $p \leq 0.05$ by F test. Means followed by the same letter did not differ according to Tukey test at 5% probability ($p<0.05$).

Figure 9. Light-adapted chlorophyll fluorescence parameters (F_s, F_{ms}, $\Delta F/F_m'$) and electron transport rate (ETR) of susceptible and partially resistant cultivars to *P. pachyrhizi* according to disease levels on the controlled-environment trials.

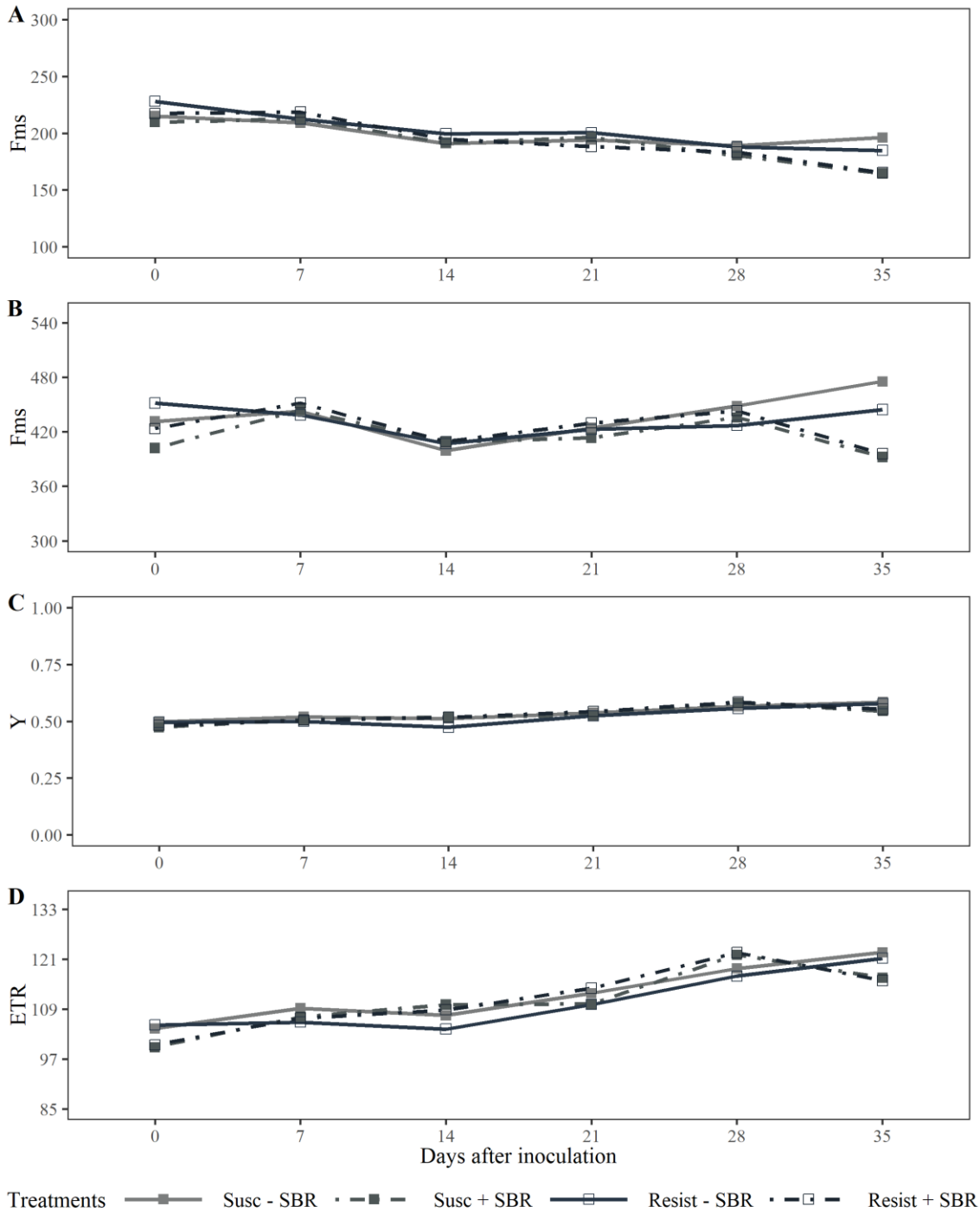

*Susc – SBR: susceptible soybean cultivar (DS6217) non-inoculated with fungicide application; Susc + SBR: susceptible soybean cultivar (DS6217) inoculated without fungicide application; Resist – SBR: partially resistant cultivar (TMG7063) non-inoculated with fungicide application; Resist + SBR: partially resistant cultivar (TMG7063) inoculated without fungicide application.

**A: steady-level fluorescence (F_s); B: maximum fluorescence at light-adapted state (F_{ms}); C: effective quantum yield of photosystem II (PSII) (Y = ΔF/Fm'); D: electron transport rate (ETR).

Figure 10. Dark-adapted chlorophyll fluorescence parameters (F_o, F_m and F_v'/F_m') of susceptible and partially resistant cultivars to *P. pachyrhizi* according to disease levels on the controlled-environment trials.

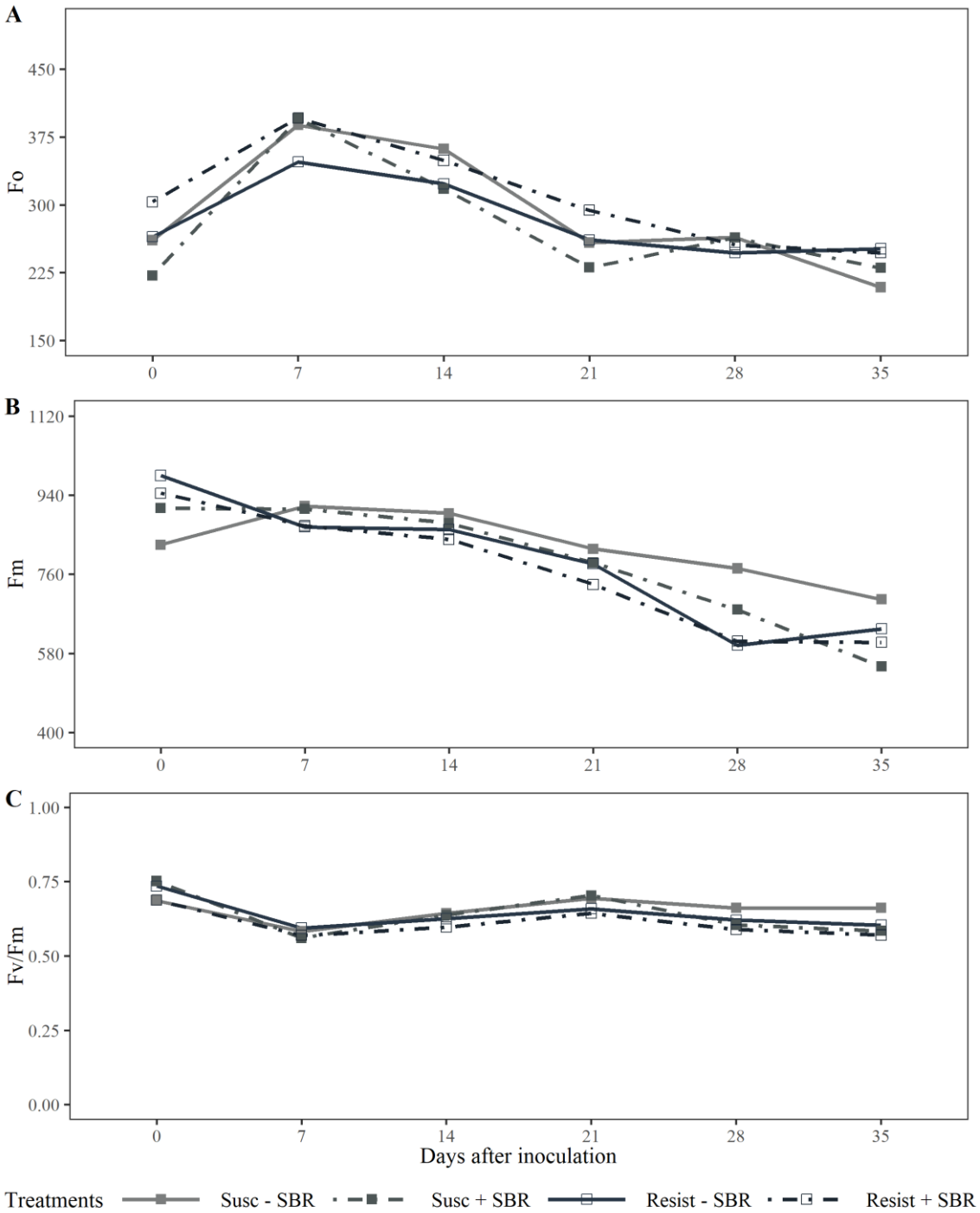

*Susc – SBR: susceptible soybean cultivar (DS6217) non-inoculated with fungicide application; Susc + SBR: susceptible soybean cultivar (DS6217) inoculated without fungicide application; Resist – SBR: partially resistant cultivar (TMG7063) non-inoculated with fungicide application; Resist + SBR: partially resistant cultivar (TMG7063) inoculated without fungicide application.
A: initial fluorescence (Fo); B: maximum fluorescence (Fm); C: maximum quantum yield of PSII (Fv'/Fm').

1.3.2.3 Leaf gas exchange

In the first evaluation of the first repetition, even under low disease severity, higher stomatal conductance, carbon assimilation and efficiency in carbon assimilation ($p<0.05$) were observed in healthy treatments compared to the SBR-infected (Table 6). In the second evaluation, with greater disease severity, there was also a difference between the treatments, with a higher transpiration rate (E) in healthy plants and lower stomatal conductance in SBR-infected plants (Table 7). On the other hand, in this evaluation, a significant difference was also observed between the factors for the assimilation rate and carboxylation efficiency variables, in which both variables were significantly higher in healthy plants (Table 8).

Table 6. Effect of *P. pachyrhizi* on transpiration rate (E), stomatal conductance (g_s), carbon assimilation rate (A), and instantaneous carboxylation efficiency (A/C_i) of susceptible and partially resistant cultivars in the first evaluation of the first repetition.

Treatment	E**	g_s	A	A/C_i
	mmol m^{-2} s^{-1}	mol H_2O m^{-2} s^{-1}	µmol CO_2 m^{-2} s^{-1}	µmol m^{-2} s^{-1} ppm^{-1}
Healthy	4.42 a	0.684 a	30.24 a	0.13 a
SBR	4.15 a	0.569 b	26.46 b	0.11 b
F	2.58^{NS}	5.03^{*}	7.65^{*}	9.02^{NS}
CV (%)	8.82	18.26	28.35	11.81

*Healthy: non-inoculated with fungicide application; SBR: inoculated without fungicide application. ^{NS}: Not significant; *significant a $p \leq 0,05$ by F test. Means followed by the same letter did not differ according to Tukey test at 5% probability ($p<0,05$). **A: carbon assimilation rate; g_s: stomatal conductance; E: transpiration rate; A/C_i: instantaneous carboxylation efficiency.

Table 7. Effect of *P. pachyrhizi* on transpiration rate (E) and stomatal conductance (g_s), of susceptible and partially resistant cultivars in the second evaluation of the first repetition.

Treatment	E	g_s
	mmol m^{-2} s^{-1}	mol H_2O m^{-2} s^{-1}
Healthy	4.03 a	0.33 b
SBR	3.21 b	0.46 a
F	18.22***	9.64***
CV (%)	11.93	22.85

*Healthy: non-inoculated with fungicide application; SBR: inoculated without fungicide application. ^{NS}: Not significant; *significant a $p \leq 0.05$ by F test. Means followed by the same letter did not differ according to Tukey test at 5% probability ($p<0.05$). ** E: transpiration rate; g_s: stomatal conductance.

Table 8. Effect of *P. pachyrhizi* on carbon assimilation rate (A) and instantaneous carboxylation efficiency (A/C_i) of susceptible and partially resistant cultivars in the second evaluation of the first repetition.

Cultivar	A		A/Ci	
	µmol CO_2 m^{-2} s^{-1}		µmol m^{-2} s^{-1} ppm^{-1}	
	Healthy	**SBR**	**Healthy**	**SBR**
Susceptible	23.2 aA	21.6 aA	0.092 aA	0.087 aA
Partially resistant	16.7 bB	23.2 aA	0.071 bB	0.098 aA
Cause of variation	**F**	**P**	**F**	**P**
Disease (D)	2.288	0.156 ^{NS}	2.935	0.112 ^{NS}
Cultivar (C)	2.728	0.124 ^{NS}	0.650	0.436 ^{NS}
D x C	7.583	0.017*	6.523	0.025*

*Healthy: non-inoculated with fungicide application; SBR: inoculated without fungicide application. ^{NS}: Not significant; *significant a $p \leq 0.05$ by F test. Means followed by the same letter did not differ according to Tukey test at 5% probability ($p<0.05$). Uppercase letters compare between means of disease level at each cultivar level (columns). Lowercase letters compare between means of cultivars at each disease level (lines). **A: carbon assimilation rate; A/C_i: instantaneous carboxylation efficiency.

In the first evaluation of the second replicate, no significant differences were found. However, in the second evaluation, the results followed the same trend of the first experiment replicate, with significantly lower values of assimilation rate and carboxylation efficiency (Table 9). Stomatal conductance and transpiration rate were higher for the partially resistant cultivar, possibly due to inherent characteristics of the cultivar (Table 10). In addition, there was an effect of the disease only for the partially resistant cultivar, with higher values found in healthier plants.

Table 9. Effect of *P. pachyrhizi* on carbon assimilation rate (A) and instantaneous carboxylation efficiency (A/C_i) of susceptible and partially resistant cultivars in the second evaluation of the second repetition.

Treatment	A	A/Ci
	µmol CO_2 m^{-2} s^{-1}	µmol m^{-2} $s^{-1}ppm^{-1}$
Healthy	8.695 a	0.026 a
SBR	5.004 b	0.014 b
F	12.137***	11.491***
CV (%)	34.58	37.76

*Healthy: non-inoculated with fungicide application; SBR: inoculated without fungicide application. ***significativo a $p \leq 0.01$ pelo teste F. Médias seguidas pela mesma letra em cada comparação não diferiram pelo teste de Tukey 5% de probabilidade ($p < 0.05$). **A: taxa de assimilação de carbono; A/C_i: eficiência instantânea da carboxilação.

Table 10. Effect of *P. pachyrhizi* on transpiration rate (E) and stomatal conductance (g_s), of susceptible and partially resistant cultivars in the second evaluation of the second repetition.

Treatment	E		g_s	
	mmol m^{-2} s^{-1}		mol H_2O m^{-2} s^{-1}	
	Healthy	**SBR**	**Healthy**	**SBR**
Susceptible	2.52 bA	2.66 aA	0.277 aA	0.319 aA
Partially resistant	3.98 aA	2.10 bB	0.415 bA	0.214 bB
Cause of variation	**F**	**P**	**F**	**P**
Disease (D)	7.446	0.018^{NS}	7.184	0.020^{NS}
Cultivar (C)	0.152	0.704^{NS}	0.309	0.588^{NS}
D x C	14.016	0.003*	16.781	0.001*

*Healthy: non-inoculated with fungicide application; SBR: inoculated without fungicide application. ^{NS}: Not significant; *significant a $p \leq 0,05$ by F test. Means followed by the same letter did not differ according to Tukey test at 5% probability ($p<0,05$). Uppercase letters compare between means of disease level at each cultivar level (columns). Lowercase letters compare between means of cultivars at each disease level (lines). ** E: transpiration rate; g_s: stomatal conductance.

1.3.2.4 Disease severity evaluation by remote sensing

No statistical difference was found in any evaluation dates. However, promising results were observed by using VIs as an indication of plant health and disease progress, with the best visual results observed for VIs correlated to pigments and morphological structures of the plant (Figure 13) when compared to VIs related to the vegetation index, leaf area and biomass (Figure 14). In general, most of the VIs presented a common pattern with an increasing or decreasing values towards the last evaluations, such as the results observed for C420, mRESR, SG, VOG1, ANTH2, DVI, mRENDVI, RVI, SR, and RENDVI. Some of the VIs excerpt in highlighting differences between the treatments, especially SIPI, PSRI, GRVI, EVI and NDVI indexes. At times of greater severity (35 – 42 DAI), more visible differences were seen between the treatments according to the disease severity.

Figure 11. Vegetation indices (VIs) calculated based on morphological factors and leaf pigments, according to the spectral curves of susceptible and partially resistant cultivars to soybean rust under the presence and absence of the disease infection throughout the experimental evaluation period.

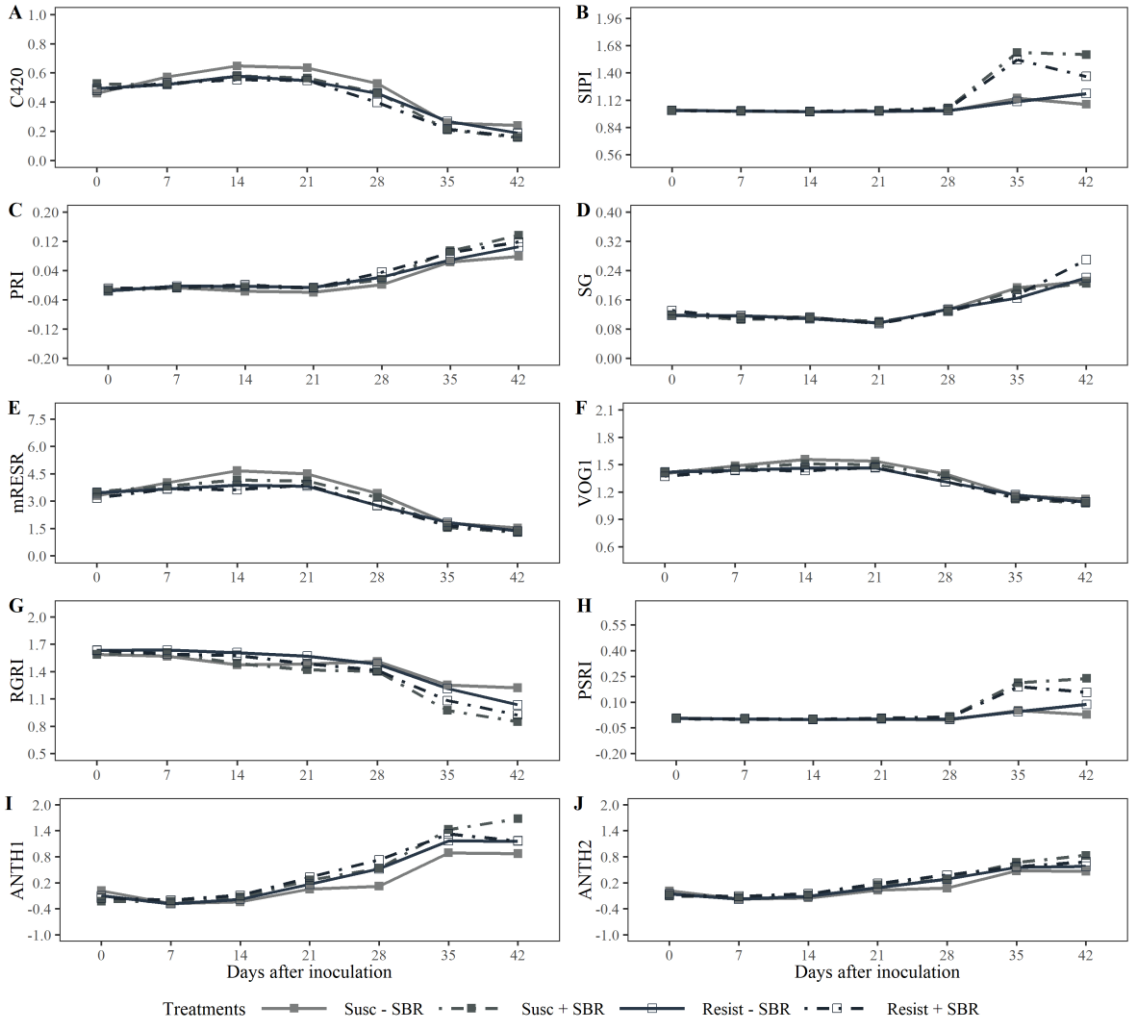

*Susc – SBR: susceptible soybean cultivar (DS6217) non-inoculated with fungicide application; Susc + SBR: susceptible soybean cultivar (DS6217) inoculated without fungicide application; Resist – SBR: partially resistant cultivar (TMG7063) non-inoculated with fungicide application; Resist + SBR: partially resistant cultivar (TMG7063) inoculated without fungicide application.

**VIs calculated based on Table A1.

Figure 12. Vegetation indices (VIs) calculated based on biomass and plant structure, according to the spectral curves of susceptible and partially resistant cultivars to soybean rust under the presence and absence of the disease infection throughout the experimental evaluation period.

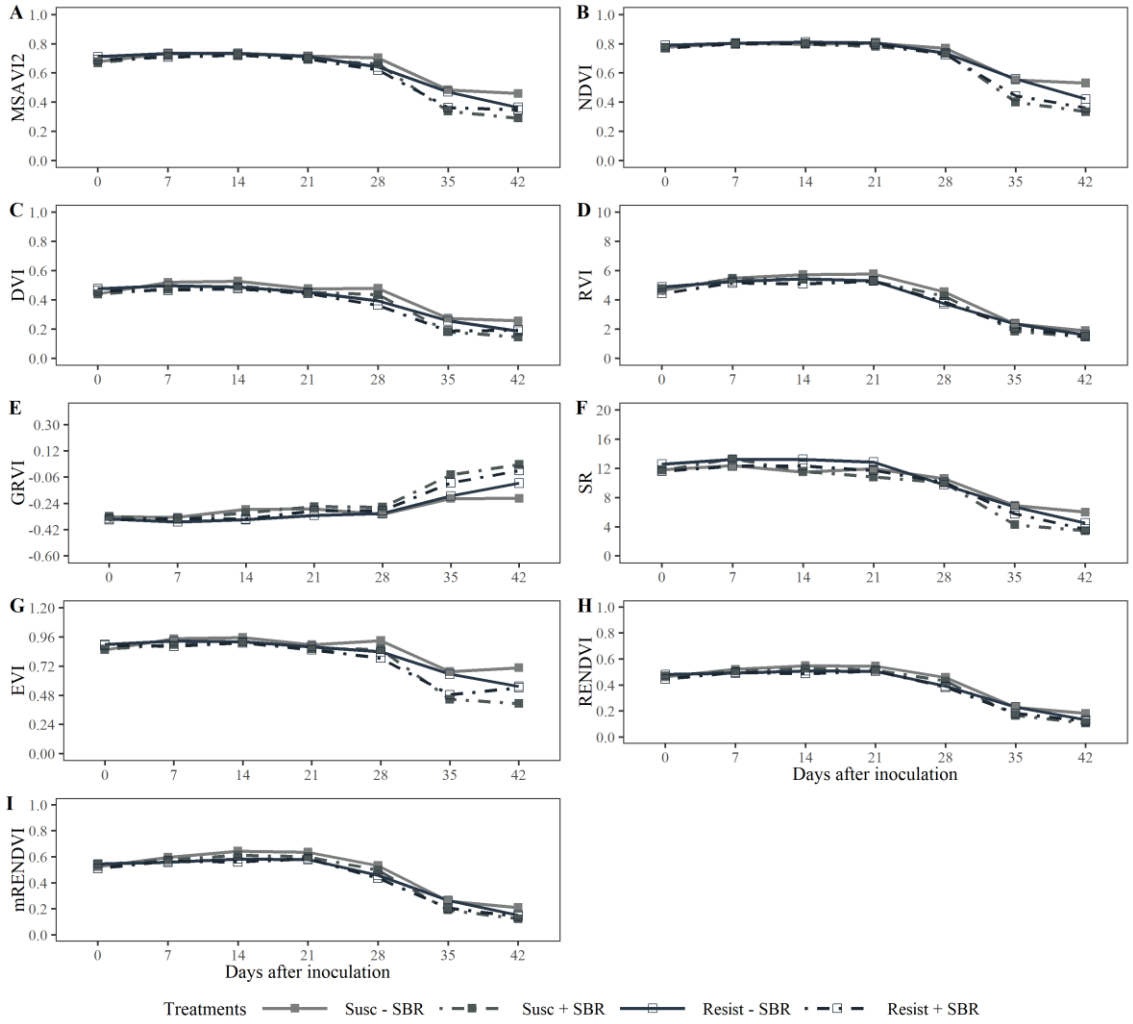

*Susc – SBR: susceptible soybean cultivar (DS6217) non-inoculated with fungicide application; Susc + SBR: susceptible soybean cultivar (DS6217) inoculated without fungicide application; Resist – SBR: partially resistant cultivar (TMG7063) non-inoculated with fungicide application; Resist + SBR: partially resistant cultivar (TMG7063) inoculated without fungicide application.

**VIs calculated based on Table A1.

1.4 DISCUSSION

In both field and laboratory trials, there was a distinct response of soybean susceptible and partially resistant cultivars according to the disease progress and symptom severity, reflecting it in the crop yield. These results were even clearer in the controlled-environment situation, where the comparison between truly healthy and SBR-infected treatments was possible. However, in general, SBR impact on soybean plants' photosynthesis capacity was inconclusive in terms of chlorophyll fluorescence and gas exchange impairments. In general, the photosynthesis parameters evaluated on both cultivars were similarly impacted by the disease.

Despite not promoting total control effectiveness in the field trials, fungicide applications promoted a lower disease severity, whereas the partially resistant cultivar also achieved a significantly reduced severity. This was not well evident in Field 2, in which the lower intensity of the disease did not promote great differences in disease severity between the treatments and cultivars. The controlled-environment condition allowed the elucidation of the biggest differences between the cultivars, mostly due to the possibility to maintain treatments without SBR infection. In this situation, disease severity was reduced by half in the partially resistant cultivar, while in field conditions AUDPC differences between cultivars were only observed at higher severity evaluations. Moreover, the same trend was found for crop yield in the field and laboratory trials, in which there was greater maintenance of crop yield in situations without the presence of the disease or with fungicide protection. On the other hand, SBR did not impact crop yield to the extend of finding differences between the cultivars, which were similarly impacted by the disease.

Soybean rust symptoms were already found at 7 DAI in both cultivars of Field 1 and in the controlled-environment trials. Since this was the first evaluation timing, the first symptoms were possibly apparent even before this period. Vittal et al. (2014) reported hyphae growth, infection, and haustoria development only 1 DAI even in partially resistant cultivars. However, the pathogen colonization in resistant cultivars was reduced by apoptosis, while in susceptible genotypes it was found expressive fungal colonization. Moreover, Vittal et al. (2014) reported a varying number of lesions cm^{-2} according to the genotype and disease reaction (TAN, RB or immune), but not outstanding differences were observed like the differences in severity found here. Furthermore, one of the greatest differences reported by Vittal et al. (2014)

were found as function of sporulating uredinia and the number of days until first symptoms, in which susceptible genotype outstood immune and partially resistant genotypes. Yamanaka et al. (2010), reported up to twice the number of lesions in susceptible cultivars compared to genotypes with varied levels of partial resistance. However, the comparison of SBR severity between genotypes in other research studies is difficult to be conducted since each genotype possesses different resistance levels according to resistant genes. Therefore, only considering the disease reaction, whether it is RB or TAN, might not be sufficient to conduct a proper comparison in this matter.

Despite the distinct effect of SBR on the susceptible and partially resistant cultivar, even on crop yield, some unclear results were found regarding the chlorophyll fluorescence parameters assessed. However, in general, a common trend was found especially for the comparison between healthy or fungicide-protected soybean plants and SBR-infected or without fungicide application, which most parameters were greater impacted by the greater SBR damage. Greater differences were found only in the last evaluations, a situation in which greater disease severity was present. Perhaps these results could be cleared out when conducted under an even higher disease severity.

Considering the laboratory trial with more data consistency and similar patterns, greater impact due to disease severity was observed in F, F_{ms}, and ETR, in which a clear division was seen between infected and non-infected plants. Among these, ETR is one of the most common parameters studied to identify plant stress by biotic factors (Berger et al. 2007; Scholes and Rolfe 2009). These studies show a high correlation between damage to the photosynthesis apparatus along with lower ETR values in infected plants. Besides, ETR has also been used to even identify different pathogen-host interactions in terms of lesion reaction types, which could be a great alternative to identifying differences between TAN and RB lesions in our study (Swarbrick et al. 2006; Scholes and Rolfe 2009).

One exception to the results observed was the proportion of absorbed light used in the PSII (Y). In the majority of the evaluations, no difference was found for cultivars or disease severity levels. Especially in the controlled-environment condition, Y was held steady across all evaluation dates in all the treatments. Oppositely, Rios et al (2017) observed an almost 31% increase in Y values of fungicide-protected plants compared to the control without application and with

higher SBR infection. It is possible that the level of damage caused by the disease was not enough to cause greater Y deficits.

Similarly, no remarkable differences were found for F_v'/F_m' in both field trials, although greater values were found in healthy plants in the laboratory assay. Usually, a value around 0.83 is expected in healthy plants, with lower values commonly observed in stressed or damaged plants (Demmig and Björkman 1987). In this study, healthier plants obtained F_v'/F_m' values around 0.75, while damaged plants ranged around 0.58. These results are similar to those found by Rios et al. (2017), where SBR-infected plants presented F_v'/F_m' around 0.5, meanwhile almost 0.75 were observed in the fungicide-protected plants. In field conditions, although greater SBR infection was observed in certain treatments, differences in chlorophyll fluorescence might not be as apparent due to other environmental conditions. Besides, the level of infection and severity also play a major role in F_v'/F_m' parameters, as reported by Tatagiba et al. (2015). According to the authors, F_v'/F_m' might not represent the best indicator of disease infection, especially in the beginning of the symptoms with lower severity. In the study of Tatagiba et al. (2015), understanding the impact of *Monographella albescens* in rice leaves, this fluorescence parameter did not follow the pattern of severity increase and disease incidence.

Furthermore, there were only a few differences in chlorophyll fluorescence between levels of SBR resistance of the genotypes assessed under SBR infection. It was expected that SBR resistance, even though partial, would ensure greater resistance to photosynthetic apparatus damage and, therefore, obtain greater fluorescence levels. However, only mild visual differences were found for most of the parameters assessed, in which the susceptible cultivar under SBR infection differed from the others, without significance. This outcome might be explained based on a few possibilities. One is due to the natural greater performance of the susceptible cultivar, observed when none of them were infected with SBR and almost all parameters assessed were higher for the susceptible cultivar compared to the partially resistant. So, even under the pathogen action, the difference between them was smaller, compensated by the cultivar performance. Moreover, Smedegaard-Peterson and Tolstrup (1985) also found a “cost effect” on the photosynthesis of resistant cultivars due to the pathogen infection. According to the authors, there is a cost of energy associated with the resistant reaction, which a high cost on ATP and

photosynthesis might be present to replenish expenses with programmed cell death and hypersensitive response.

Leaf gas exchange rates were also similar to those effects on chlorophyll fluorescence. Studies have reported a high correlation between these two sets of parameters, especially in correlation to different disease severity levels (Kumudini et al. 2008b; Baker et al. 2008; Scholes and Rolfe 2009). One of the comparisons is between ETR and CO_2 assimilation rate (A), reported as an important parameter for the identification of pathogen-host interactions due to the similar linear relationship between them (Scholes and Rolfe 2009). In our study, a significant effect was seen for CO_2 assimilation rate in the controlled-environment conditions, with lower rates due to SBR infection regardless of the cultivar, matching the results from ETR evaluation. Overall, transpiration rate, stomatal conductance, CO_2 assimilation, and instantaneous carboxylation efficiency (A/Ci) were all impacted by SBR infection, especially at higher severity (second evaluation), while only few differences were found in the comparison between susceptible and partially resistant cultivars. Once more, the cost of resistance and the presence of symptoms and cell death might be also related to this outcome, such as those found in chlorophyll fluorescence (Smedegaard-Peterson and Tolstrup, 1985).

Lower chlorophyll fluorescence values might represent in this scenario damage to the photosynthetic apparatus and, therefore, lower photosynthesis capacity (Berger et al. 2007). It was also demonstrated by CO_2 and gas exchange parameters' impact. Besides using host's carbohydrate, the disease infection usually causes necrotic or chlorotic areas that impacts the production of photosynthetic assimilates (Berger et al. 2007). It potentially means a deficit in photosynthesis efficiency, which is readily assessed through chlorophyll fluorescence and efficiency to convert energy in the PSII. In consequence, lower photosynthesis will lead to lower carbohydrate production and a change in the host's sink metabolism (Berger et al., 2004; Bonfig et al. 2006).

Kumudini et al. (2008b) also reported a significant impact of SBR on soybean physiology. Besides decreasing crop yield, the authors reported an effect on radiation interception and reduced radiation efficiency, which was associated with reduced photosynthesis capacity due to the reduction of healthy green leaves. Furthermore, the carbon exchange rate was also impacted by SBR infection with exponential decline according to severity increase. In both compatible and incompatible (partial)

interaction between *P. pachyrhizi* and soybean, the infection process after urediniospores deposition in the leaf happens by appressorial penetration through the epidermis and hyphae growth through intercellular space and epidermal cell, which then evolves to haustoria formation and uredia formation in the epidermis (Vittal et al. 2014). Thereby, besides cell damage and infection process, green leaf area are reduced by the uredinia, affecting its photosynthesis capacity.

Besides chlorophyll fluorescence and photosynthesis activity, the usage of VIs as a path to identify plant-pathogen interactions was also seen as a great tool. Although most of the VIs tested presented the same pattern, which is possibly related to the plant senescence towards the end of the evaluations (Gitelson and Merzlyak 1994), some of the VIs were able to better distinguish between treatments. From this list, SIPI, PSRI, and RGRI which correlate to pigment and morphological structure of the plants, as well as GRVI, EVI, and NDVI, which correlate to the structural characteristics and biomass, were those that stood out. In all of these VIs, at the last evaluation, there is a clear division especially between SBR-infected and healthy plants, regardless of the cultivar.

As discussed, the main purpose of VIs is to estimate morphological and physiological features of the plants, such as healthy biomass, leaf density, pigments, and chlorophyll content (Meena et al. 2020), using this data to compare plants under different situations (healthy and infected) and inferring the plant health (Xue and Su 2017). Hyperspectral data, such as those collected here, can supply a quite amount of information that is sometimes not even visible (Behmann et al. 2014). Therefore, VIs represent a simpler way to extract valuable information from all spectral datasets that, as seen, can also be used to complement and understand plant behavior in the plant-pathogen interaction. Nonetheless, we encourage new research studies to be conducted unveiling the interaction of this VIs tested with other diseases or biotic stresses, such as plant nutrition. This will add great value to distinguish some of these effects and aid to get a clearer sight of the results achieved here.

Therefore, the hypothesis that partial resistance to SBR promotes lower impact of the disease in terms of severity and yield was partially confirmed, since it demonstrated distinct effects over the genotypes tested, especially regarding SBR severity and crop yield. Nonetheless, the impact on physiological parameters such as chlorophyll fluorescence and leaf gas exchange was not fulfilled. The results presented here show a significantly different effect of SBR infection on soybean

plants, with most parameters differing between healthy and SBR-infected plants, but it was not as clear in the comparison between partially resistant and susceptible cultivars. Despite the heterogeneity found in the field trials, SBR seems to have affected soybean photosynthesis capacity in different ways in both cultivars, reducing both cultivars' capacity to some extent. More studies are encouraged to be conducted focusing on the evaluation under even higher SBR severities, which should clarify the differences between the treatments. Moreover, as seen in the field trials, even under fungicide protection, a considerable severity was found in the treatments, which reinforces the need for new tools to be implemented in the IDM. In this scenario, the full comprehension of the efficacy and applicability of resistant cultivars might be a key factor to improve SBR management.

In conclusion, partially resistant cultivars promoted less SBR severity but were similarly affected by the disease in terms of chlorophyll fluorescence and leaf gas exchange. In addition, the use of spectral values in the assessment of plant health may be of great value as a quick and reliable source of information but still requires more studies to obtain a more robust database.

1.5 REFERENCES

Azevedo, L. A. S. D., Juliatti, F. C., & Barreto, M. (2007). Resistência de genótipos de soja à *Phakopsora pachyrhizi*. *Summa Phytopathologica*, *33*(3), 252-257.

Baker, N. R. (2008). Chlorophyll fluorescence: a probe of photosynthesis in vivo. *Annual Review of Plant Biology*, *59*, 89-113.

Bajwa, S. G., Rupe, J. C., & Mason, J. (2017). Soybean disease monitoring with leaf reflectance. Remote Sensing, 9(2), 127.

Behmann, J., Steinrücken, J., & Plümer, L. (2014). Detection of early plant stress responses in hyperspectral images. *ISPRS Journal of Photogrammetry and Remote Sensing*, 93, 98-111.

Berger, S., Papadopoulos, M., Schreiber, U., Kaiser, W., & Roitsch, T. (2004). Complex regulation of gene expression, photosynthesis and sugar levels by pathogen infection in tomato. *Physiologia Plantarum*, *122*(4), 419-428.

Berger, S., Sinha, A. K., & Roitsch, T. (2007). Plant physiology meets phytopathology: plant primary metabolism and plant–pathogen interactions. *Journal of experimental botany*, *58*(15-16), 4019-4026.

Bohnenkamp, D., Behmann, J., & Mahlein, A. K. (2019). In-field detection of yellow rust in wheat on the ground canopy and UAV scale. *Remote Sensing*, 11(21), 2495.

Bonfig, K. B., Schreiber, U., Gabler, A., Roitsch, T., & Berger, S. (2006). Infection with virulent and avirulent *P. syringae* strains differentially affects photosynthesis and sink metabolism in *Arabidopsis* leaves. *Planta*, *225*(1), 1-12.

Brasil (2009). Ministério da Agricultura, Pecuária e Abastecimento. *Regras para Análise de Sementes*. Ministério da Agricultura, Pecuária e Abastecimento. Secretaria de Defesa Agropecuária. Brasília, DF: Mapa/ACS, 395p.

Brevant Sementes (2020). Cultivares de soja: DS6217IPRO. https://www.brevant.com.br/produtos/soja/ds6217ipro.html.

Bromfield, K. R. (1984). *Soybean Rust,* Monograph Nº. 11. American Phytopathological Society, St. Paul, MN.

Campbell, C. L., & Madden, L. V. (1990). *Introduction to plant disease epidemiology*. John Wiley & Sons.

Cattelan, A. J., & Dall'Agnol, A. (2018). The rapid soybean growth in Brazil. *Oilseeds and fats, Crops and Lipids*, 25 (1), 1-12.

Childs, S. P., Buck, J. W., & Li, Z. (2018). Breeding soybeans with resistance to soybean rust (*Phakopsora pachyrhizi*). *Plant Breeding*, 137(3), 250-261.

Cui, D., Zhang, Q., Li, M., Zhao, Y., & Hartman, G. L. (2009). Detection of soybean rust using a multispectral image sensor. *Sensing and Instrumentation for Food Quality and Safety*, 3(1), 49-56.

Demmig, B., & Björkman, O. (1987). Comparison of the effect of excessive light on chlorophyll fluorescence (77K) and photon yield of O_2 evolution in leaves of higher plants. *Planta*, *171*(2), 171-184.

Gamon, J. A., & Surfus, J. S. (1999). Assessing leaf pigment content and activity with a reflectometer. The New Phytologist, 143(1), 105-117.

Gamon, J., Serrano, L., & Surfus, J. S. (1997). The photochemical reflectance index: an optical indicator of photosynthetic radiation use efficiency across species, functional types, and nutrient levels. Oecologia, 112(4), 492-501.

Gitelson, A.A., & Merzlyak, M.N. (1994). Spectral reflectance changes associated with autumn senescence of *Aesculus hippocastanum* L. and *Acer platanoides* L. leaves. Spectral features and relation to chlorophyll estimation. *Journal of Plant Physiology*. 143, 286–292.

Gitelson, A. A., Merzlyak, M. N., & Chivkunova, O. B. (2001). Optical properties and nondestructive estimation of anthocyanin content in plant leaves¶. Photochemistry and photobiology, 74(1), 38-45.

Godoy, C. V., Koga, L. J., & Canteri, M. G. (2006). Diagrammatic scale for assessment of soybean rust severity. *Fitopatologia Brasileira*, 31, 63-68.

Godoy, C. V., Seixas, C. D. S., Soares, R. M., Marcelino-Guimarães, F. C., Meyer, M. C., & Costamilan, L. M. (2016). Asian soybean rust in Brazil: past, present, and future. *Pesquisa Agropecuária Brasileira*, *51*, 407-421.

Huete, A. R., Liu, H. Q., Batchily, K. V., & Van Leeuwen, W. J. D. A. (1997). A comparison of vegetation indices over a global set of TM images for EOS-MODIS. Remote sensing of environment, 59(3), 440-451.

Juliatti, B. C. M., Pozza, E. A., & Juliatti, F. C. Severity of rust infection in soybean genotypes with partial resistance as a function of temperature and leaf wetness duration. *Genetics and Molecular Research*, 20 (2), 1-19.

Juliatti, F. C., Azevedo, L. A. S., & Cristina, J. (2017). *Strategies of chemical protection for controlling soybean rust*. In M. Kasai (Ed.), Soybean (pp. 35–62). London: Intech Open.

Kumudini, S., Godoy, C. V., Board, J. E., Omielan, J., & Tollenaar, M. (2008a). Mechanisms involved in soybean rust-induced yield reduction. Crop Science, 48(6), 2334-2342.

Kumudini, S., Prior, E., Omielan, J., & Tollenaar, M. (2008b). Impact of *Phakopsora pachyrhizi* infection on soybean leaf photosynthesis and radiation absorption. *Crop science*, *48*(6), 2343-2350.

Lana, D. F., Paul, P. A., Godoy, C. V., Utiamada, C. M., da Silva, L. H. C., Siqueri, F. V., et al. (2018). Meta-analytic modeling of the decline in performance of fungicides for managing soybean rust after a decade of use in Brazil. *Plant Disease*, 102(4), 807–817.

Langenbach, C., Campe, R., Beyer, S. F., Mueller, A. N., & Conrath, U. (2016). Fighting Asian soybean rust. *Frontiers in Plant Science*, *7*, 797.

Meena, S. V., Dhaka, V. S., & Sinwar, D. (2020, November). Exploring the Role of Vegetation Indices in Plant Diseases Identification. In *2020 Sixth International Conference on Parallel, Distributed and Grid Computing (PDGC)* (pp. 372-377). IEEE.

Merzlyak, M. N., Gitelson, A. A., Chivkunova, O. B., & Rakitin, V. Y. (1999). Non-destructive optical detection of pigment changes during leaf senescence and fruit ripening. Physiologia plantarum, 106(1), 135-141.

Pearson, R. L., & Miller, L. D. (1972). Remote mapping of standing crop biomass for estimation of the productivity of the shortgrass prairie. Remote sensing of environment, VIII, 1355.

Penuelas, J., Baret, F., & Filella, I. (1995). Semi-empirical indices to assess carotenoids/chlorophyll a ratio from leaf spectral reflectance. Photosynthetica, 31(2), 221-230.

Qi, J., Chehbouni, A., Huete, A. R., Kerr, Y. H., & Sorooshian, S. (1994). A modified soil adjusted vegetation index. Remote sensing of environment, 48(2), 119-126.

Miles, M. R., Bonde, M. R., Nester, S. E., Berner, D. K., Frederick, R. D., & Hartman, G. L. (2011). Characterizing resistance to *Phakopsora pachyrhizi* in soybean. *Plant Disease*, *95*(5), 577-581.

R CORE TEAM (2019). R: A language and environment for statistical computing. R Foundation for Statistical Computing, Vienna, Austria.

Richardson, A. J., & Wiegand, C. L. (1977). Distinguishing vegetation from soil background information. Photogrammetric engineering and remote sensing, 43(12), 1541-1552.

Rios, V. S., Rios, J. A., Aucique-Pérez, C. E., Silveira, P. R., Barros, A. V., & Rodrigues, F. Á. (2018). Leaf gas exchange and chlorophyll a fluorescence in soybean leaves infected by *Phakopsora pachyrhizi*. *Journal of Phytopathology*, *166*(2), 75-85.

Rouse, J. W., Haas, R. H., Schell, J. A., Deering, D. W., & Harlan, J. C. (1974). Monitoring the vernal advancement and retrogradation (green wave effect) of natural vegetation. NASA/GSFC Type III Final Report, Greenbelt, Md, 371.

Savitzky, A., & Golay, M. J. (1964). Smoothing and differentiation of data by simplified least squares procedures. *Analytical chemistry*, 36(8), 1627-1639.

Scholes, J. D., & Rolfe, S. A. (2009). Chlorophyll fluorescence imaging as tool for understanding the impact of fungal diseases on plant performance: a phenomics perspective. *Functional Plant Biology*, *36*(11), 880-892.
Smedegaard-Petersen, V., & Tolstrup, K. (1985). The limiting effect of disease resistance on yield. *Annual Review of Phytopathology*, *23*(1), 475-490.

Shiratsuchi, L.S.; Brandão, Z.N.; Vicente, L.N.; Victoria, D.C.; Ducati, J.R.; Oliveira, R.P.; Vilela, M.F (2014). Sensoriamento Remoto: conceitos básicos e aplicações na Agricultura de Precisão. In: Bernardi, A.C.C.; Naime, J.M.; Resende, A.V.; Bassoi, L.H.; Inamasu, R.Y (Eds.), *Agricultura de precisão: Resultados de um novo olhar* (pp. 58-73). Embrapa.

Sims, D. A., & Gamon, J. A. (2002). Relationships between leaf pigment content and spectral reflectance across a wide range of species, leaf structures and developmental stages. Remote sensing of environment, 81(2-3), 337-354.

Sripada, R. P., Heiniger, R. W., White, J. G., & Meijer, A. D. (2006). Aerial color infrared photography for determining early in-season nitrogen requirements in corn. Agronomy Journal, 98(4), 968-977.

Swarbrick, P. J., Schulze-Lefert, P. A. U. L., & Scholes, J. D. (2006). Metabolic consequences of susceptibility and resistance (race-specific and broad-spectrum) in barley leaves challenged with powdery mildew. *Plant, Cell & Environment*, *29*(6), 1061-1076.

Tatagiba, S. D., DaMatta, F. M., & Rodrigues, F. Á. (2015). Leaf gas exchange and chlorophyll a fluorescence imaging of rice leaves infected with *Monographella albescen*s. *Phytopathology*, *105*(2), 180-188.

Thenkabail, P. S., Smith, R. B., & De Pauw, E. (2000). Hyperspectral vegetation indices and their relationships with agricultural crop characteristics. *Remote sensing of Environment*, *71*(2), 158-182.

Toloi, M. N. V., Bonilla, S. H., Toloi, R. C., Silva, H. R. O., & Nääs, I. D. A. (2021). Development Indicators and Soybean Production in Brazil. *Agriculture*, *11*(11), 1164.

Tropical Melhoramento Genético (TMG) (2020). Cultivares de soja: TMG 7063 IPRO. 2020. http://www.tmg.agr.br/ptbr/cultivar/tmg-7063-ipro

Vittal, R., Paul, C., Hill, C. B., & Hartman, G. L. (2014). Characterization and quantification of fungal colonization of *Phakopsora pachyrhizi* in soybean genotypes. *Phytopathology*, 104, 86-94.

Vogelmann, J. E., Rock, B. N., & Moss, D. M. (1993). Red edge spectral measurements from sugar maple leaves. Remote Sensing, 14(8), 1563-1575.

Xue, J., & Su, B. (2017). Significant remote sensing vegetation indices: A review of developments and applications. *Journal of sensors*, *2017*.

Yamanaka, N., Yamaoka, Y., Kato, M., Lemos, N. G., Passianotto, A. L. D. L., dos Santos, J. V., ... & Suenaga, K. (2010). Development of classification criteria for resistance to soybean rust and differences in virulence among Japanese and Brazilian rust populations. *Tropical Plant Pathology*, *35*(3), 153-162.

Zanatta, T., Reis, E. M., & Zanatta, M. (2012). Adjuvant concentrations and uredospore densities on *Phakopsora pachyrhizi* infection efficiency in soybean. *Summa Phytopathologica*, *38*, 148-151.

1.6 APPENDICES

Table A1. Vegetation indices (VIs) representative to the disease effect on the soybean crop used to assess to correlation of disease severity and spectral signatures.

Vegetation Indices (VI)	Description	Formula	Reference
C420	*C420*	$\frac{R_{420}}{R_{695}}$	Bajwa et al. (2017)
MSAVI2	*Modified Chlorophyll Absorption Ratio Index Improved*	$\frac{1}{2}[\,2(R_{810}+1)-\sqrt{(2R_{810}+1)^2-8(R_{810}-R_{690})}$	Qi et al. (1994)
NDVI	*Normalized Difference Vegetation Index*	$\frac{(R_{810}-R_{690})}{(R_{810}+R_{690})}$	Rouse et al. (1974)
DVI	*Difference vegetation Index*	$R_{755}-R_{698}$	Richardson & Wiegand (1977)
RVI	*Ratio vegetation Index*	$\frac{R_{775}}{R_{698}}$	Pearson & Miller (1972)
GRVI	*Green normalized Difference vegetation index*	$\frac{(R_{690}-R_{560})}{(R_{690}+R_{560})}$	Sripada et al. (2006)
SIPI	*Structure Independent Pigment Index*	$\frac{(R_{800}-R_{445})}{(R_{800}-R_{680})}$	Penuelas et al. (1995)
PRI	*Photochemical reflectance Index*	$\frac{(R_{570}-R_{531})}{(R_{570}+R_{531})}$	Gammon et al. (1997)
SR	*Simple ratio index*	$\frac{R_{800}}{R_{670}}$	Rouse et al. (1974)

Continuation of Table A1. Summary of vegetation indices (VIs)

Vegetation Indices (VI)	Description	Formula	Reference
EVI	*Enhanced vegetation index*	$2{,}5 * \frac{(R_{800} - R_{670})}{(R_{800} + 6 * R_{670} - 7{,}5 * R_{490} + 1)}$	Huete et al. (1997)
SG	*Sum green index*	$\frac{1}{n}\sum_{i=500}^{599} Ri$	Gamon & Surfus (1999)
RENDVI	*Red edge NDVI*	$\frac{(R_{750} - R_{705})}{(R_{750} + R_{705})}$	Gitelson & Merzlyak (1994)
mRENDVI	*Modified red edge NVDI*	$\frac{(R_{750} - R_{705})}{(R_{750} + R_{705} - 2R_{445})}$	Sims & Gamon (2002)
mRESR	*Modified red edge simple ratio index*	$\frac{(R_{750} - R_{445})}{(R_{705} - R_{445})}$	Sims & Gamon (2002)
VOG1	*Vogelmann Red Edge Index 1*	$\frac{R_{740}}{R_{720}}$	Vogelmann et al. (1993)
RGRI	*Red green ratio index*	$\frac{mean(R_{500-600})}{mean(R_{600-700})}$	Gamon & Surfus (1999)
PSRI	*Plant senescence reflectance index*	$\frac{R_{680} - R_{500}}{R_{750}}$	Merzlyak et al. (1999)
ANTH1	*Anthocyanin reflectance index (1)*	$\frac{1}{R_{550}} - \frac{1}{R_{700}}$	Gitelson et al. (2001)
ANTH2	*Anthocyanin reflectance index (2)*	$R_{800}\left[\frac{1}{R_{550}} - \frac{1}{R_{700}}\right]$	Gitelson et al. (2001)

Figure A1. Laboratory trials conduction in controlled-environment conditions under humidity, temperature, and irrigation control.

Figure A2. Visual evaluation of soybean rust symptoms (A) and analysis of chlorophyll fluorescence with pulse-modulated fluorometer in light-adapted (B) and dark-adapted (C) states.

Figure A3. Evaluation of soybean reflectance under biotic stress caused by *P. pachyrhizi* using a spectroradiometer ASD FieldSpec Dual Spectroradiometer (Analytical Spectral Devices, Boulder, CO, USA): equipment calibration (A), reading of soybean leaflets reflectance (A) and documentation of the spectral curve (C).

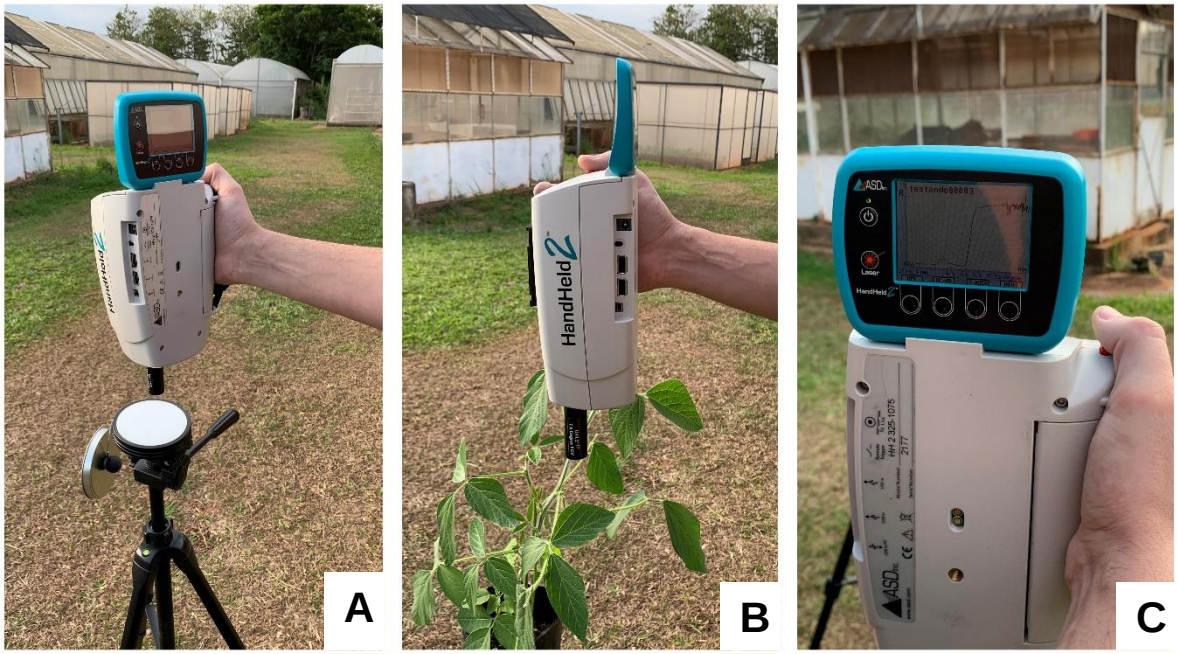

Figure A4. Portable photosynthesis system (IRGA) use to analyze the effect of the disease on the gas exchange and photosynthetic capacity of the crop.

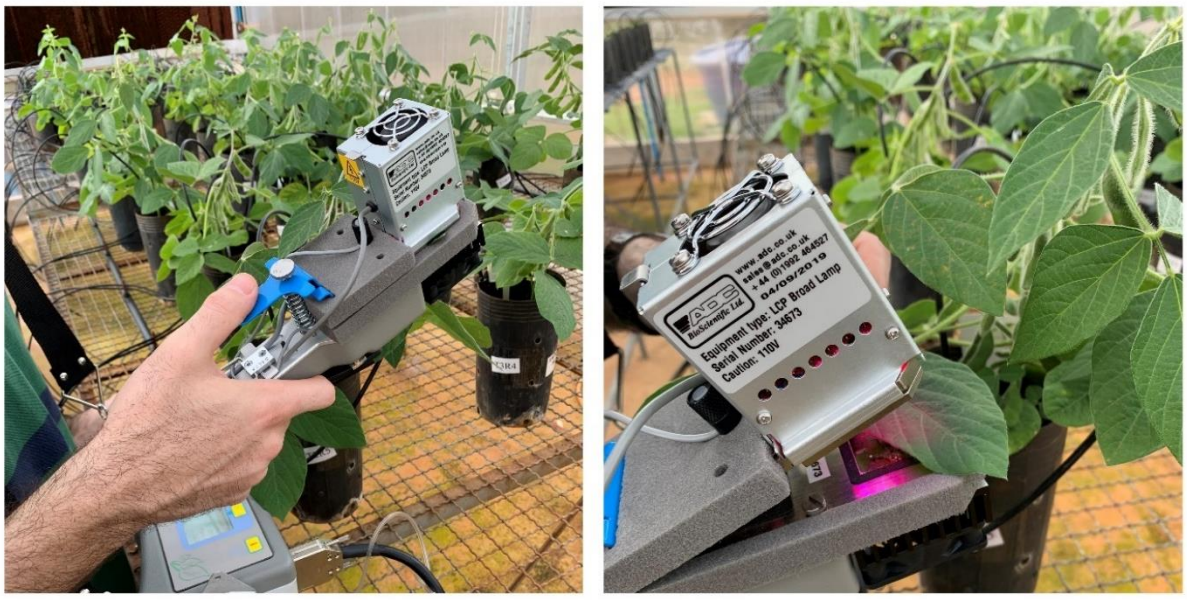

CHAPTER 2

Soybean rust detection and disease severity classification by remote sensing[2]

Detecção da ferrugem da soja e classificação da severidade da doença por sensoriamento remoto

RESUMO

A detecção e monitoramento da ferrugem da soja (FAS) por meio de sensoriamento remoto é promissor devido à importância da cultura e os aspectos da doença. Avaliamos os efeitos de diferentes níveis de severidade de FAS na refletância de folíolos de soja visando a construção de um modelo de classificação de doenças. O efeito do SBR na refletância dos folíolos da soja foi avaliado em duas cultivares (suscetível e parcialmente resistente) em quatro níveis de severidade da doença: sadio, baixo, moderado e alto, quando as plantas se encontravam no estádio reprodutivo R5. Os folíolos foram coletados a campo e levados ao laboratório para a avaliação espectral através do espectrofotômetro UV 2700 (Shimadzu) acoplado ao *Integrating Sphere Attachment* ISR-603, avaliando a refletância de cada amostra na faixa de 270 a 1000 nm em um intervalo de 3,0 nm. A viabilidade do uso de uma coleção de 19 Índices Vegetativos (IVs) e redução da dimensionalidade dos dados por meio de Análise Fatorial Múltipla (MFA) foram avaliadas e um modelo de classificação foi construído por meio de algoritmos estatísticos e de aprendizado de máquina. Dez algoritmos foram avaliados com base em parâmetros de precisão, sensibilidade e acurácia, utilizando 80% do conjunto de dados como dados de treinamento e 20% como conjunto de dados de teste. A faixa visível do espectro e a faixa *Red Edge* foram consideradas as melhores para auxiliar na predição da doença e no modelo de classificação. A MFA teve um desempenho satisfatório na redução da dimensionalidade dos dados e revelou o efeito de comprimentos de onda específicos na classificação de cada classe e na redução da dimensionalidade dos dados. A maioria dos IVs estudados obteve alta correlação entre as classes de severidade. A acurácia e a precisão da classificação da doença foram superiores a

[2]Artigo aceito para publicação na Agronomy Journal (ISSN: 1435-0645) e redigido de acordo com as normas da revista.

70% para todos os modelos estudados. A máquina de vetores de suporte linear com a base de dados dos VIs obteve os melhores resultados. Este estudo oferece um bom caminho para o desenvolvimento de um modelo de detecção a ser integrado aos programas de gestão de SBR.

Palavras-chave: Sensoriamento remoto, doenças de plantas, sistemas de manejo de doenças, soja.

ABSTRACT

The detection and monitoring of soybean rust (SBR) through remote sensing is promising due to the importance of the crop and the aspects of the disease. We evaluated the effects of different levels of SBR severity on soybean leaflets reflectance aiming the construction of a disease classification model. The effect of SBR on soybean leaflet reflectance was evaluated on two cultivars (susceptible and partially resistant) at four disease severity levels: healthy, low, moderate, and high severity levels, when the plants were at R5 reproductive stage. Leaflet samples were collected in the field and taken to the laboratory for the spectral evaluation through the spectrophotometer UV 2700 (Shimadzu) coupled with Integrating Sphere Attachment ISR-603, evaluating the reflectance of each sample in the range of 270 to 1000 nm at an interval of 3.0 nm. The feasibility of using a collection of 19 Vegetation Indices (VIs) and data dimensionality reduction through Multiple Factor Analysis (MFA) were evaluated and a classification model was constructed through statistical and machine learning algorithms. Ten algorithms were assessed based on precision, sensibility, and accuracy parameters, using 80% of the dataset as training data, and 20% as testing dataset. The visible range of spectrum and red edge region were considered the best ones to aid in the prediction of the disease and classification model. MFA performed satisfactorily in the dimensionality data reduction and unveiled the effect of specific wavelengths on the classification of each class and on the data dimensionality reduction. Most of the VIs studied had high correlation performance across the severity classes. Classification accuracy and precision was above 70% for all models. Linear support vector machine with the collection of VIs achieved the best results. This study provides a practical path for developing a detection model to be integrated into SBR management programs.

Keywords: Remote sensing, plant disease, pest management systems, soybean.

2.1 INTRODUCTION

Soybean crop yield is affected by phytosanitary problems globally. Soybean rust (SBR), caused by *Phakopsora pachyrhizi* Sydow & Syd. was responsible for more than US$15 billion losses from 2001 to 2015 (IEAg/ABAG, 2015), and is currently considered the most important disease of the crop. This pathogen can cause up to 80% yield reduction and its control is based on fungicides, of which there are only few options available due to exponential growth of fungus resistant populations (Deising et al. 2008; Kelly et al. 2015; Godoy et al., 2015; Godoy et al., 2021). Therefore, the need for innovative techniques to be integrated into the disease management is evident in order to obtain greater control efficacy and loss reduction.

In this scenario, monitoring is the basis for integrating different tactics into the Integrated Disease Management (IDM), supporting decision-making of control and, therefore, promoting greater sustainability of soybean production (Wylie & Speight, 2012). However, it is considered one of the costliest procedures and the least employed in the field, where farmers choose using pesticides on a scheduled basis as a guarantee of crop production. Besides potential inputs losses, this action can lead to selection of fungi populations resistant to fungicides, greater environmental contamination, and reduced control effectiveness (Godoy et al., 2015). Conventional monitoring was conducted through extensive scouting and visual evaluation in the field, which takes great number of employees and high expertise.

After years of optimizations in techniques and equipment, remote sensing can reduce the cost and time spent on disease monitoring, improving both operational and financial capacity by providing data and information that are not visible or apparent. On this matter, hyperspectral sensors have been one of the most used for plant diseases detection and monitoring of cropping fields through differences in reflectance (Khaled et al., 2018; Kelly & Guo, 2007; Shiratsuchi et al., 2014; Ahmed et al., 2016; Mahlein, 2016).

One of the key features to identify plant stress and, thereby, plant disease incidence, is to analyze the “spectral signature” of the elements (Shiratsuchi et al., 2014; Khaled et al., 2018). Each pathogen can affect the plant structure in a particular way, either by altering its pigmentation, solutes chemical concentration, cell structure, nutrient balance, water absorption, or gas exchange (Hatfield & Pinter, 1993). Soybean rust symptoms are firstly visible on the leaves at the bottom of the plant canopy, with chlorosis and presence of reddish-brown (RB) or tan (TAN)

pustules, depending on the cultivar susceptibility to the disease (Rupe & Sconyers, 2008; Kelly et al., 2015). Partially resistant cultivars produce RB lesions, while susceptible reactions produce TAN lesions. As the disease progresses, symptoms are aggravated with the appearance of more uredia, progressing to intense defoliation and reduced photosynthesis (Kelly et al., 2015). Few studies have observed the application of remote sensing in the identification of stress and diseased plants in soybean crops (Cui et al., 2009; Hikishima et al., 2010; Bajwa et al., 2017).

Remote sensing primarily aids identifying the plant stress suffered from the disease based on the biophysical principles (Martinelli et al., 2015). The faster the monitoring and detection, the greater the chance of success for the IDM. For that, the construction of a prediction or detection model has to go through extensive study to firstly identify the possibility of a disease to be identified remotely. Once knowing the effects of the disease on the plant, it is possible to build a correlation with the spectral values obtained in the monitoring and subsequently construct the so-called classification model.

Techniques have been used to help in the interpretation of the outcomes from hyperspectral sensors, since they gather high quantities of data. The first one is data dimensionality reduction, such as Principal Component Analysis (PCA) and Multiple Factors Analysis (MFA). These techniques aid reducing the quantity of data while preserving relevant information from the original data (Abdi et al., 2013; Feng et al., 2017). Another alternative is through Vegetation Indices (VI) calculations based on reflectance values (Behmann et al., 2014; Al Saddik et al., 2019). Vegetation Indices are divided into indices sensitive to pigment concentration, using the characteristics observed in the visible range, and indices sensitive to the structure of the plant, with the analysis of structural properties through the near infrared spectrum band (Shiratsuchi et al., 2014). Several VIs showed a high correlation on the identification of diseases in soybean crops (Mahlein et al., 2013; Bajwa et al., 2017), although only few specifically for SBR.

For soybean IDM, the timing of fungicide application is very important to improve the spraying technology (Negrisoli et al., 2019) and to avoid an epidemic outbreak in the field. Besides, remote sensing has been applied successfully at different phytopathosystems and has a great potential for SBR management. Only a few studies have been conducted identifying SBR on soybean leaves through remote

sensing techniques and more work need to be conducted. The effect of RB or TAN lesions from different cultivars on the reflectance are also not yet well comprehended. The hypothesis of this study is that relevant differences can be found based on leaf reflectance under different disease severity levels, especially between healthy and low severity levels. These differences may allow an early detection of the disease and, thereby, to build a classification model based on the reflectance data. Therefore, the objective of this study was to construct a detection and classification model for future applications on IDM based on the effects of different levels of soybean rust severity on soybean leaflets reflectance by remote sensing.

2.2 MATERIAL AND METHODS

Soybean cultivation was conducted in two experimental areas (replicates) in Botucatu, São Paulo State, Brazil, with geographic coordinates 22° 48' 48"S; 48° 25' 37"W (Site 1) and 22° 49' 38"S; 48º 25' 40"W (Site 2), during the 2019/2020 crop season. In both experimental sites, no-tillage system was adopted and all sowing operations, crop protection management, fertilization, and evaluations were carried out homogeneously. The soybean crop was sown simultaneously on December 6, 2019, with row spacing of 0.45 m and a population of 299,000 plants ha^{-1} in Site 1 and 288,000 plants ha^{-1} in Site 2.

2.2.1 Experimental design

The field trials were carried out in a randomized block design and the treatments were distributed in a 2 x 2 factorial scheme: 2 soybean cultivars (Brevant DS6217 IPRO, susceptible to SBR; TMG IPRO 7063, partially resistant to SBR) and 2 disease situations (diseased plants without chemical control; healthy plants with chemical control), in five replications. Both cultivars are recommended for the region where the study was conducted and have the same indeterminate growth habit. This design refers only to the installation of field trials to collect samples homogeneously. The experimental units (plots) of each site was composed of six 3 x 5 m soybean rows (width x length), totaling an area of 15 m^2.

Treatments kept with chemical control were carried out using protective and curative fungicides. Starting at the vegetative growth stage V6, three applications of the systemic fungicide trifloxystrobin (150.0 g L^{-1}) + prothioconazole (175.0 g L^{-1}) (Fox®) along with the fungicide multisite mancozeb (750 g kg^{-1}) (Unizeb Gold®) were

carried out fortnightly (at V6, R1 and R3 growth stages). Fox® and Unizeb Gold® were applied at a constant rate of 0.4 L ha^{-1} and 2.5 kg ha^{-1}, respectively, as recommended by the manufacturers. Sprayings were uniformly carried out with a CO_2 pressurized backpack sprayer equipped with a 3-meter boom and six flat fan nozzles XR 11002 (TeeJet). The displacement speed was 5.0 km h^{-1} and the working pressure 200 kPa, providing an application rate of 150 L ha^{-1}.

After V6 vegetative growth stage, 10 leaflets per plot were collected weekly from the bottom of the canopy and taken to the laboratory for better visualization of symptoms and fungal structures under a stereoscopic microscope to monitor the onset and evolution of the disease. Disease severity was estimated by assigning severity levels based on visual observation of the symptoms using a diagrammatic disease scale proposed by Godoy et al. (2006).

2.2.2 Spectral data evaluation

The effect of SBR on the leaflets was evaluated when the crop was at the R5 reproductive growth stage and with the presence of plants with high disease severity. Due to the epidemiology of the disease, it is common to find in the same area (i.e. plots) plants with different levels of disease severity (Kelly et al., 2015). Ten leaflets were collected according to each disease situation (severity levels), from each cultivar (susceptible and partially resistant), and at each experimental site, that is, randomly collected among the plots conducted in the field. According to the methodology proposed by Cui et al. (2009), the severity levels were divided into: i) healthy leaflets (no symptoms); ii) low severity (2% severity); iii) moderate severity (10% severity); iv) high severity (30% severity), being the severity percentage evaluated based on the diagrammatic scale proposed by Godoy et al. (2006) (Figure 1).

The spectral evaluation was conducted through the spectrophotometer UV 2700 (Shimadzu) coupled with integrating spheres (Integrating Sphere Attachment ISR-603), evaluating the reflectance of each sample in the range of 270 to 1000 nm at an interval of 3.0 nm. Integrating spheres-based reflectance analysis were carried out by setting a sample facing the incident light window and focusing the light reflected from the sample in the detector using a coated-barium sulfate sphere known as standard white board that presents 100% reflectance (Figure 2). The value obtained becomes the sample reflectance (relative reflectance) in relation to the

reference standard whiteboard reflectance (Shimadzu, 2020). Specular and diffuse reflected light are measured through models of integrating spheres across different incidence angles. Each sample (leaflet) was evaluated separately, generating the reflectance values of each sample in the previously mentioned spectral range interval.

Figure 1. Soybean rust severity scale (%) classes used for reflectance assessments, based on the scale proposed by Godoy et al. (2006).

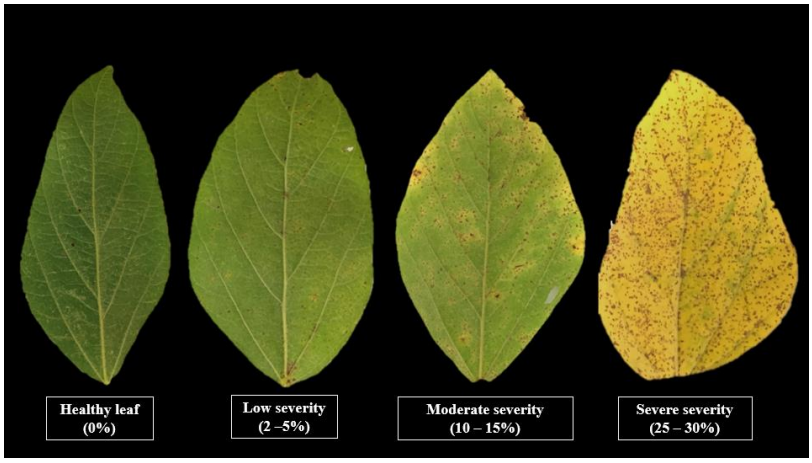

Figure 2. Schematic example of samples placements in the Integrating Sphere Attachment (ISR-603) of the spectrophotometer UV 2700 (Shimadzu) for reflectance evaluations.

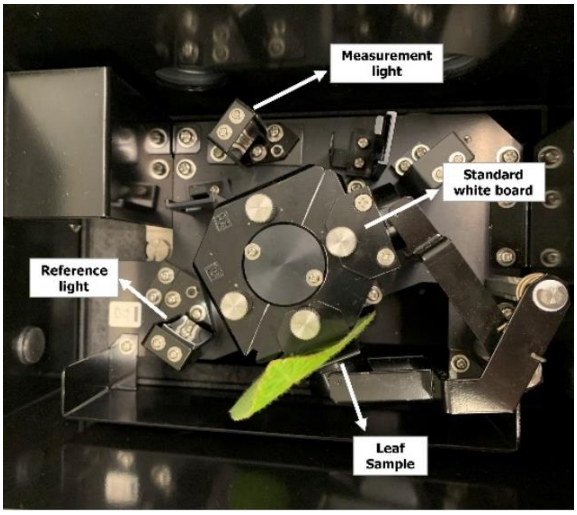

Leaflets were collected and evaluated 95 and 96 days after planting (DAP) for Site 1 and Site 2, respectively. All leaves with petiole were collected and placed in a

falcon tube with water to maintain leaves turgidity. The evaluation was carried out immediately after sampling in the laboratory.

2.2.3 Prediction model building

Data processing and model construction analysis are shown in Figure 3, considering all steps of noise reduction, Savitzky Golay filtering, feature extraction methods based on VI calculations and data dimensionality reduction by MFA, as well as model construction steps for learning and testing to obtain final metrics.

The reflectance data of the four classifications were considered based on four levels of disease severity (Figure 1) as fore mentioned: healthy, low, moderate, and high severity (severe) of two cultivars (susceptible and partially resistant to SBR). Each classification consisted of 10 repetitions of each area, totaling 20 repetitions per classification and a total of 80 units (considered as “individuals” for the models applied below) for the whole study. Therefore, samples from both sites were considered in the model construction.

In order to process the reflectance data, the spectral curve from 270 – 1000 nm was initially reduced to 270 – 900 nm, aiming to reduce high noise levels that normally occur at the extremities (Abdel-Rahman et al., 2014). From this, two distinct analyses were carried out to extract information that were more relevant to the model construction and to optimize the classification performance: i) data dimensionality reduction and ii) VIs calculation.

Prior to applying any information extraction techniques, one more data treatment was necessary to smooth the curves and reduce noise. Savitzky-Golay filter was applied to the spectral curves used in the VIs calculations, using 11 central points and a third-degree polynomial, according to Savitzky and Golay (1964) and Bohnenkamp et al. (2019). To reduce data dimensionality, the first derivative was also calculated in addition to this data smoothing filter.

Figure 3. Methodology development diagram for the construction and testing of disease classification and prediction models based on data from dimensionality reduction and collection of vegetative indices.

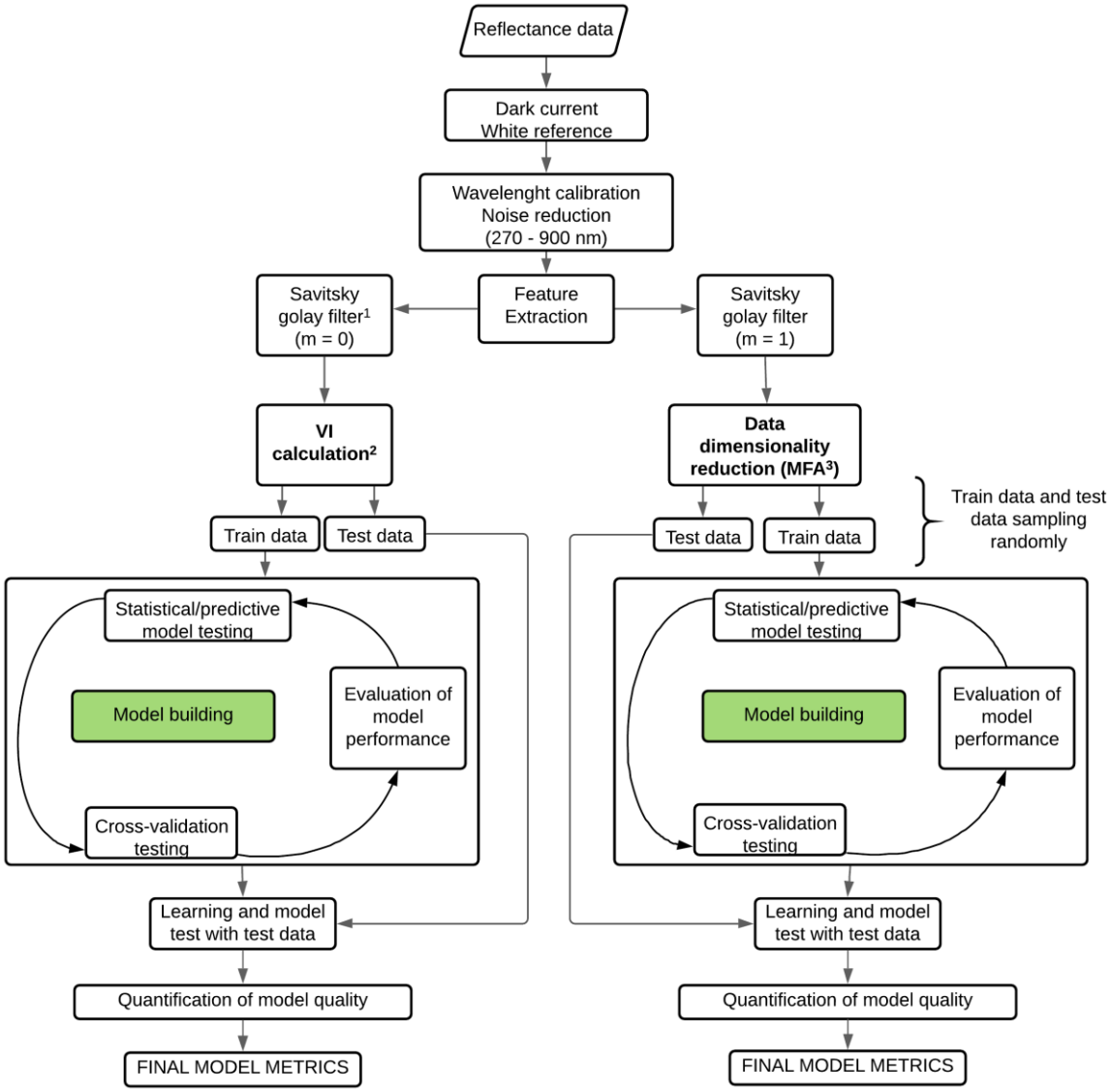

[1]Savitsky-Golay smoothing filter = (*m*=0) and with first derivative (*m*=1);

[2]VI calculation: vegetation indices calculation

[3]MFA: Multiple factor analysis

[*]Diagram created through Lucidchart® plataform

2.2.4 Data dimensionality reduction

Multiple Factor Analysis (MFA) was adopted to reduce data dimensionality. MFA is a multivariate analysis method that consider both quantitative and qualitative variables in the data dimensionality reduction process. It means that, in addition to

the quantitative variables of the spectral bands, it was also possible to take into account the qualitative variable of the two cultivars analyzed (Abdi et al., 2013). Besides, this analysis allows structuring the variables into groups, which were divided into: i) UV: comprising the spectral range of ultraviolet region (UV), between 270 – 400 nm; ii) VIS: comprising the spectral range of the visible region (VIS), between 400 – 700 nm; iii) NIR: comprising the spectral range of the near infrared region (NIR), between 700 – 900 nm. As each spectral band expresses unique information for classification (Behmann et al., 2014), as well as each soybean cultivar can also have different reactions for each disease severity level (Vittal et al., 2013), these distribution into groups and different variables were important to properly reduce data and to help understand the impact of each factor.

Multiple factor analysis considers the contribution of all groups of variables to define the distance between the individuals analyzed. The analysis is based on a combination of PCA (quantitative variables) and Multiple Correspondence Analysis (categorical or qualitative variables). Data are initially normalized, and their variance is decomposed by PCA, generating new orthogonal variables called dimensions or components, which are then ordered by the amount of explanation of the data variance (Abdi et al., 2013). The number of components or dimensions varies depending on the data. The number of components was decided based on a scree plot when the percentage of variance explanation is stabilized and the curve if flattened, representing the number of components that have significant effect to the new data (Abdi et al., 2013).

In each new dimension, the so-called data coordinates or scores (factor scores) are present, which are new data for each individual in each dimension. These values were then used for the classification model construction. The scores obtained from each individual allow the interpretation of how each variable or group of variables influenced data variance, that is, how each band or spectral band is influencing the classification of groups and which ones are the most important for the data representativeness.

2.2.5 Vegetation Indices calculation

In order to unveil the best data analysis for this model, another model was constructed based on VIs that were previously studied for soybean diseases monitoring that showed high correlation (Cui et al., 2009; Bajwa et al., 2017).

Vegetation Indices are excellent resources to help interpret this type of data, optimizing the understanding and application of data to identify plant stresses (Shiratsuchi et al., 2014; Bajwa et al., 2017). Besides, it allows other sensors such as multispectral sensors to be also able to obtain enough information to estimate these values, not requiring hyperspectral sensors.

With the advance of machine learning algorithms and other artificial intelligence techniques becoming widely used in data modeling, a collection of several VIs that are representative for morphophysiological changes started to be used instead of just one VI at a time, improving overall model performance (Abdi et al., 2013). Thus, for this study, the results of a collection of 19 VIs were used (Table 1).

The VIs were chosen based on the indices adopted by Abdi et al. (2013) for the analysis of stresses caused by plant diseases, and by Cui et al. (2009) to analyze the effect of SBR on soybean. Only VIs that showed more than 70% of data correlation were selected to compose the VI collection. The calculation and reference of all VIs are described in Table 1. Some of the indices, such as NDVI, were calculated based on single bands of the wavelength instead of the whole visible or NIR range, according to Gago et al. (2015), Xue and Su (2017), and Prada et al. (2020).

Pearson's linear correlation (r) of each VI was calculated as function of the corresponding disease severity level, considering the healthy, mild, moderate, and severe levels as 0, 2, 10 and 30% severity, respectively (Table 1). Correlation percentages were calculated based on all replicates data from both sites.

Table 1. Summary of Vegetation Indices (VIs) used to assess to correlation of disease severity and spectral signatures, and for the classification model. Formulas and descriptions were based on Cui et al. (2009) and Behmann et al. (2014).

Vegetation Indices (VI)	Description	Formula	Reference
C420	*C420*	$\frac{R_{420}}{R_{695}}$	Bajwa et al. (2017)
MSAVI2	*Modified Chlorophyll Absorption Ratio Index Improved*	$\frac{1}{2}[\,2(R_{810}+1)-\sqrt{(2R_{810}+1)^2-8(R_{810}-R_{690})}$	Qi et al. (1994)
NDVI	*Normalized Difference Vegetation Index*	$\frac{(R_{810}-R_{690})}{(R_{810}+R_{690})}$	Rouse et al. (1974)
DVI	*Difference vegetation Index*	$R_{755}-R_{698}$	Richardson & Wiegand (1977)
RVI	*Ratio vegetation Index*	$\frac{R_{775}}{R_{698}}$	Pearson & Miller (1972)
GRVI	*Green normalized Difference vegetation index*	$\frac{(R_{690}-R_{560})}{(R_{690}+R_{560})}$	Sripada et al. (2006)
SIPI	*Structure Independent Pigment Index*	$\frac{(R_{800}-R_{445})}{(R_{800}-R_{680})}$	Penuelas et al. (1995)
PRI	*Photochemical reflectance Index*	$\frac{(R_{570}-R_{531})}{(R_{570}+R_{531})}$	Gammon et al. (1997)
SR	*Simple ratio index (clorofila)*	$\frac{R_{800}}{R_{670}}$	Rouse et al. (1974)

Continuation of Table 1. Summary of Vegetation Indices (VI)

Vegetation Indices (VI)	Description	Formula	Reference
EVI	*Enhanced vegetation index*	$2{,}5 * \frac{(R_{800} - R_{670})}{(R_{800} + 6 * R_{670} - 7{,}5 * R_{490} + 1)}$	Huete et al. (1997)
SG	*Sum green index*	$\frac{1}{n}\sum_{i=500}^{599} Ri$	Gamon & Surfus (1999)
RENDVI	*Red edge NDVI*	$\frac{(R_{750} - R_{705})}{(R_{750} + R_{705})}$	Gitelson & Merzlyak (1994)
mRENDVI	*Modified red edge NVDI*	$\frac{(R_{750} - R_{705})}{(R_{750} + R_{705} - 2R_{445})}$	Sims & Gamon (2002)
mRESR	*Modified red edge simple ratio index*	$\frac{(R_{750} - R_{445})}{(R_{705} - R_{445})}$	Sims & Gamon (2002)
VOG1	*Vogelmann Red Edge Index 1*	$\frac{R_{740}}{R_{720}}$	Vogelmann et al. (1993)
RGRI	*Red green ratio index*	$\frac{mean(R_{500-600})}{mean(R_{600-700})}$	Gamon & Surfus (1999)
PSRI	*Plant senescence reflectance index*	$\frac{R_{680} - R_{500}}{R_{750}}$	Merzlyak et al. (1999)
ANTH1	*Anthocyanin reflectance index (1)*	$\frac{1}{R_{550}} - \frac{1}{R_{700}}$	Gitelson et al. (2001)
ANTH2	*Anthocyanin reflectance index (2)*	$R_{800}\left[\frac{1}{R_{550}} - \frac{1}{R_{700}}\right]$	Gitelson et al. (2001)

2.2.6 Data modeling

Disease classification and prediction models were constructed for each dataset (MFA and VIs). Total database of each dataset was randomly divided into training (80%) and testing (20%) data. Training data were used in the calibration and construction of each algorithm, and, after construction, test data were used to evaluate the performance and classification metrics and, therefore, were not considered during models construction. Therefore, 128 individuals were randomly selected to compose the training dataset and 32 to test and validation dataset, considering same individuals for the data from the dimensionality reduction and VI collection.

Ten classification algorithms that are most used for hyperspectral data were analyzed: Linear (LDA) and Quadratic (QDA) Discriminant Analysis, Logistic Regression (RL), Linear and Radial Support Vector Machine (SMV), K-Nearest Neighbors (KNN), Random Forests (RF), Decision Tree (DT), Learning by Vector Quantization (LVQ), and Partial Least Squares Regression (SPLS).

All techniques were evaluated in the R environment using the 'caret' statistical package for construction and testing (R CORE TEAM, 2019). The parameters of the algorithms were defined based on cross-validations (n=10) by the statistical package in order to obtain the best accuracy and overall performance. Likewise, models performance classifying disease levels based on the test data was calculated through cross-validations (n=10).

The performance of the classification models were evaluated based on six parameters considered suitable for these types of models: accuracy, precision, sensitivity, specificity, F1 and Kappa (Hossin & Sulaiman, 2015). The entire set of model performance results are important for determining the best model for disease classification and prediction. However, some of the factors may have greater importance based on the main goals of this study, such as the precision and sensitivity, which are indications of how much important information has been retrieved.

Therefore, precision and sensitivity values were considered the most decisive for choosing the best model, since the main goal is to extract the maximum amount of relevant information for the classification of disease severity levels. As the F1 value correlates the two measures, it was also considered to be of greater importance. This is

especially true for the healthy and low severity levels, since a greater sensitivity along with low error rates may provide a better indication of the onset of the disease, which is a result of paramount importance for decision-making of control.

Performance metrics were calculated based on the confusion matrix of the results of each model. The equations for calculating each parameter are shown in Table 2. All analyses were conducted in R environment (R Core Team, 2019).

Table 2. Model performance evaluation and equations for each metric parameter.

Evaluation metrics	Equations[1]
Accuracy	$\frac{(FP+FN)}{(TP+TN+FP+FN)}$
Error	$1-Accuracy$
Precision	$\frac{TP}{(TP+FP)}$
Sensibility	$\frac{TP}{(TP+FN)}$
Specificity	$\frac{TN}{(TN+FP)}$
F1	$2\,x\,\frac{Precision\ x\ Sensibility}{Precision+Sensibility)}$
Kappa	$\frac{p_o-p_e}{1-p_e}$ $p_o = accurary$ $p_e = \frac{1}{N^2}\sum_k n_{k1}n_{k2}$ *k* = categories, *N*= observations, n_{ki}= number of times model *i* predicted category *k*

[1]TP: true positive; TN: true negative; FP: false positive; FN: false negative

2.3 RESULTS AND DISCUSSION

2.3.1 Spectrum reflectance analysis

Disease severity levels of each soybean cultivar produced different spectral signatures (Figure 4). Although each class spectral curve distinguished from each other, a similar trend was found, especially comparing between disease severities. Besides,

susceptible soybean cultivar presented different spectral curve compared to the partially resistant cultivar.

Each waveband of the reflectance spectrum has a distinguished importance helping to understand the stress caused by the disease, besides yielding good indicators to differentiate between classes. In the VIS range, as symptoms severity increased, greater reflectance was found, especially at wavelength around 550 nm, in which severely affected leaves presented much higher reflectance than the ones with milder symptoms or healthy leaves. On the other hand, an inversion was found in NIR region, with the highest reflectance found on healthier leaves. There were no remarkable visual differences in the UV range for any of the classes analyzed.

Figure 4. Mean spectrum reflectance (spectral signature) of soybean leaflets susceptible and partially resistant to *P. pachyrhizi* under different levels of disease severity.

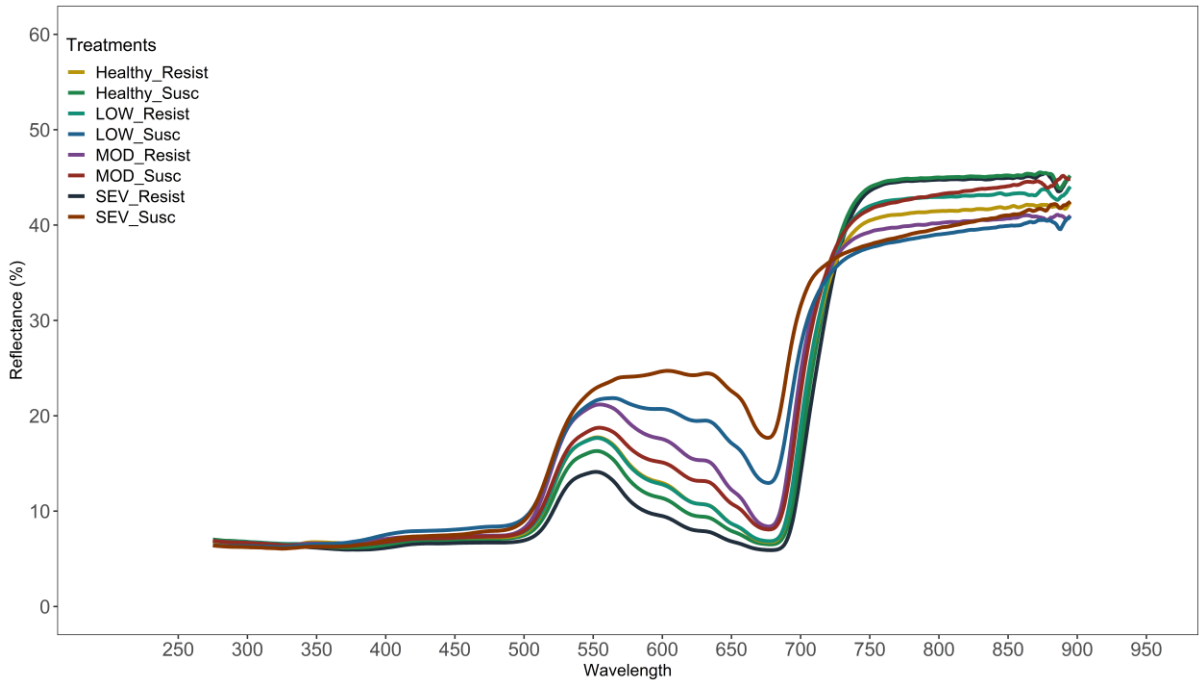

[1]Healthy_Resist: partially resistant cultivar, no disease; Healthy_Susc: susceptible cultivar, no disease; LOW_Resist: partially resistant cultivar, low disease severity; LOW_Susc: susceptible cultivar, low disease severity; MOD_Resist: partially resistant cultivar, moderate disease severity; MOD_Susc: susceptible cultivar, moderate disease severity; SEV_Resist: partially resistant cultivar, high disease severity; SEV_Susc: susceptible cultivar, high disease severity.

The lowest reflectance value, which is around 680 nm (Appeltans et al., 2021), also changed according to the severity classes, with the highest reflectance found again on leaflets with severer symptoms. Moreover, leaflets with severer symptoms had the lowest reflection in NIR region, producing a quite different spectral curve shape and smaller increase in the red edge region (680-690 nm). While healthier leaflets presented the highest reflectance around 740-750 nm, severer affected leaflets presented the highest reflectance around 690 nm. The highest values were also observed in healthier leaflets irrespective of the position. It is known that healthy plants have low radiation reflectance in the visible and mid-infrared region and high reflectance in the near-infrared (Hatfield & Pinter, 1993; Ahmed et al., 2016).

In general, lower reflectance was found for all disease severities of partially resistant cultivars compared to the susceptible one, including healthy leaves. Therefore, these small spectral differences were possibly due to morphological structures of each cultivar rather than due to differences in disease symptoms. Nonetheless, similar spectral responses were observed across disease severity levels evaluated on both cultivars and, therefore, they could potentially be considered together in modeling disease severity levels classification.

Based on visual observations, the VIS range and red edge region were considered the best ones to aid in the prediction and classification model. Therefore, these spectral regions can be better explored to find differences that can be used to differentiate each class, and to increase model performance.

2.3.2 Feature analysis

2.3.2.1 Multiple factor analysis

The MFA performed satisfactorily in the dimensionality data reduction, reducing 620 units to only 5 components (dimensions) with approximately 60% of variance explanation. The first and second dimensions represented the most important contributors of variables explanation, with 26.7 and 9.4% of explanation, respectively.

The MFA also unveiled the effect of specific wavebands or wavelengths on the classification of each class and on the data dimensionality reduction (Figure 5). In general, NIR and VIS regions were the ones that most contributed to data variability

explanation, *i.e.*, the most important to the discrimination of disease severity levels and cultivars. In the first dimension, which is the most important for variance explanation of the model, both NIR (38%) and VIS region (37%) stood out (Figure 5A). In the second dimension, VIS range performed the greatest importance to data explanation (57%), followed by NIR region (29%) (Figure 5B). Ultraviolet region did not contribute significantly to any dimension.

Figure 5. Percentage of contribution to variability explanation of wavebands to the first (A) and second (B) dimensions and of wavelengths to the first (C) and second (D) dimension.

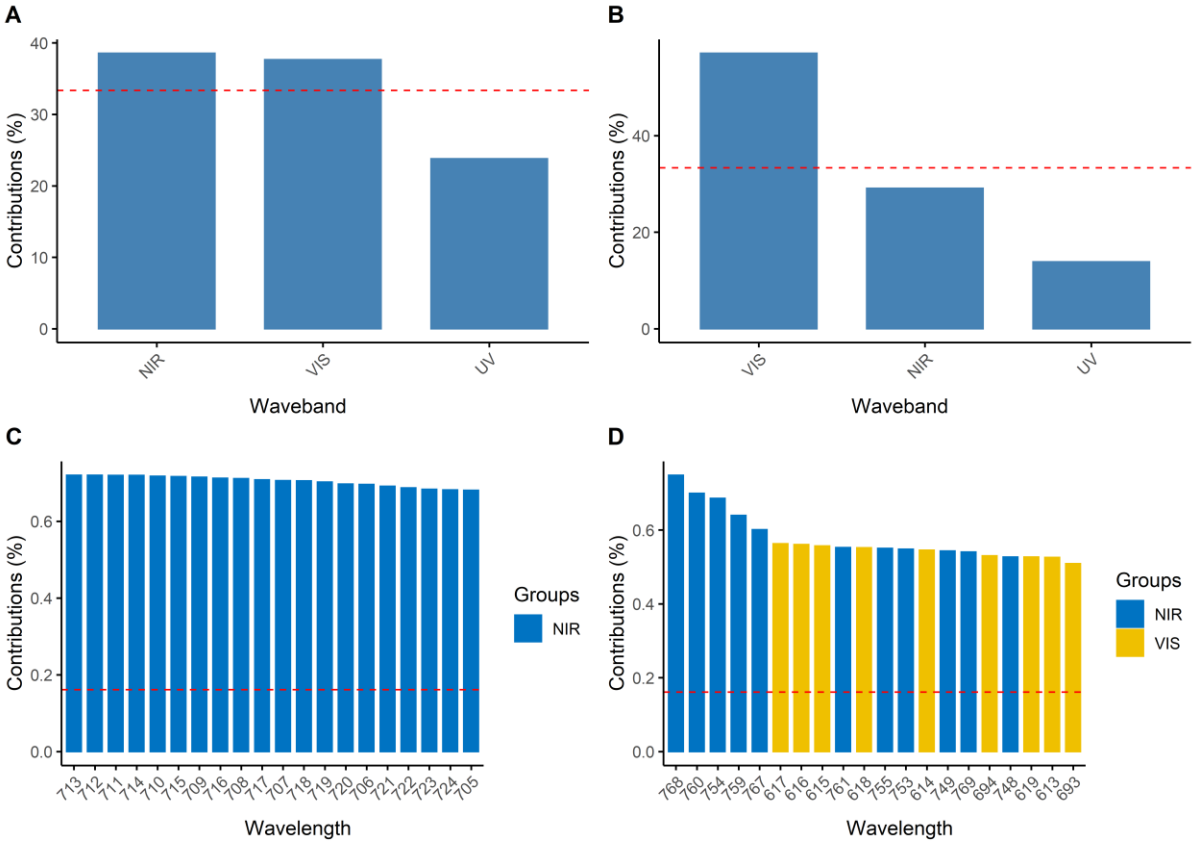

NIR: Near infrared region (700-800 nm); VIS: Visible region (300-700 nm)
Red dashed-line indicates the expected average value of contribution

In terms of specific spectrum wavelengths, the range from 705 to 725 nm (NIR range) was the most important for data variance explanation in the first dimension (Figure 5C), while VIS range predominately influenced the second dimension (Figure

5D). This outcome corroborates the percentage of contribution for each dimension found in each waveband and the visual analysis of the spectrum reflectance curve (Figure 4), where NIR and VIS regions were remarkably more suitable for classification between individuals.

Lastly, a clear distinction between the four levels of disease severity were observed when comparing the classification of individuals based on the eigenvalue in the first and second dimension (Figure 6). Few observations can be done in the separation of the groups. Firstly, healthy leaflets seemed to produce more consistent, and less variability compared to the severely affected leaflets, since the healthy ones were all majorly clustered together while the other group seemed more scattered through the graph. Same trend was found for moderate and low severity levels.

Figure 6. Individual separation according to values found in the first and second dimension after MFA and data dimensionality reduction.

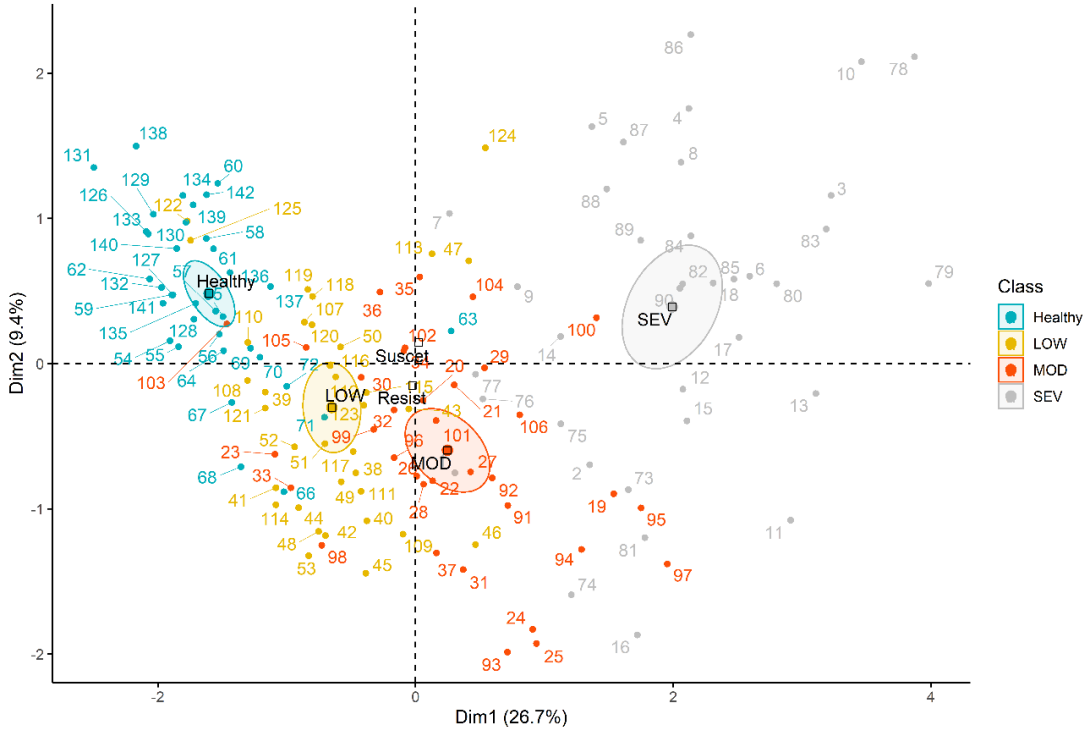

[1]Dim1: Dimension 1; Dim2: Dimension 2;
[2]Class: Healthy: healthy leaflets; Low: low disease severity; MOD: Moderate disease severity; SEV: Severe disease severity
[3]Suscet: soybean cultivar susceptible to soybean rust; Resist: soybean cultivar partially resistant to soybean rust

Healthy and severely affected leaflets were both positively affected by Dim-2, while moderate and low disease severities were negatively affected (Figure 6). On the other hand, leaflets with no symptoms and low severity were negatively affected by Dim-1, meanwhile severer leaflets (moderate and severe) were positively affected. Considering that Dim-1 has the highest contribution to data variability explanation, and that NIR region is the one with the highest importance, it can be inferred that NIR region plays a key role at the classification of the disease severity levels.

The categorical values of susceptible and partially resistant cultivars (represented as "*Suscet* and *Resist*" in the graph) seemed to not affect the classification, being positioned in the middle of the graph. Nonetheless, the clear separation of the groups shows the efficacy of the data dimensionality reduction and the possibility to use the new data for classification models.

2.3.2.2 Vegetation Indices

The heatmap matrix shows the correlation of all VIs tested in this study as well as the correlation of disease severity classes to each VIs (Table 3). Since the correlation of the severity classes to the VIs are the most important to decide which indices are more appropriate to be used in the classification model construction, the discussion will focus on this subject.

Overall, most of the VIs studied performed reasonably well in the correlations with the severity classes, except for REP, MCARI, CAR1 and CAR2 (Table 3). The rest of the VIs presented at least 70% of either positive or negative correlation according to the classes, which indicates great parameters to be used in the classification models. Vegetation Indices that correlate mostly to chlorophyll content, such as NDVI, DVI, SR and EVI, and to the plant stress or senescence (mRENDVI) showed high negative correlation to severity levels, indicating that increased disease severity led to lower VIs values. This information is valid since SBR disease interferes with the plant's photosynthetic apparatus, decreasing chlorophyll content with chlorosis and necrosis, leading to leaf senescence and defoliation (Kelly et al., 2015).

Oppositely, VIs that correlate to other pigmentation alterations in the leaf, such as PSRI, SIPI, ANTH1 and SG, presented high positive correlation to the disease severity

levels. Most of these indices are intended to unveil certain alterations in plant's pigmentation that indicates plant stress, such as greenness level and carotenoid content (Al-Saddik et al., 2019). Foliar diseases are majorly affected by changes in color and indices, that can correlate to these alterations have great importance to first detect a diseased plant and to evaluate the level of damage caused (Tetila et al., 2017).

Table 3 Pearson's linear correlation coefficient (*r*) of 23 Vegetation Indices (VI) according to soybean rust severities (healthy, low, moderate, and severe symptoms).

VIs[1]	**ANTH1**	**ANTH2**	**SG**	**SIPI**	**PSRI**	**GRVI**	**PRI**	**REP**
Pearson's correlation	0.73	0.71	0.70	0.75	0.79	0.87	0.80	-0.50
VIs	**RENDVI**	**C420**	**mRESR**	**VOG1**	**RVI**	**mRENDVI**	**EVI**	**RGRI**
Pearson's correlation	-0.74	-0.78	-0.74	-0.76	-0.78	-0.81	-0.88	-0.87
VIs	**DVI**	**SR**	**NDVI**	**MSAVI2**	**MCARI**	**CAR1**	**CAR2**	
Pearson's correlation	-0.86	-0.87	-0.88	-0.88	-0.11	-0.41	-0.01	

[1]Vegetation indices (Table 1)

Therefore, since each VIs correspond to a specific parameter of the individual that is affected by the disease, a collection of them may bring good benefits to the model fitting and performance, since it is possible to achieve a greater percentage of understanding and differentiation from each class. Thus, likewise the visual comparison of each class spectral signature, VIs may be useful for this classification model. Since REP, MCARI, CAR1 and CAR2 did not perform well in the correlation analyzes, they were considered not adequate to the VIs collection group and, therefore, were not considered in the model.

2.3.3 Performance and metrics of prediction and classification model

2.3.3.1 Dimensionality reduction and feature selection (MFA)

The models tested based on data from MFA performed reasonably well in the classification of disease severity levels in terms of overall performance metrics (Table 4) and error index (Table 5). Classification accuracy and precision was above 70% for all models, except for KNN (67%), while sensibility ranged from 60 to 87%. Among those models, LR and LDA outstood the others due to the best precision (86 and 85%) and

lowest error for the classifications levels healthy (0%) and low severity (14%). Besides, LDA achieved better sensibility (87%), accuracy (85%) and F1 score (86%), and thereby, being considered the best model for this dataset. It is important to note similar performance of LVQ and linear SVM models. However, considering its precision, it is still below the LDA model results.

Table 4. Performance parameters of prediction and classification models of soybean rust, as function of disease severity levels and based on results from dimensionality reduction by multiple factor analysis (MFA).

Model	Precision	Accuracy	Kappa	F1	Sensibility	Specificity
	%					
LDA[1]	85.71	85.71	80.95	86.05	87.49	95.27
QDA	71.43	71.43	61.90	71.20	72.23	90.60
LR	86.07	78.57	71.43	77.50	77.50	93.10
SVM linear	78.57	78.57	71.43	78.57	78.57	92.85
SVM radial	71.43	71.43	61.90	67.93	74.64	90.90
KNN	82.14	67.86	57.14	66.51	66.58	89.70
RF	71.43	82.14	76.19	83.03	60.00	94.06
DT	82.14	71.43	61.90	72.17	76.78	90.52
LVQ	71.43	82.14	76.19	82.08	82.43	94.09
SPLS	85.71	75.00	66.67	73.92	74.86	92.08

[1] LDA: linear discriminant analysis; QDA: quadratic discriminant analysis; LR: logistic regression; SVM: support vector machine (linear and radial); KNN: k-nearest neighbours; RF: random forest; DT: decision tree; LVQ: learning vector quantization; SPLS: sparse partial least square regression

For all models, higher percentage of error and, therefore, lower percentage of precision were found for classes with severer symptoms (moderate and high severity) (Table 5). As observed in the discrimination and classification graph of MFA (Figure 6), as the disease severity increases, higher heterogeneity was found and data seemed to be more scattered, probably due to the similar symptoms and similarities in spectral values. Contrariwise, for healthy and low severity, low percentage of error was found, possibility due to differences in the pigmentation and healthier leaf structure when comparing to the severer symptoms, besides the presence of other pigments and structures in the leaf in comparison to having no symptoms at all (healthy and low

severity). Therefore, it is important to highlight the differentiation of healthy individuals from the others, since it will allow better prediction of diseased classes, besides showing the possibility of identifying diseased plants even under low severity indices (detection of disease incidence).

Table 5. Percentage of error of 10 classification models according to disease severity levels and spectral data, after data dimensionality reduction by Multiple Factor Analysis.

Model	Error (%)				
	Healthy	**Low**	**Moderate**	**Severe**	**Average**
LDA[1]	00.00	14.29	14.29	28.57	**14.29**
QDA	14.29	42.86	28.57	28.57	**28.57**
RL	00.00	14.29	27.14	14.29	**13.93**
SVM linear	00.00	14.29	42.86	28.57	**21.43**
SVM radial	14.29	28.57	57.14	14.29	**28.57**
KNN	00.00	28.57	57.14	14.29	**25.00**
RF	14.29	14.29	28.57	14.29	**17.86**
DT	14.29	42.86	28.57	28.57	**28.57**
LVQ	14.29	14.29	14.29	28.57	**17.86**
SPLS	00.00	42.86	42.86	28.57	**28.57**

[1] LDA: linear discriminant analysis; QDA: quadratic discriminant analysis; LR: logistic regression; SVM: support vector machine (linear and radial); KNN: k-nearest neighbours; RF: random forest; DT: decision tree; LVQ: learning vector quantization; SPLS: sparse partial least square regression

2.3.3.2 Vegetation Indices collection

The performance of the prediction and classification models using the collection of VIs were similarly comparable to the ones from MFA. Overall, high accuracy was found especially for linear SVM (93%), radial SVM (85%), LDA (85%), QDA (82%) and SPLS (82%) (Table 6). Similar values were also found for precision and percentage of error (Table 7). Overall, linear SVM model achieved the highest precision (93%), low error for classification as healthy (14.5%) and low severity (0%), high sensibility (93%), and accuracy (93%), and, therefore, it was considered the best one for VIs collection.

Table 6. Performance parameters of prediction and classification models of soybean rust as function of disease severity levels and based on results from vegetation indices collection based on spectral reflectance.

Model	Precision	Accuracy	Kappa	F1	Sensibility	Specificity
LDA[1]	85.71	85.71	80.95	85.62	86.46	95.34
QDA	82.14	82.14	76.19	81.77	82.54	91.76
LR	75.00	75.00	66.67	73.45	79.11	92.37
SVM linear	92.86	92.86	80.48	92.82	93.75	92.73
SVM radial	85.71	85.71	80.95	85.18	89.38	95.74
KNN	75.00	75.00	66.67	74.67	74.70	90.69
RF	78.57	78.57	71.43	78.69	80.36	92.95
DT	67.86	67.86	57.14	66.97	69.50	89.58
LVQ	71.43	71.43	61.90	69.95	70.07	90.93
SPLS	82.24	82.39	76.52	82.00	81.96	94.23

[1] LDA: linear discriminant analysis; QDA: quadratic discriminant analysis; LR: logistic regression; SVM: support vector machine (linear and radial); KNN: k-nearest neighbours; RF: random forest; DT: decision tree; LVQ: learning vector quantization; SPLS: sparse partial least square regression

The error percentage of the models using VIs collection (Table 7) were also similar to the ones found using MFA data (Table 5). The biggest errors in most models were found in individuals with severer symptoms, while there was low error and higher precision in healthier plants. It is important to note again that both moderate and severely affected leaflets presented chlorosis, necrosis and pustules spread in the surface, in addition to expected damages to the cell structure, only differing on the damage level (Figure 1). However, linear SVM also performed better than the others in this parameter, achieving high precision (low error) for severer symptoms as well (14% error for moderate and 0% error for severe). On the other hand, the models were also able to properly identify diseased plants and distinguish them from healthy ones, which is the main focus of the model. Thus, the use of VIs collection was also considered to have potential to SBR prediction and classification.

Table 7. Percentage of error of 10 classification models according to disease severity levels and collection of Vegetation Indices based on spectral data.

Model	Error (%)				
	Healthy	Low	Moderate	Severe	Average
LDA[1]	14.29	00.00	28.57	14.29	14.29
QDA	14.29	14.29	42.86	00.00	17.86
RL	14.29	28.57	57.14	00.00	25.00
SVM linear	14.29	00.00	14.29	00.00	7.15
SVM radial	14.29	00.00	42.86	00.00	14.29
KNN	14.29	14.29	42.86	28.57	25.00
RF	28.57	14.29	28.57	14.29	21.43
DT	14.29	57.14	42.86	14.29	32.15
LVQ	14.29	00.00	71.43	28.57	28.57
SPLS	08.33	34.29	22.86	05.56	17.76

[1] LDA: linear discriminant analysis; QDA: quadratic discriminant analysis; LR: logistic regression; SVM: support vector machine (linear and radial); KNN: k-nearest neighbours; RF: random forest; DT: decision tree; LVQ: learning vector quantization; SPLS: sparse partial least square regression

Bajwa et al. (2017) also reported satisfactory results using VIs for the identification of soybean disease monitoring. In this study, the VIs NDVI, MSAVI2, PRI, SIPI, and C420 showed the highest correlation according to the disease symptoms. Besides, LDA was also applied to construct the detection model on a collection of VIs, which also resulted in high performance of classification accuracy, close to 91%. Moreover, VIs data from hyperspectral imaging was also considered a powerful tool for predicting general plant stresses (Behmann et al., 2014). The authors were able to identify several stress conditions, such as senescence stages and drought stress through a collection of VIs that were highly correlated to the data.

Comparing both groups of data (MFA and VIs), linear SVM model using the collection of VIs achieved the best results. Besides, VIs are considered an easy method to extract information from spectral reflectance and it is one of the most common methods applied in this matter (Behmann et al., 2014). In a scenario of field application, VIs are easier to be applied and with greater background knowledge, in addition to not require complex statistical analysis. Furthermore, data dimensionality reduction

techniques may affect the final data, since the new components generated are based on the data being analysed, thereby subjected to changes depending on the database used initially.

Therefore, the identification of initial stages of the disease are of paramount importance to avoid an epidemic outbreaks and disease spread throughout the field. Since even low severity levels were highly identifiable based on reflectance data, these models can be a potential tool to support disease monitoring in the field. Especially with advances in remotely piloted aircrafts (RPA) with hyperspectral cameras, this task could be quickly conducted over a wide area, outperforming traditional monitoring methods (Tetila et al., 2017; Ahmad et al., 2021). Future research on the application of the models tested in this study should be conducted in the field to improve model efficacy and to improve the viability of this tools in the IDM.

2.4 CONCLUSION

Based on the results found herein, each soybean rust severity level presented a different behaviour on spectral data, allowing the differentiation between each level and the construction of a detection and classification model. The collection of Vegetation Indices were the best suitable for the model construction, which is considered a powerful tool to be integrated in the disease management to support decision-making of control. Initial stages of the disease were identified, reassuring its potential to support disease monitoring. Therefore, the use of remote sensing based on the reflectance for different levels of disease severity proved to be an adequate path for the construction of a soybean rust disease prediction model in disease management. Nonetheless, the evaluation of other diseases and plant nutrition effect on this model are also encouraged to be conducted. Moreover, the possibility of using remote sensing techniques to detect SBR also unleash new questions on how this can impact the disease control and crop yield. Therefore, new studies are encouraged to be conducted assessing the applicability of these findings in the field, especially in terms of impact of different application timings based on the detection model on the disease control.

2.5 REFERENCES

Abdi, H., Williams, L. J., & Valentin, D. (2013). Multiple factor analysis: principal component analysis for multitable and multiblock data sets. *Wiley Interdisciplinary reviews: computational statistics*, *5*(2), 149-179.

Abdel-Rahman, E. M., Mutanga, O., Odindi, J., Adam, E., Odindo, A., & Ismail, R. (2014). A comparison of partial least squares (PLS) and sparse PLS regressions for predicting yield of Swiss chard grown under different irrigation water sources using hyperspectral data. Computers and Electronics in Agriculture, 106, 11-19.

Ahmad, A., Ordoñez, J., Cartujo, P., & Martos, V. (2021). Remotely Piloted Aircraft (RPA) in Agriculture: A Pursuit of Sustainability. Agronomy, 11(1), 7.

Ahmed, M. R., Yasmin, J., Mo, C., Lee, H., Kim, M. S., Hong, S. J., & Cho, B. K. (2016). Outdoor applications of hyperspectral imaging technology for monitoring agricultural crops: A review. Journal of Biosystems Engineering, 41(4), 396-407.

Al-Saddik, H., Simon, J. C., & Cointault, F. (2019). Assessment of the optimal spectral bands for designing a sensor for vineyard disease detection: the case of 'Flavescence dorée'. Precision Agriculture, 20(2), 398-422.

Appeltans, S., Pieters, J. G., & Mouazen, A. M. (2021). Detection of Leek Rust Disease under Field Conditions Using Hyperspectral Proximal Sensing and Machine Learning. Remote Sensing, 13(7), 1341.

Bajwa, S. G., Rupe, J. C., & Mason, J. (2017). Soybean disease monitoring with leaf reflectance. Remote Sensing, 9(2), 127.

Behmann, J., Steinrücken, J., & Plümer, L. (2014). Detection of early plant stress responses in hyperspectral images. ISPRS Journal of Photogrammetry and Remote Sensing, 93, 98-111.

Bohnenkamp, D., Behmann, J., & Mahlein, A. K. (2019). In-field detection of yellow rust in wheat on the ground canopy and UAV scale. Remote Sensing, 11(21), 2495.

Cui, D., Zhang, Q., Li, M., Zhao, Y., & Hartman, G. L. (2009). Detection of soybean rust using a multispectral image sensor. Sensing and Instrumentation for Food Quality and Safety, 3(1), 49-56.

Deising, H. B., Reimann, S., & Pascholati, S. F. (2008). Mechanisms and significance of fungicide resistance. Brazilian Journal of Microbiology, 39, 286-295.

Feng, F., Li, W., Du, Q., & Zhang, B. (2017). Dimensionality reduction of hyperspectral image with graph-based discriminant analysis considering spectral similarity. Remote sensing, 9(4), 323.

Gago, J., Douthe, C., Coopman, R. E., Gallego, P. P., Ribas-Carbo, M., Flexas, J., & Medrano, H. (2015). UAVs challenge to assess water stress for sustainable agriculture. Agricultural Water Management, 153, 9-19.

Gamon, J., Serrano, L., & Surfus, J. S. (1997). The photochemical reflectance index: an optical indicator of photosynthetic radiation use efficiency across species, functional types, and nutrient levels. Oecologia, 112(4), 492-501.

Gamon, J. A., & Surfus, J. S. (1999). Assessing leaf pigment content and activity with a reflectometer. The New Phytologist, 143(1), 105-117.

Gitelson, A., & Merzlyak, M. N. (1994). Spectral reflectance changes associated with autumn senescence of *Aesculus hippocastanum* L. and *Acer platanoides* L. leaves. Spectral features and relation to chlorophyll estimation. Journal of plant physiology, 143(3), 286-292.

Gitelson, A. A., Merzlyak, M. N., & Chivkunova, O. B. (2001). Optical properties and nondestructive estimation of anthocyanin content in plant leaves. Photochemistry and photobiology, 74(1), 38-45.

Godoy, C., Utiamada, C., Meyer, M., Campos, H., Lopes, I., Muhl, A., & Carlin, V. (2021). Eficiência de fungicidas para o controle da ferrugem-asiática da soja, *Phakopsora pachyrhizi*, na safra 2020/2021: resultados sumarizados dos ensaios cooperativos. Embrapa Soja-Circular Técnica (INFOTECA-E).

Godoy, C. V., Bueno, A. D. F., & Gazziero, D. L. P. (2015). Brazilian soybean pest management and threats to its sustainability. Outlooks on Pest management, 26(3), 113-117.

Godoy, C. V., Koga, L. J., & Canteri, M. G. (2006). Diagrammatic scale for assessment of soybean rust severity. Fitopatologia Brasileira, 31, 63-68.

Hatfield, P. L., & Pinter Jr, P. J. (1993). Remote sensing for crop protection. Crop protection, 12(6), 403-413.

Hikishima, M., Canteri, M. G., Godoy, C. V., Koga, L. J., & Silva, A. J. D. (2010). Quantificação de danos e relações entre severidade, medidas de refletância e produtividade no patossistema ferrugem asiática da soja. Tropical Plant Pathology, 35, 96-103.

Hossin, M., & Sulaiman, M. N. (2015). A review on evaluation metrics for data classification evaluations. International Journal of Data Mining & Knowledge Management Process, 5(2), 1.

Huete, A. R., Liu, H. Q., Batchily, K. V., & Van Leeuwen, W. J. D. A. (1997). A comparison of vegetation indices over a global set of TM images for EOS-MODIS. Remote sensing of environment, 59(3), 440-451.

IEAg/ABAG – Instituto de Estudos do Agronegócio/Associação Brasileira do Agronegócio (2015). O futuro da soja nacional. Available at: http://www.abag.com.br/media/images/0-futuro-da-soja-nacional---ieag---abag.pdf.

Kelly, H. Y., Dufault, N. S., Walker, D. R., Isard, S. A., Schneider, R. W., Giesler, L. J., & Hartman, G. L. (2015). From select agent to an established pathogen: the response to *Phakopsora pachyrhizi* (soybean rust) in North America. Phytopathology, 105(7), 905-916.

Kelly, M., & Guo, Q. (2007). Integrated agricultural pest management through remote sensing and spatial analyses. In General Concepts in Integrated Pest and Disease Management (pp. 191-207). Springer, Dordrecht.

Khaled, A. Y., Abd Aziz, S., Bejo, S. K., Nawi, N. M., Seman, I. A., & Onwude, D. I. (2018). Early detection of diseases in plant tissue using spectroscopy–applications and limitations. Applied Spectroscopy Reviews, 53(1), 36-64.

Mahlein, A. K. (2016). Plant disease detection by imaging sensors–parallels and specific demands for precision agriculture and plant phenotyping. Plant disease, 100(2), 241-251.

Mahlein, A. K., Rumpf, T., Welke, P., Dehne, H. W., Plümer, L., Steiner, U., & Oerke, E. C. (2013). Development of spectral indices for detecting and identifying plant diseases. Remote Sensing of Environment, 128, 21-30.

Martinelli, F., Scalenghe, R., Davino, S., Panno, S., Scuderi, G., Ruisi, P.,… & Dandekar, A. M. (2015). Advanced methods of plant disease detection. A review. Agronomy for Sustainable Development, 35(1), 1-25.

Merzlyak, M. N., Gitelson, A. A., Chivkunova, O. B., & Rakitin, V. Y. (1999). Non-destructive optical detection of pigment changes during leaf senescence and fruit ripening. Physiologia plantarum, 106(1), 135-141.

Negrisoli, M. M., Raetano, C. G., de Souza, D. M., e Souza, F. M. S., Bernardes, L. M., Junior, L. D. B., ... & Sartori, M. M. P. (2019). Performance of new flat fan nozzle design in spray deposition, penetration and control of soybean rust. European Journal of Plant Pathology, 155(3), 755-767.

Prada, M., Cabo, C., Hernández-Clemente, R., Hornero, A., Majada, J., & Martínez-Alonso, C. (2020). Assessing canopy responses to thinnings for sweet chestnut coppice with time-series vegetation indices derived from landsat-8 and sentinel-2 imagery. Remote Sensing, 12(18), 3068.

Pearson, R. L., & Miller, L. D. (1972). Remote mapping of standing crop biomass for estimation of the productivity of the shortgrass prairie. Remote sensing of environment, VIII, 1355.

Penuelas, J., Baret, F., & Filella, I. (1995). Semi-empirical indices to assess carotenoids/chlorophyll a ratio from leaf spectral reflectance. Photosynthetica, 31(2), 221-230.

Qi, J., Chehbouni, A., Huete, A. R., Kerr, Y. H., & Sorooshian, S. (1994). A modified soil adjusted vegetation index. Remote sensing of environment, 48(2), 119-126.

R CORE TEAM (2019). R: A language and environment for statistical computing. R Foundation for Statistical Computing, Vienna, Austria.

Richardson, A. J., & Wiegand, C. L. (1977). Distinguishing vegetation from soil background information. Photogrammetric engineering and remote sensing, 43(12), 1541-1552.

Rouse, J. W., Haas, R. H., Schell, J. A., Deering, D. W., & Harlan, J. C. (1974). Monitoring the vernal advancement and retrogradation (green wave effect) of natural vegetation. NASA/GSFC Type III Final Report, Greenbelt, Md, 371.

Rupe, J.; Sconyers, L. Soybean Rust. *The Plant Health Instructor*. 2008. DOI: 10.1094/PHI-I-2008-0401-01

Savitzky, A., & Golay, M. J. (1964). Smoothing and differentiation of data by simplified least squares procedures. Analytical chemistry, 36(8), 1627-1639.

Shimadzu. UV-Vis-NIR Spectroscopy: Suspension and Opaque Sample Measurement. ISR-603 IntegratingSphereAttachment. Available at: <https://www.shimadzu.com/an/molecular_spectro/uv/accessory/liquidsample/liquid8.html>.

Shiratsuchi, L.S.; Brandão, Z.N.; Vicente, L.N.; Victoria, D.C.; Ducati, J.R.; Oliveira, R.P.; Vilela, M.F (2014). Sensoriamento Remoto: conceitos básicos e aplicações na Agricultura de Precisão. In: Bernardi, A.C.C.; Naime, J.M.; Resende, A.V.; Bassoi, L.H.; Inamasu, R.Y (Eds.), *Agricultura de precisão: Resultados de um novo olhar* (pp. 58-73). Embrapa.

Sims, D. A., & Gamon, J. A. (2002). Relationships between leaf pigment content and spectral reflectance across a wide range of species, leaf structures and developmental stages. Remote Sensing of Environment, 81(2-3), 337-354.

Sripada, R. P., Heiniger, R. W., White, J. G., & Meijer, A. D. (2006). Aerial color infrared photography for determining early in-season nitrogen requirements in corn. Agronomy Journal, 98(4), 968-977.

Tetila, E. C., Machado, B. B., Belete, N. A., Guimarães, D. A., & Pistori, H. (2017). Identification of soybean foliar diseases using unmanned aerial vehicle images. IEEE Geoscience and Remote Sensing Letters, 14(12), 2190-2194.

Vittal, R., Paul, C., Hill, C. B., & Hartman, G. L. (2014). Characterization and quantification of fungal colonization of *Phakopsora pachyrhizi* in soybean genotypes. Phytopathology, 104(1), 86-94.

Vogelmann, J. E., Rock, B. N., & Moss, D. M. (1993). Red edge spectral measurements from sugar maple leaves. Remote Sensing, 14(8), 1563-1575.

Wylie, F. R., & Speight, M. R. (2012). Insect pests in tropical forestry. CABI.

Xue, J., & Su, B. (2017). Significant remote sensing vegetation indices: A review of developments and applications. Journal of Sensors, 2017.

CHAPTER 3

Impact of fungicide application timing based on soybean rust prediction model on application technology and disease control[3]

Impacto da época de aplicação de fungicida com base no modelo de previsão da ferrugem da soja na tecnologia de aplicação e no controle de doenças

ABSTRACT

The application of remote sensing techniques and prediction models for soybean rust (SBR) monitoring may result in different fungicide application timings, control efficacy, and spraying performance. This study aimed to evaluate the applicability of a prediction model as a threshold for disease control decision-making and to identify the effect of different application timings on SBR control as well as on the spraying technology. Two experimental trials were conducted in a 2 x 4 factorial scheme: 2 cultivars (susceptible and partially resistant to SBR); and four application timings (conventional chemical control at a calendarized system basis; based on prediction model; at the appearance of the first visible symptoms; and control without fungicide application). Spray deposit and coverage at each application timing were evaluated in the lower and upper region of the soybean canopy through quantitative analysis of a tracer and water-sensitive papers. The prediction model was calculated based on leaf reflectance data collected by remote sensing. Application timings impacted the application technology as well as control efficacy. Calendarized system applications were conducted earlier, promoting different spray performances. Spraying at moments when the leaf area index was higher obtained poorer distribution. None of the treatments were capable of achieving high spray penetration into the canopy. The partially resistant cultivar was effective in holding disease progress during the crop season, whereas all treatments with chemical control resulted in less disease impact. The use of the prediction model was effective and promising to be integrated into disease management programs.

[3]Artigo aceito para publicação na Agronomy (ISSN: 2073-4395) e redigido de acordo com as normas da revista.

Keywords: *Phakopsora pachyrhizi*, Integrated disease management, Spraying technology, Remote sensing.

RESUMO

A aplicação de técnicas de sensoriamento remoto e modelos de predição no monitoramento da ferrugem da soja (FAS) pode resultar em diferentes momentos de aplicação de fungicidas, eficácia de controle e desempenho da pulverização. Este estudo teve como objetivo avaliar a aplicabilidade de modelos de predição como limiar para a tomada de decisão no controle da FAS e identificar o efeito de diferentes momentos de aplicação no controle da FAS e na tecnologia de pulverização. Dois experimentos foram conduzidos no esquema fatorial 2 x 4, sendo: 2 cultivares (suscetível e parcialmente resistente ao FAS); e quatro momentos de aplicação: controle químico convencional calendarizado (R1); baseado em modelo de predição; no aparecimento dos primeiros sintomas visíveis; e a testemunha sem aplicação de fungicida. A deposição e cobertura da pulverização em cada momento de aplicação foram avaliadas na região inferior e superior do dossel da cultura da soja por meio da análise quantitativa de um marcador e papéis hidrossensíveis. O modelo de predição foi calculado com base em dados de refletância foliar coletados por sensoriamento remoto. Os tempos de aplicação impactaram a tecnologia de aplicação, bem como a eficácia do controle. As aplicações do sistema calendarizado foram realizadas previamente as demais, promovendo diferentes desempenhos de pulverização. A pulverização foi prejudicada nos momentos em que o índice de área foliar era maior. Nenhum dos tratamentos foi capaz de atingir alta penetração da pulverização no dossel. O cultivar parcialmente resistente foi eficaz na contenção do progresso da doença durante a safra, enquanto todos os tratamentos com controle químico resultaram em menor impacto da doença. O uso do modelo de predição mostrou-se eficaz e promissor para ser integrado aos programas de manejo da doença.

Palavras-chave: *Phakopsora pachyrhizi*, manejo integrado de doenças, tecnologia de aplicação, sensoriamento remoto.

3.1 INTRODUCTION

Soybean rust (SBR) causes significant crop yield losses throughout the world [1-2]. The disease is caused by *Phakopsora pachyrhizi* Sydow and is controlled mostly by fungicide application at pre-determined scheduled timings of the soybean growth stages, usually regardless of disease incidence and pressure level [1,3]. Due to constant fungicide spraying over the seasons and several times at the same season, a large number of fungi populations resistant to different chemical groups of fungicides have also been reported [4-5], significantly reducing fungicide efficacy over time [6].

Most soybean cultivation is conducted in extensive field areas, which hardens disease monitoring conductance. Nowadays, specialists monitor SBR in the field through extensive scouting based on disease symptom recognition. However, monitoring is usually absent, and farmers choose to spray on a calendarized system basis (i.e., at a pre-determined period) as a guarantee of crop yield. Besides input losses, these practices can lead to fungicide resistance selection pressure, poor spraying quality at periods not appropriate to achieve the best spray distribution, as well as possible wrong timing, which also leads to lower efficacy [1, 6-9]. Other techniques are being applied to the integrated disease management (IDM) of the soybean – *P. pachyrhizi* pathosystem, such as resistant or partially resistant cultivars [10-11], planting dates restrictions [1-2], and biological control [12]. Nonetheless, disease monitoring is considered the basis of any control method applied.

One of the alternatives to aid in disease control decision-making is the use of remote sensing technologies to facilitate data acquisition in wider fields as well as the obtainment of reliable information. It means that these technologies can precisely detect the disease remotely and at a faster pace since it allows the monitoring of wider fields depending on the sensor and where it is based [13-15]. Studies have reported the possibility of identifying SBR by remote sensing techniques [16-18], as well as for other diseases and crops [15,19]. Moreover, researchers have been applying all of this information in data modeling so that remote sensing could serve as the background information in the construction of disease prediction models as decision support systems [14,20]. These models are expected to improve the application timing, control

effectiveness as well as spraying performance regarding its uniform distribution in the crop.

Fungicide application timing strongly influences disease control, and it may vary depending on the fungicide mode of action and translocation capacity [8,21]. Besides reaching the target at the moment of most fungicide susceptibility, the application timing may influence the application technology in terms of product distribution, coverage, and penetration into the canopy [9,22]. Different timings also represent variations in soybean canopy density, especially due to leaf area index (LAI) and vegetation density [23] which play a major role as a barrier to the spray reaching the interior of the canopy. Most fungicide applications target the lower region of the soybean canopy since this is where SBR starts its development [1]. Therefore, applications at moments of higher LAI tend to have reduced penetration capacity and worse spray distribution [24].

According to Müller et al. [8], effective monitoring along with fungicide application as soon as the disease is identified in the field is a key factor to mitigate excessive and unnecessary application. However, since most systemic fungicides used for SBR control have both curative and preventive action modes, it is unknown how the application timing will affect control efficacy. The hypothesis is that SBR monitoring through prediction models based on remote sensing can help identify the first appearance of the disease in the field, and, thereby, improve application timing accuracy. Moreover, different application timings will potentially influence product distribution across soybean canopy regions.

The goal of this study was to evaluate the applicability of prediction models as the threshold for disease control decision-making and to identify the effect of different application timings on soybean rust control as well as on the spraying technology. This study is a continuation of the research conducted by Negrisoli et al. [18], using a prediction model to determine the fungicide application timing and how it differs from conventional methods.

3.2 MATERIAL AND METHODS

Two experiment replications were carried out in the field over the 2020/2021 crop season, in different experimental areas of Botucatu, SP, Brazil (Field 1: 22° 48' 48” S

and 48° 25' 37" W; Field 2: 22° 49' 38" S and 48º 25' 40" W). In both experimental fields, no-tillage system was adopted, and all sowing operations, phytosanitary management, and evaluations were carried out homogeneously (Figure 1). Figures of the trials conduction in the field, as well as fungicides application and evaluations are shown in the appendices (Figure A1 – A3).

Figure 1. Study area map of both field trial replications.

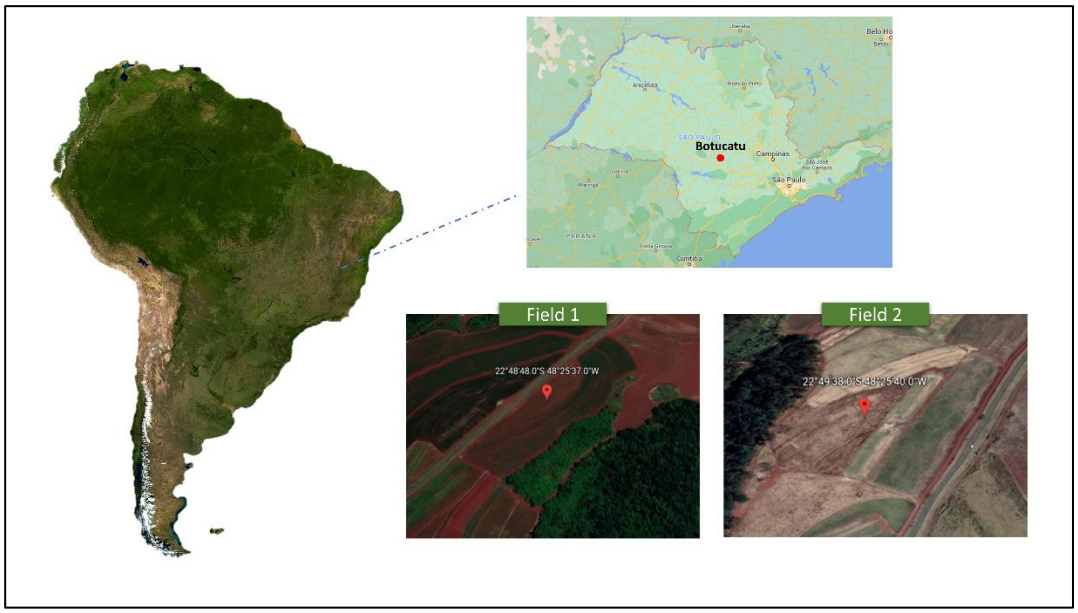

The trials were sown on December 8, 2020, spaced at 0.45 m between rows, and with a population of 196,528 plants ha^{-1} in Field 1 and 211,806 plants ha^{-1} in Field 2. The crop was fertilized with 250 kg ha^{-1} of the commercial formula 02-20-20 (NPK) homogeneously throughout the experimental area.

The experiments were carried out in a completely randomized blocks design and the treatments were distributed in a 2 x 4 factorial scheme: 2 cultivars (Brevant DS6217 IPRO, susceptible to SBR; TMG 7063 IPRO, partially resistant to SBR); and 4 application timings based on different parameters as decision-making of control: conventional chemical control, spraying at a scheduled basis at the soybean reproductive stage R1 and R1+15 days; application timing (A1) defined based on the disease prediction model and A1+15 days; application timing (A2) at the appearance of the first visible symptoms and A2+15 days; control treatments without fungicide

application (Table 1), and all in four repetitions. The descriptions of each cultivar are shown in Table 2.

Table 1. Description of the treatments according to the soybean cultivar and application timing.

Treatments	Cultivar	First Application Timing	Second Application Timing
1	DS6217 IPRO (Susceptible)	-	-
2	TMG 7063 (Partially resistant)	-	-
3	DS6217 IPRO (Susceptible)	Calend*	Calend+15
4	TMG 7063 (Partially resistant)	Calend	Calend+15
5	DS6217 IPRO (Susceptible)	Model	Model+15
6	TMG 7063 (Partially resistant)	Model	Model+15
7	DS6217 IPRO (Susceptible)	Sympt	Sympt+15
8	TMG 7063 (Partially resistant)	Sympt	Sympt+15

*Calend: calendarized application at reproductive stage R1; Model: spraying according to SBR prediction model; Sympt: spraying at the first symptoms observations; "+15": second application conducted at 15 days after the first application; "-": no application (control treatments).

The definition of the application timings "A1" and "A2" were based on weekly disease severity monitoring starting at the vegetative growth stage V6 in each plot. Firstly, the definition of A1 was conducted using an SBR prediction model proposed by Negrisoli et al. [18], based on the leaf reflectance, as the decision support system of control, as described subsequently herein.

Table 2. Description of the cultivars adopted in the experimental trials.

Description	Brevant DS6217 IPRO[1]	TMG 7063[2]
P. pachyrhizi susceptibility	Susceptible	Partially resistant (Inox)
Maturity groups	6,2	6,3
Growth habit	Indeterminate	Indeterminate
Traits	Intacta RR2 PRO®	Intacta RR2 PRO®

[1]BREVANT SEMENTES (2020); [2]TROPICAL MELHORAMENTO GENÉTICO (2020)

3.2.1 Leaf reflectance assessment

This assessment was conducted every five days after the V6 vegetative growth stage, by randomly collecting 5 leaflets per plot from the lower region of the canopy for leaf reflectance analysis. The UV 2700 non-imaging spectrophotometer (Shimadzu) was used coupled to an integrated base ISR-603: Integrating Sphere Attachment, analyzing the reflectance of each leaflet in the range of 270 to 1000 nm with an interval of 3.0 nm, as described by Negrisoli et al. [18]. Each sample (leaflet) was evaluated separately, generating the reflectance values of each sample in the previously mentioned spectral range interval.

The spectral curves were reduced from 270 – 1000 nm to 270 – 900 nm for high noise levels reduction [27] and the Savitzky-Golay filter was applied using 11 central points and a third-degree polynomial [28-29]. The data was used to calculate a list of 19 vegetation indices (VIs) that was representative of the disease effect on the crop and to allow disease severity classification and, therefore, to predict or detect diseased plants among the samples [16,18,30]. Vegetation indices were chosen to be used instead of the full spectra length so that other spectral sensors besides the hyperspectral ones could be used to acquire the data required to run this model [18], besides being able to supply valuable information for disease detection and plant stress identification [14].

The VIs were calculated for each sample at every reflectance evaluation date and this database was used to supply the prediction model based on the Support Vector Machine (SVM) algorithm, which is programmed to classify into four classes: “healthy”, “low severity”, “moderate severity”, “high severity”. At the moment when samples from susceptible (T5) and partially resistant (T6) cultivars averaged 1 plant per plot classified at “low severity” (diseased plant), the application was thereafter immediately conducted. All the VIs calculations, evaluation methodologies, and prediction model construction are fully described by [18]. The formulas and list of VIs used are attached in the supplementary material (Appendices, Table S1).

For the definition of “A2” application timing, 10 leaflets were collected from the lower region of the canopy in each plot for visual assessment of the symptoms. The samples were taken to a laboratory for better visualization of fungal structures and symptoms under a stereoscopic microscope. Susceptible and resistant reactions may

result in different SBR symptoms. A susceptible reaction results in tan to light-brown lesions (TAN reaction type) and the presence of uredinia throughout the leaf, while in partially resistant cultivars the lesions are characterized by reddish-brown lesions (RB-reaction type) and a lower quantity of uredinia [3,11]. The spraying was conducted at the time when the first SBR symptoms were detected in the plots of susceptible (T7) and partially resistant cultivars (T8).

The standard application timing was conducted at the end of the vegetative growth and the beginning of the reproductive stage (R1) of susceptible (T3) and partially resistant cultivars (T4). This application timing is common throughout the country and was used as the standard timing parameter.

3.2.2 Fungicide sprayings

The fungicide Elatus®, Syngenta (azoxystrobin 60 g L^{-1} + benzovindiflupyr 30 g L^{-1}) was used for SBR control at a dose of 0.250 kg ha^{-1}, following the manufacturer's recommendations. The spraying was carried out with a CO_2 pressurized backpack sprayer with a 2.0-meter boom equipped with four flat fan spray nozzles (Teejet XR110-02), displacement speed of 5 km h^{-1}, and working pressure of 200 kPa, providing a spraying volume of 150 L ha^{-1}.

3.2.3 Quali-quantitative analysis of spraying

Spray deposit capacity as well as the percentage of coverage of each treatment were evaluated in both first and second applications (Table 1). For the quantitative analysis of the deposit, the food dye Brilliant Blue marker (Duas Rodas Industrial Ltda) was applied immediately before fungicide spraying to avoid the influence of the fungicide formulation on the optical reading of the marker by spectrophotometry. The Brilliant Blue marker dye was solubilized in distilled water at a concentration of 3,000 mg L^{-1}. After spraying, three samples composed of 10 leaflets each were randomly collected from the upper and lower region of the plant canopy in the central lines of each plot, also evaluating the ability of the treatments to penetrate the crop canopy.

The samples were taken to the laboratory and processed according to Palladini et al. [44]. Each sample received 100 mL of distilled water, stirred for 15 seconds, and the

resulting solution was transferred to plastic containers. The quantification of deposits was performed in a spectrophotometer (Shimadzu VIS 1601 PC) with an absorbance reading at a wavelength of 630 nm [44]. After the tracer was washed, the leaf area of each sample was evaluated with the aid of a benchtop leaf area meter (LICOR, model LI-3100). The readings of known concentrations of the dye were correlated to the absorbance values obtained in the spectrophotometer and the calibration curve was constructed, obtaining the dye concentration in the target in mg L^{-1}. Finally, the volume found in the target was established by correlating the dye concentration in the samples washing solution with the dye concentration in the final spray solution, presenting the data in µL cm^{-2}.

The qualitative analysis of the spraying was carried out through the evaluation of the spray coverage using water-sensitive papers (WSP) (26 x 76 mm) distributed in each plot. Two WSPs were used attached to a metal rod in the central lines of the plots, one located horizontally at the top and the other at the bottom part of the canopy. Spray coverage and deposit evaluations were performed at the same time.

After spraying, the WSPs were placed in Petri dishes to prevent moisture absorption and taken to the laboratory for analysis. These samples were scanned at a resolution of 600 dpi and the digitalized images were analyzed by the “GOTAS” software (Embrapa®) to obtain the percentage of surface coverage.

The leaf area index (LAI) of the plots was also measured in the period between 50 to 70 days after emergence (DAE) (Field 1) and 50 – 88 DAE (Field 2), corresponding to the range of all application timings in each field. Therefore, at 50, 60, and 70 DAE of Field 1, and 50, 65, and 88 DAE of Field 2, 10 plants of each cultivar were randomly collected across each experimental field trial. The whole plants were taken to the laboratory, completely defoliated and the leaves were measured by a benchtop leaf area meter (LICOR, model LI-3100). The total leaf area measured of each sample was converted to m^2 and divided by the mean number of plants m^{-1} (Field 1 = 9.93 plants m^{-1} of the susceptible cultivar; 7.75 plants m^{-1} of the partially resistant cultivar; Field 2 = 10.34 plants m^{-1} of the susceptible cultivar; 8.72 plants m^{-1} of the partially resistant cultivar) [45]. The LAI is an important factor to understand spraying

quality behavior as well as the capacity of each operational parameter according to the leaf density as a barrier to spraying.

3.2.4 Assessment of disease severity and control efficacy

Starting at the V6 growth stage, 10 leaflets were collected weekly per plot from the lower third of the plant and taken to the laboratory for better visualization of fungal structures and symptoms under a stereoscopic microscope. Disease severity (%) was estimated based on the SBR diagrammatic scale proposed by Godoy et al. [46], based on visual observation of the symptoms. The Area Under the Disease Progress Curve (AUDPC) was calculated according to Campbell and Madden [47] using the mean values of disease severity obtained in the plots and on the respective evaluation dates.

In addition, disease severity was indirectly assessed by the defoliation level. The evaluations started at 85 DAE, the moment when the highest level of severity began, and no defoliation was still detected. The evaluation was carried out using the ASD FieldSpec Dual Spectroradiometer (Analytical Spectral Devices, Boulder, CO, USA), with a spectral range from 350 to 1070 nm and 7.5º of field of view. A white panel with approximately 100% reflectance (*Spectralon*) was used as a reference for calibration. Calibration and optimization of the equipment were conducted every 10 minutes.

The evaluations were conducted weekly under intense sunlight at around 11:00 am, performing three readings in the central region of each plot in each experimental trial, maintaining uniform height and equipment position. The reflectance data obtained was smoothed by Savitsky-Golay filtering as described above. The reflectance database was then used to calculate the VIs that was the most correlated to the effect of SBR on crop defoliation. For that, the calculation of the LAI through the Normalized Difference Vegetation Index (NDVI) and Beer-Lambert law [48] stood out and was used as a reference for evaluating crop defoliation by the disease. Tan et al. [48] proposed the calculation of the LAI through the integration of the Beer-Lambert Law and the NDVI of the samples, also considering its leaf orientation values. Here, the soybean crop was considered as a middle-type plants with leaf orientation values ranging from 30 to 60º, and the whole model is fully described by the authors [48].

3.2.5 Evaluation of the effect of control on crop yield

At the end of the crop season, each plot was individually harvested to determine the influence of disease control effectiveness on soybean crop yield. One meter of the three center rows of each plot was manually harvested. The production was weighed on a precision scale to determine the weight of a thousand seeds (TSW) (g) and crop yield (kg ha^{-1}) of each treatment, considering humidity correction to 13% [49].

3.2.6 Data analysis

Statistical analysis for the construction of the disease prediction model was performed according to the procedure already described, using the same script for data processing [18]. The prediction model was executed during the experiment to aid in the decision-making of control and it was cross-validated (n=10) with the original database used for the construction of this prediction model to confirm the disease severity classes identification [18].

The results were analyzed in the factorial scheme described and submitted to the analysis of homogeneity and normality. The data were submitted to analysis of variance (ANOVA) using the F test and, when significant, compared by Tukey's test, both at 5% probability.

Since a significant difference was found between experimental field replications ($p<0.01$), both areas were compared separately. In both fields, spray deposit and coverage mean values were compared separately for each region of the canopy (upper and lower). The percentage of control was calculated based on the AUDPC of the control without application of each cultivar (T1 and T2). All statistical analyses and models were conducted using the R 3.6.3 software [50].

3.3 RESULTS

3.3.1 Soybean rust detection and application timings

The periods of disease detection in the field trials according to each treatment are shown in Figure 2. In Field 1, SBR's first symptoms were detected in both cultivars (Treatments 7 and 8) concomitant to the scheduled application (R1) at 50 DAE, and, therefore, T7 and T8 were sprayed on the same date as T3 and T4. The model was able to detect plants classified as "low severity" 6 days after that and in both cultivars when

symptoms were about 0.2% severity. In the second experimental replication (Field 2), disease symptoms were detected in susceptible and partially resistant cultivars (T7 and T8) at 70 DAE, as well as the model was also able to detect diseased plants in the susceptible cultivar (T5), which had more characteristic symptoms of the disease at this time. For the partially resistant cultivars, which demonstrated significantly slower disease progression, the model detected diseased plants 7 days after that. The calendarized application (R1) was sprayed at the same time as in Field 1 (50 DAE).

At both Fields 1 and 2, a peak of LAI was observed around 60-65 DAE, occurring concurrently with the second application of the treatments (Figure 3). This period corresponds to the moment when higher foliar density is found, offering greater deposit and spray penetration challenges.

Figure 2. Graphical representation of fungicide application timings along with qualitative and quantitative spraying evaluations as a function of disease detection proposed for each treatment.

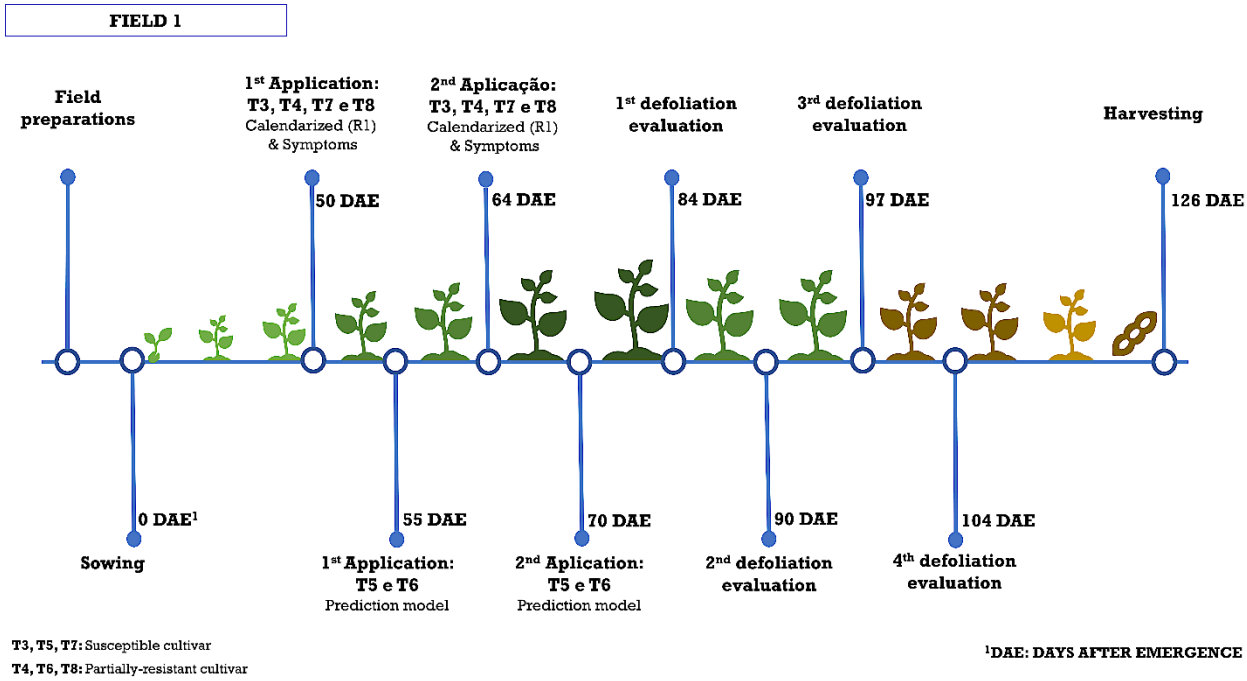

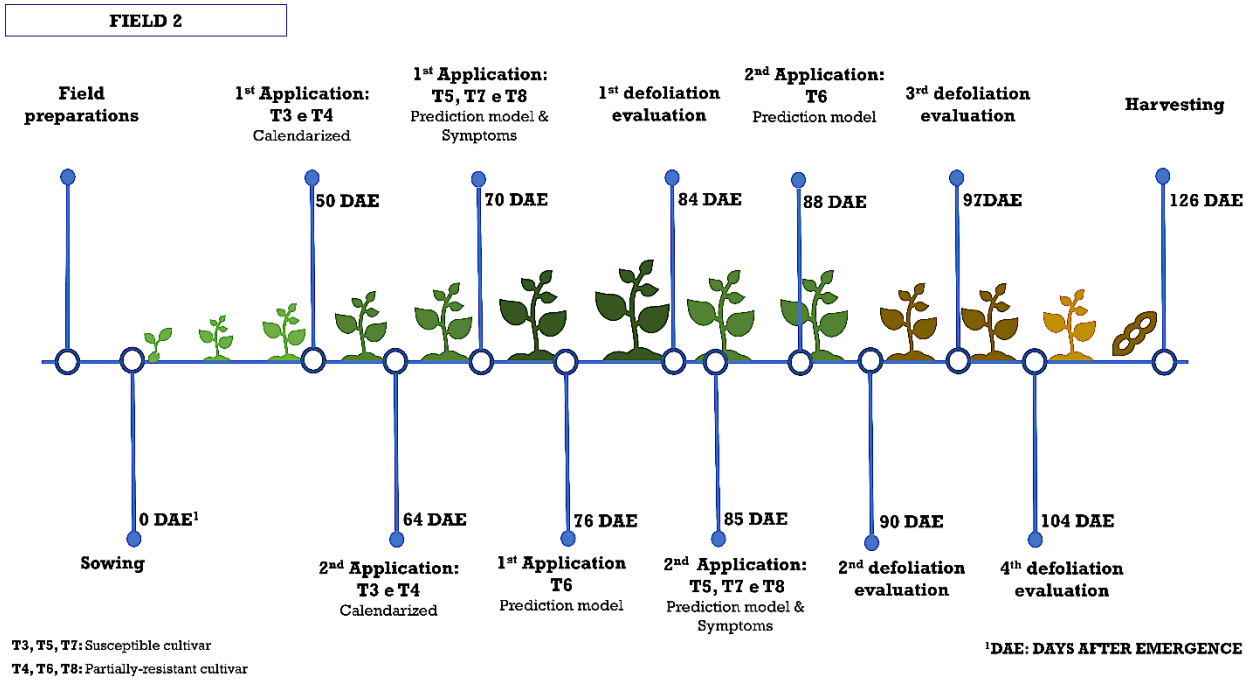

Figure 3. Leaf area index (LAI) of both field trials repetitions analyzed during the period interval of the fungicide applications.

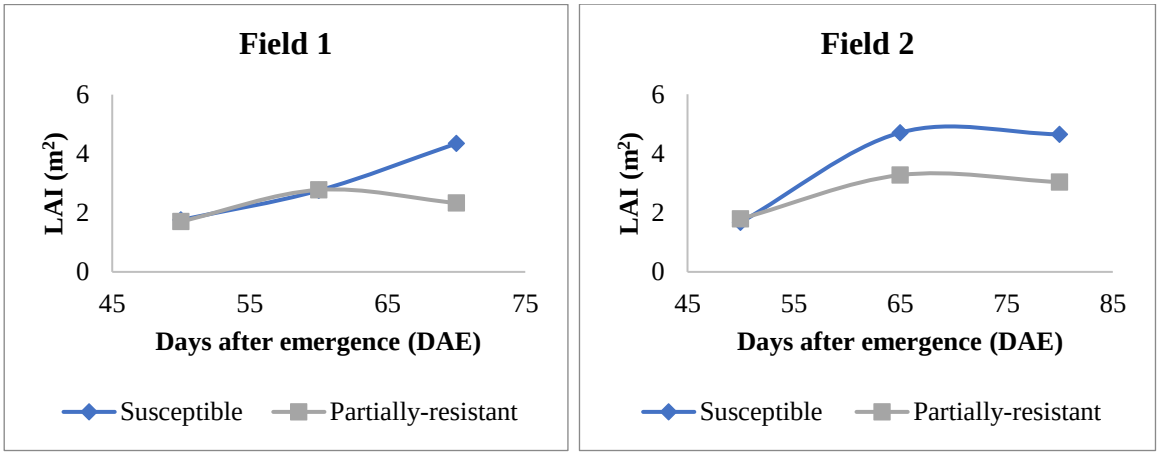

3.3.2 Spray deposit

Consistent results were observed between field trials and regarding the effect of application timings on the qualitative and quantitate spraying variables. No significant effect was found in the interaction of the factors for any deposit values in both field trial replications.

In the first application of Field 1, a greater spray deposit was observed in the upper region of the crop canopy when spraying based on the prediction model (0.85 µL cm^{-2}), compared to when based on symptoms (0.65 µL cm^{-2}) and calendarized (0.55 µL cm^{-2}) that were sprayed previously (Figures 4). In the lower region of the canopy, a significant difference was found only between cultivars, where higher spray deposits ($p<0,01$) were found in partially resistant cultivars (0.30 µL cm^{-2}) than in the susceptible cultivar (0.09 µL cm^{-2}) (Figure 5).

In the second application, the application timings affected the deposit values at both upper and lower canopy regions, disregarding the cultivar used. Greater spray deposit was found when spraying based on the prediction model at the upper (0.98 µL cm^{-2}) and lower (0.21 µL cm^{-2}) canopy regions (Figure 6). The prediction model application timings (T5 and T6) occurred at a different moment than the other two treatments.

Figure 4. Mean deposit values (µL cm^{-2}) collected in the upper region of the soybean canopy at different application timings in the first application of Field 1.

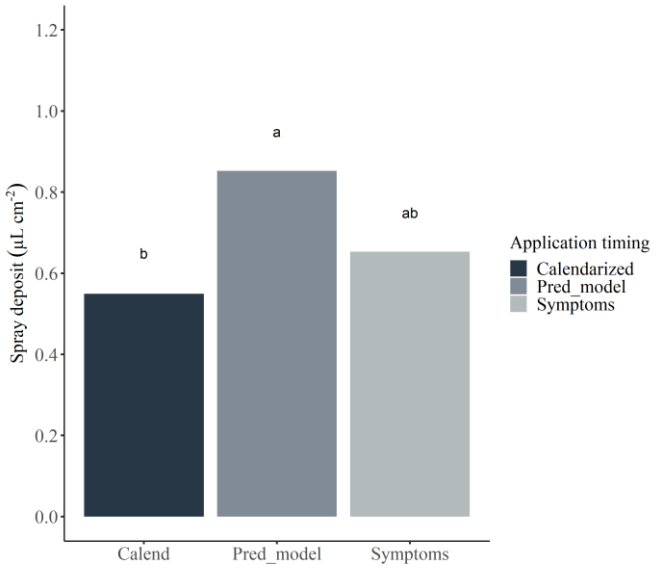

Means followed by the same letter did not differ by the Tukey test at 5% probability ($p<0.05$).

Figure 5. Mean deposit values (µL cm-2) collected in the lower region of the soybean canopy of different soybean cultivars in the first application of Field 1.

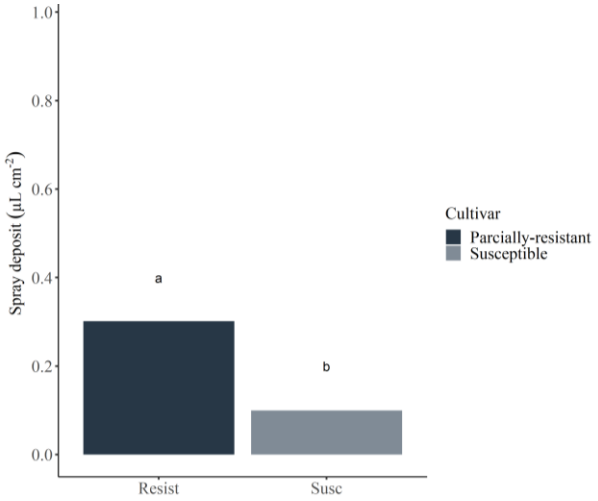

Means followed by the same letter did not differ by the Tukey test at 5% probability ($p<0.05$).

Figure 6. Mean deposit values (µL cm^{-2}) collected in the upper (A) and lower (B) regions of the soybean canopy at different application timings in the second application of Field 1.

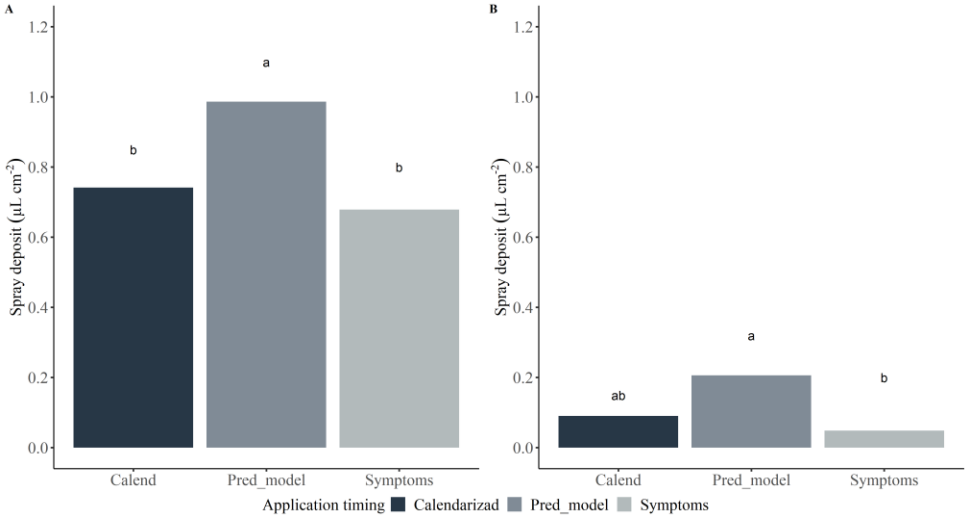

Means followed by the same letter did not differ by the Tukey test at 5% probability ($p<0.05$) in each comparison.

Furthermore, the cultivar also affected the quantity of deposits found in the lower region of the canopy, in which the partially resistant cultivar (0.17 µL cm^{-2}) significantly overcame the susceptible cultivar (0.05 µL cm^{-2}) (Figure 7). Irrespective of the

application timing, expressive reduction in spray deposit was found again at the lower region of the canopy, demonstrated by an uneven spray distribution across canopy regions and reduced capacity of droplets penetration into lower regions.

Figure 7. Mean deposit values (µL cm^{-2}) collected in the lower region of the soybean canopy of different soybean cultivars in the second application of Field 1. Means followed by the same letter did not differ by the Tukey's test at 5% probability ($p<0.05$).

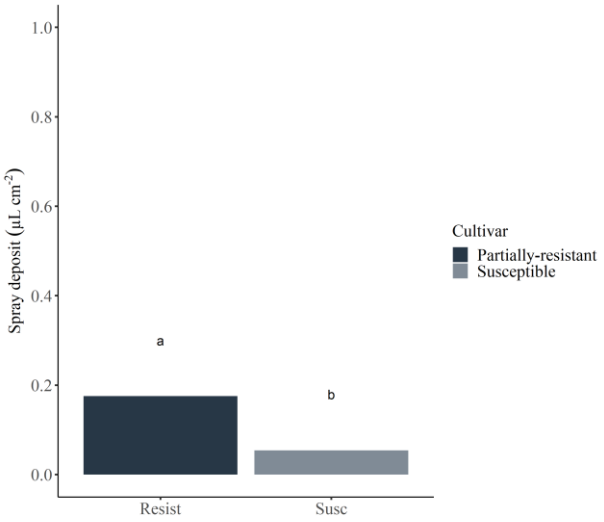

Means followed by the same letter did not differ by the Tukey test at 5% probability ($p<0.05$).

The second experimental field trial presented a similar trend in deposit values. In the first application, a significantly greater deposit was found in the upper region in treatments sprayed at the first symptoms appearance (0.82 µL cm^{-2}) and prediction model decision (0.84 µL cm^{-2}) (Figure 8). These applications happened 20 days after the calendarized application (0.66 µL cm^{-2}), once more demonstrating better spray deposit in the region with the later application. Moreover, a higher mean deposit value was found in the lower region of partially resistant cultivars (0.13 µL cm^{-2}) than those found in the susceptible cultivar (0.05 µL cm^{-2}) (Figure 9).

Figure 8. Mean deposit values (µL cm^{-2}) collected in the upper region of the soybean canopy at different application timings in the first application of Field 2.

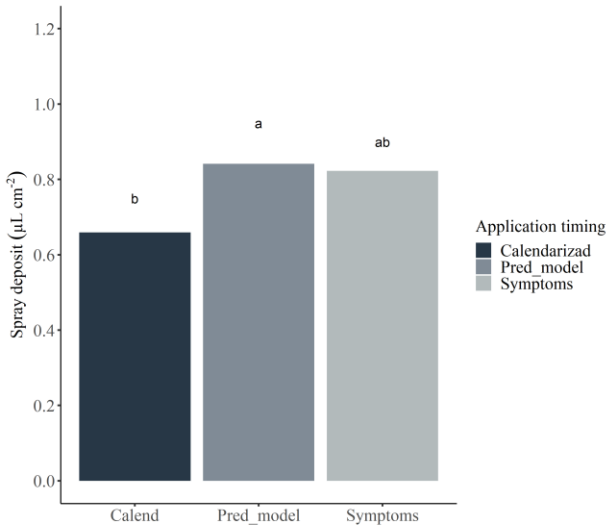

Means followed by the same letter did not differ by the Tukey test at 5% probability ($p<0.05$).

Figure 9. Mean deposit values (µL cm^{-2}) collected in the lower region of the soybean canopy of different soybean cultivars in the first application of Field 2.

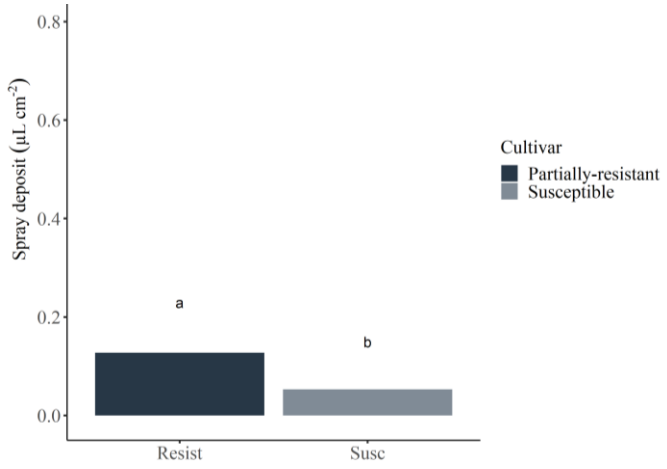

Means followed by the same letter did not differ by the Tukey test at 5% probability ($p<0.05$).

In the second application of Field 2, significant differences were found only in the lower region of the canopy. Application timings based on the prediction model and symptoms, applied on the same date, obtained significantly higher deposition than the scheduled application (Figure 10). Higher mean deposit values were also found in the lower region of the canopy of partially resistant cultivars (Figure 11).

Figure 10. Mean deposit values (µL cm^{-2}) collected in the upper region of the soybean canopy at different application timings in the second application of Field 2.

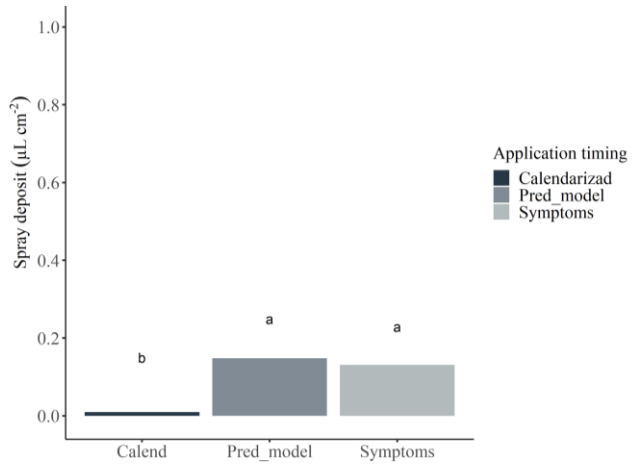

Means followed by the same letter did not differ by the Tukey test at 5% probability ($p<0.05$).

Figure 11. Mean deposit values (µL cm^{-2}) collected in the lower region of the soybean canopy of different soybean cultivars in the second application of Field 2.

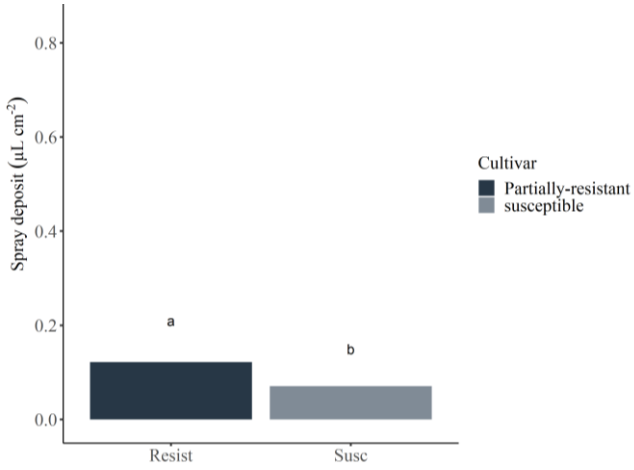

Means followed by the same letter did not differ by the Tukey test at 5% probability ($p<0.05$).

3.3.3 Spray coverage

Finally, the qualitative evaluations based on the percentage of spray coverage were also consistent between experimental trials. For Field 1, no significant difference was found in the first application, irrespective of application timing, cultivar, or canopy region. In the second application, a higher percentage of coverage was observed in the

lower region of the canopy according to the cultivar, in which there was greater coverage in the partially resistant cultivar (42,3%), compared to the susceptible one (31,8%) (Figure 12).

Figure 12. Mean percentage of coverage (%) in water-sensitive papers located at the lower region of the soybean canopy, according to different soybean cultivars in the second application of Field 1.

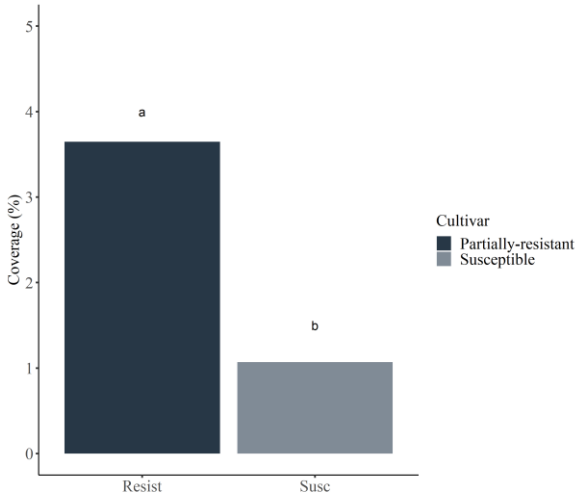

Means followed by the same letter did not differ by the Tukey test at 5% probability ($p<0.05$).

On the other hand, a significant difference was found in the interaction between the factors in the first application of Field 2, only in the lower region of the canopy (Table 3). A higher percentage was found at the lower-positioned targets of partially resistant cultivar treatments (21.9%) compared to the susceptible cultivars (5.14%) when spraying at a calendarized timing. Moreover, the coverage of the partially resistant cultivar was also significantly higher compared to the other application timings. In the second application, another difference was found in the lower region of the canopy as a function of application timings, in which the scheduled spraying timing presented significantly lower values compared to the others (Figure 13).

Table 3. Mean percentage coverage (%) on water-sensitive papers in the first application of Field 2, according to different application timings and soybean cultivars, compared separately in each canopy region.

Application timing	Cultivar	
	Susceptible	**Partially resistant**
Calendarized	5.14 aB	21.97 aA
Prediction model	6.57 aA	2.06 Ba
Symptoms	6.74 aA	4.27 bA
Cause of Variation		
Application timing (AT)	2.885	0.087^{NS}
Cultivar (C)	0.922	0.352^{NS}
AT x C	3.958	0.042*
CV(%)		-

^{NS}: Not significant; *significant a p ≤ 0.05 by F test. Means followed by the same letter did not differ according to Tukey test at 5% probability (p<0,05). Lowercase letters compare between means of application timings at each cultivar level (lines). Uppercase letters compare between means of cultivars at each application timing (columns). Each statistical comparison was conducted separately for each canopy region (upper and lower).

Figure 13. Mean percentage of coverage (%) in water-sensitive papers located at the lower region of the soybean canopy, according to different application timings in the second application of Field 2.

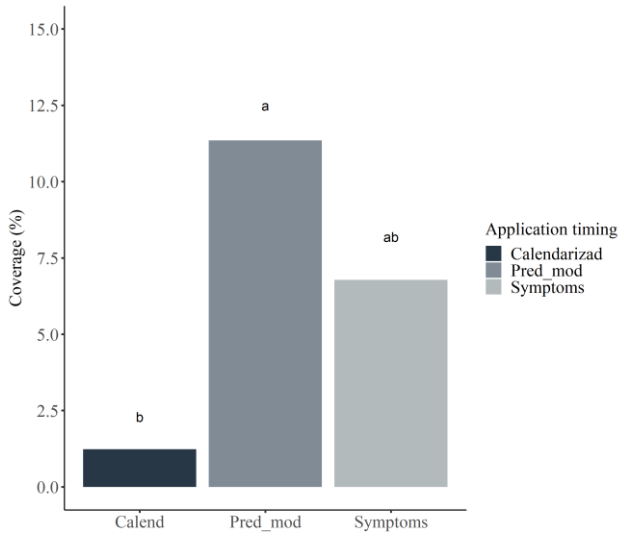

Means followed by the same letter did not differ by the Tukey test at 5% probability (p<0.05).

3.3.4 Effect of application timings on SBR control and crop defoliation

Disease severity (AUDPC) and the control efficacy in both experimental fields are shown in Table 4. In general, a significant reduction in disease severity was observed in all treatments with the fungicide application compared to the control. In addition, there was also a significant difference between cultivars, in which the partially resistant cultivar presented lower AUDPC, regardless of the application timing. For the percentage of control, a difference was found only in Field 2, where a higher disease severity was observed in all treatments and, therefore, with higher disease pressure. In this field trial, the percentage of control with the scheduled application (R1) in the partially resistant cultivar was significantly lower than in the others. Although the percentage of control seems much lower in partially resistant cultivars, it is possibly due to the lower severity found even for the control treatment without applications.

Table 4. Mean values of disease severity (AUDPC) and control (%) according to application timings and susceptible and partially resistant soybean cultivars, for each field trial replication.

Field	Application timing	AUDPC		CONTROL (%)	
		Cultivar		Cultivar	
		Susceptible	P. Resistant	Susceptible	P. Resistant
FIELD 1	Control	200.80 aA	40.50 aB	-	-
	Calendarized	68.90 bA	18.10 aB	64.40	51.50
	Prediction model	54.60 bA	15.90 aB	71.60	59.20
	Symptoms	63.00 bA	15.00 aB	67.90	58.90
	Causes of Variation	**F**	**P**	**F**	**P**
	Application timing (AT)	53.450	<0.001***	0.576	0.574^{NS}
	Cultivar (C)	177.450	<0.001***	3.772	0.071^{NS}
	AT x C	26.450	<0.001***	0.042	0.959^{NS}
FIELD 2	Control	519.20 aA	65.70 aB	-	-
	Calendarized	138.90 bA	32.50 aB	72.50 aA	47.80 bB
	Prediction model	142.50 bA	22.40 aB	71.70 aA	65.70 aA
	Symptoms	191.00 bA	27.10 aB	62.10 aA	56.74 abA
	Causes of Variation	**F**	**P**	**F**	**P**
	Application timing (AT)	43.076	<0.001***	143.823	<0.001***
	Cultivar (C)	188.949	<0.001***	8.577	0.008*
	AT x C	28.402	<0.001***	5.019	0.009*

^{NS}: Not significant; *significant a p ≤ 0.05 by F test. Means followed by the same letter did not differ according to Tukey test at 5% probability (p<0.05). Lowercase letters compare between means of application timings at each cultivar level (lines). Uppercase letters compare between means of cultivars at each application timing (columns). Each statistical comparison was conducted separately for each canopy region (upper and lower).

The disease progress curves were considerably similar between both experimental fields (Figure 14). It is possible to observe greater development starting at 42 days after the first application (DAA) and rapid growth after this moment. On the other hand, greater severity progress was found at Field 2, where other treatments were also affected by the disease and promoted greater disease development. Overall, susceptible cultivars showed greater development, especially the control without fungicide application.

Figure 14. Soybean rust disease progress curve at Field 1 and Field 2 trial repetitions, according to different soybean cultivars and application timings (treatments).

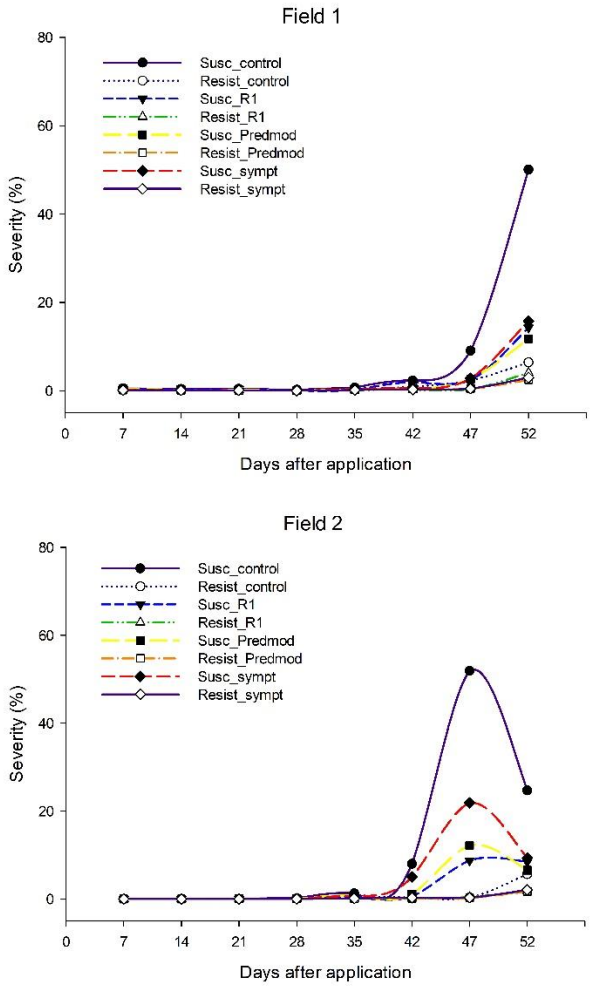

*Susc_: susceptible soybean cultivar (DS6217); Resist_: partially resistant soybean cultivar (TMG7063). Control: without fungicide application; Calend: calendarized application (reproductive growth stage R1); Model: application timing based on prediction model; Sympt: application timing based first symptoms appearance.

For the level of defoliation as an indirect severity evaluation, the spectroradiometer proved to be effective in representing the leaf stand level of the treatments (Figure 15). As the crop moved towards the end of the season, a clear reduction in LAI was observed in both field trials regardless of the treatment.

Figure 15. Defoliation assessment based on the leaf area index (LAI) through the integration of NDVI and Beer-Lambert law, according to the spectral curves of susceptible and partially resistant soybean cultivars under soybean rust effect, across experimental evaluation periods of Field 1 (A) and Field 2 (B).

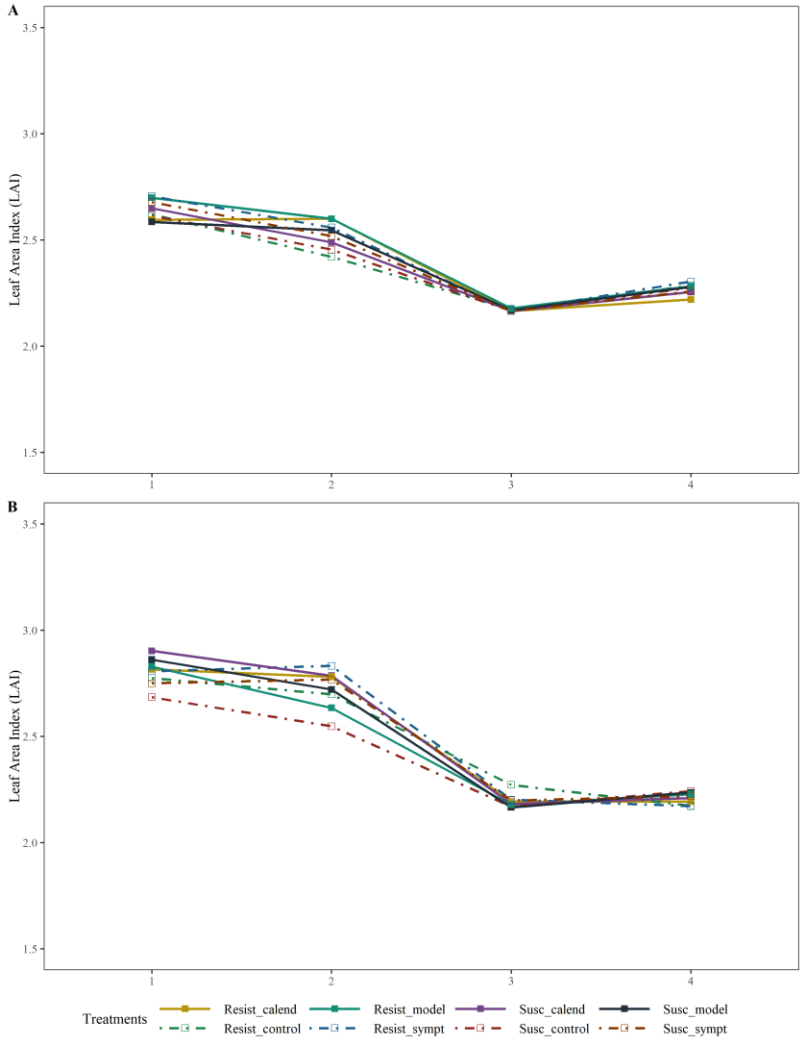

*Susc_: susceptible soybean cultivar (DS6217); Resist_: partially resistant soybean cultivar (TMG7063). Control: without fungicide application; Calend: calendarized application (reproductive growth stage R1); Model: application timing based on prediction model; Sympt: application timing based first symptoms appearance.
**VI calculated according to Tan et al. [48].

3.3.5 Effect of SBR on crop yield

Regarding the effect of the disease on the crop yield (kg ha^{-1}), no significant differences were found in the interaction of factors. However, the application timings affected the crop yield in Field 2, in which the control treatment without application presented a lower crop yield ($p<0.05$) compared to the other application timings (Table 5). The numerical difference was kept similar in Field 1.

Table 5. Mean values of soybean crop yield (kg ha^{-1}) and thousand seeds weight (TSW) (g), according to soybean rust effect of different application timings and soybeans cultivars, for each field trial repetition.

Application timing	Crop yield		TSW	
	kg ha^{-1}		g	
	FIELD 1	**FIELD 2**	**FIELD 1**	**FIELD 2**
Control	2393.714	2799.833 b	151.79 b	159.56
Calendarized	3143.054	3462.89 a	167.52 a	173.26
Prediction model	2738.061	3055.73 ab	171.71 a	173.02
Symptoms	2817.034	3169.037 ab	168.13 a	173.75
F value	2.713^{NS}	4.092*	5.510***	1.804 ^{NS}
CV (%)	19.05	12.31	6.47	8.54

^{NS}: Not significant; ***significant at p ≤ 0,01; *significant at p ≤ 0,05 by F test. Means followed by the same letter did not differ according to Tukey test at 5% probability (p<0,05).

Likewise, lower TWS was observed for the control treatment without control, significantly ($p<0.05$) for Field 1 (Table 5). Furthermore, the effect of cultivars was also observed for TWS in Field 2, in which the susceptible cultivar presented lower TWS (160.9 g) than the partially resistant cultivar (178.8 g) (Figure 16).

Figure 16. Mean values of thousand seeds weight (TSW) (g) as a function of soybean rust effect over different soybean cultivars in the experimental Field 2.

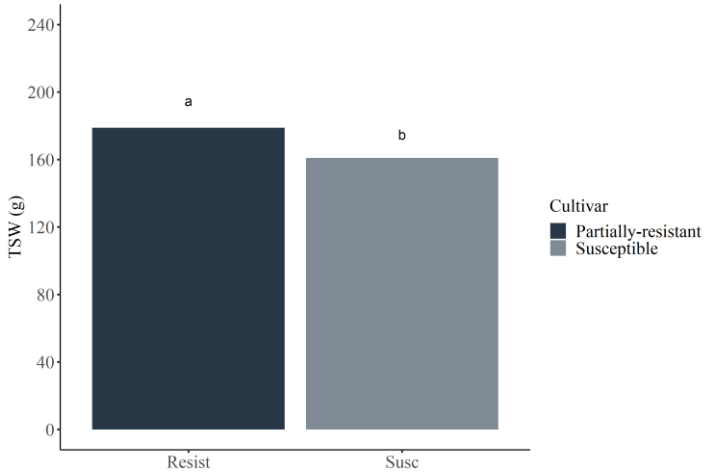

Means followed by the same letter did not differ by the Tukey test at 5% probability ($p<0.05$).

3.4 DISCUSSION

This study evaluated the applicability of an SBR prediction model and the effect of different fungicide application timings on the spraying quality as well as on disease control and crop yield. Based on the disease epidemiology, it is important to provide proper SBR control as soon as possible, aiming to avoid the quick dispersal of spores and the emergence of epidemics in the field [2,51]. In this scenario, adequate disease monitoring is key to improving application timing accuracy, spraying quality, and control efficacy. Besides, remote sensing and the usage of prediction models as support decision system showed to be a valuable tool for IDM of SBR.

The prediction model applied here was able to identify plants with severity levels as low as 0.2% severity. The disease detection matched with the first appearance of symptoms, which can be considered an advantage since remote sensing may be applied in a simpler and faster way than extensive scouting in the field [15], especially with innovations in technology such as hyperspectral cameras and drone imaging of wide fields in lesser times [13]. The possibility of identifying the disease as quickly as possible can provide greater chances of a successful disease management program.

The application timings impacted the spraying quality, resulting in significant differences in spray deposit and coverage at different parts of the crop canopy. A

difference in the quantity of product deposited in the leaves, as well as the area covered by the spraying, may play a significant effect on the control of the biological agent, interfering with the control effectiveness and epidemic management. For instance, Berger-Neto et al. [52] reported higher white mold (*Sclerotinia sclerotiorum*) incidence in soybean with treatments that produced lower spray deposits, especially in lower canopy regions.

In our study, a marked difference was found mainly with later application timings. It promoted greater retention of spray deposit on the upper region of the canopy, therefore demonstrating a greater barrier for spray penetration. This outcome was also observed as the percentage of coverage. In Field 1, spraying based on the prediction model was conducted 6 days later than the others, which already promoted slightly greater retention in the upper section. None of the treatments were able to promote proper deposition and coverage in the lower region of the canopy. Meanwhile, the second application was conducted when a reduction of LAI was already started due to crop defoliation [23], influencing the penetration of the spray into the canopy and, therefore, promoting better deposition.

Nonetheless, the recommended timing of application at the end of the vegetative growth stage and reproductive growth stage is due to the possibility of still reaching the entire vertical profile of the plants and, therefore, achieving a better spray distribution, besides targeting the period of greater disease development [51]. However, it was seen that even spraying on R1 did not provide uniform distribution. Furthermore, most fungicides recommended for SBR control act preventively and curatively, while most applications aim to act preventively to avoid any disease incidence and proliferation throughout the field [1]. Oppositely, when sprayed too far away from the first disease incidence in the field it is possible that the residual of the fungicide may not still be as active as needed, leading to lower efficacy [53].

Müller et al. [8] reported similar results of soybean rust severity at different application timings. Higher SBR severity (AUDPC) was observed when the application was the furthest from the first disease incidence. So, an application after R3 produced the best control when the disease incidence happened only after this period, whereas an application at R1 resulted in the best control efficacy when the disease was first seen

before this growth stage and, therefore, closer to the disease incidence. Although an earlier application during the vegetative growth stage may provide better fungicide distribution in the canopy [24], the residual effect of the fungicide may not last until the period of higher disease incidence [53].

Moreover, Müller et al. [8] found that applications conducted closer to the first disease observations resulted in higher crop yields than compared to other treatments that were sprayed after a longer time. This information also reassures the importance of proper disease monitoring to reduce both unnecessary fungicide applications in the field and to improve application timing accuracy and disease epidemic control. Especially considering a country with proper environmental conditions for SBR development, along with fungicide application as the main source of control that is majorly characterized by several application of only a few chemical choices (triazole, strobilurin, and carboxamides) that contributes to the selection of resistant populations [1,5-6].

In this study, especially for Field 2 where the disease started only 20 days after the calendarized application, at least one application would have been saved considering the whole crop season and the 15-day interval between applications. A smaller number of applications could reduce chemical usage and, therefore, decrease fungal exposition to these fungicides, while a more accurate application has the potential to cease fungal development at determinant points that can increase control efficacy and decrease the chance of fungal survival in the field [8]. Finally, a better distribution throughout the crop canopy could also ensure a lower risk of over or under-application rate, which could also lead to fungicide resistance [54]. Therefore, the benefits of sensor-based prediction models might come from the reduction of the number of applications or the fungicide efficacy that it might achieve.

The structural differences of the cultivars also played a major role in the spraying technology. The partially resistant cultivar (TMG7063) visually had less inter-row canopy closure compared to the susceptible cultivar (DS6217), in addition to a lower LAI. Therefore, the architecture format of the cultivar allowed a better penetration into the canopy, represented by a better spray distribution. Thereby, in most spraying conducted, better spray deposition and coverage were observed in the lower section of the plants.

A study unveiled the dynamic spray deposition according to different soybean cultivars' architecture, reporting a significant increase in spray coverage and overall penetration capacity when spraying in cultivars with lower height, LAI, and numbers of branches [22]. An increase in coverage of almost 96% at the lower canopy regions was found for these cultivars.

Coverage and spray deposit results were very similar and consistent. The significant reduction in spraying reaching capacity into the innermost regions of the canopy stood out in all cases. Therefore, it highlights the need to adjust the technology according to the application timing, especially based on LAI and canopy closure [22]. Alternatives such as using specialized spray nozzles or higher application volumes can be very responsive to provide significant improvements [9,52,55-56].

The results obtained on the application technology corroborate the disease severity found. The treatments with higher spray deposit and coverage also promoted slightly lesser disease severity, such as those observed when spraying based on the prediction model and first symptoms. Therefore, in general, the spraying decision-making based on remote sensing data improved or at least maintained the control effectiveness level of conventional methods. Furthermore, greater disease development was observed 42 days after the first application (DAA). Therefore, the earlier applications may have promoted a lower control rate due to greater distance from the peak of disease severity and lower fungicide residual.

As regards disease severity, the partially resistant cultivar was also considered to be highly effective in terms of suppressing the level of disease growth, with a marked progress curve reduction and lower severity indexes, even when without application. Along with the aforementioned cultivar structure that allowed a better spray distribution, all these features contribute to disease management and are, therefore, considered an excellent tool for the IDM.

To date, seven soybean resistance loci were identified [57-58]. Vittal et al. [11] identified varied infection capacities of *P. Pachyrhizi* among different soybean genotypes tested, reporting reduced hyphae development in resistant soybean cultivars. Resistant (immune reaction) and partially resistant cultivars are known to produce fewer pustules, lesions, and longer latent periods [10].

Another important factor is that, in this study, the disease incidence happened later than the usual first appearance, which can be visually identified in the curve progress. In this study, later application timings at the disease onset provided better control. It is possible that in regions where there is higher disease pressure, monitoring by remote sensing can even anticipate the application compared to the calendarized applications. Improvements in disease monitoring to supply information to the decision support system have the potential to improve control efficacy as well as to even reduce the number of applications in regions of lower disease pressure [13,59-61].

Moreover, the use of remote sensing to assess the disease severity and defoliation was also considered successful, as reported by other authors [48,62]. Although no significant difference was found between the treatments, the LAI calculated through the integration of NDVI and the Beer-Lambert law [48] represented properly the defoliation levels, allowing better visualization of the effect of the disease on the crop leaf mass throughout the crop season.

The fungicide application promoted a reduced disease effect on the soybean crop yield, allowing greater yields irrespective of the cultivar or application timings. However, the differences found for each treatment control and spraying quality were not fully correlated to the crop yield, despite the proximity of the values found. For example, in both field repetitions, the calendarized application which obtained poorer spraying quality and higher disease severity, also achieved slightly higher crop yield than the others, even though only numerical. Crop yield is mostly affected when disease pressure is high, such as in the values observed in the control treatment without application. Besides, the effect of SBR on crop yield is most pronounced when its progression occurs at pod formation and filling [57,63]. Other injuries than visual symptoms may also play an important role in affecting the crop yield, such as on the carbon exchange rates [64].

Overall, the model was considered an effective tool and showed promising results to be used as a tool in the integrated management of SBR, since detection periods were similar to those based on visual diagnosis and with potential for maintenance or improvement of disease control. In addition, improvements in assessment techniques are reported as a result of time savings compared to visual assessments. For cultivars

with lower disease severity, or situations where there is a lower risk of epidemic or lower disease severity and incidence, it could be considered even more effective. It is important to state that the applicability of remote sensing techniques and data obtainment to supply these types of prediction models is difficult since many variables can interfere with the optical analyses, such as climate conditions and the presence of other injuries [13,19]. More studies are encouraged to be conducted to improve the prediction model database as well as to implement it in IDM programs.

Our results denote the practicality of using remote sensing and prediction models in the integrated management of the disease. Positive results were found, indicating the possibility of integrating it among the currently present management techniques. In addition, the timing of application impacted the application technology, resulting in significant differences in spray deposition and coverage, which have a high potential to also interfere with the effective control and management of epidemics. Application at lower LAI promoted better spray distribution and better SBR control efficacy. Finally, partially resistant cultivars also played a major role in the SBR control and as a powerful tool of the IDM.

3.5 REFERENCES

1. Godoy, C.V.; Seixas, C.D.S.; Soares, R.M.; Marcelino-Guimarães, F.C.; Meyer, M.C.; Costamilan, L.M. Asian soybean rust in Brazil: past, present, and future. *Pesqui. Agropecu. Bras* 2016, 51, 407-421.
2. Langenbach, C.; Campe, R.; Beyer, S. F.; Mueller, A. N.; Conrath, U. Fighting Asian soybean rust. *Front Plan Sci* 2016, *7*, 797, 1-13.
3. Juliatti, F.C.; Azevedo, L.A.S.; Cristina, J. Strategies of chemical protection for controlling soybean rust. In *Soybean*; M. Kasai; IntechOpen: London, 2017; Volume 1, pp. 35–62.
4. Hossain, M.M.; Yamanaka, N. Pathogenic variation of Asian soybean rust pathogen in Bangladesh. *J Gen Plant Pathol* **2019**, *85*, 90-100.
5. Müller, M.A.; Stammler, G.; De Mio, L.L.M. Multiple resistance to DMI, QoI and SDHI fungicides in field isolates of *Phakopsora pachyrhizi*. *Crop Prot* **2021**, *145*, 105618.
6. Dalla Lana, F.; Paul, P.A.; Godoy, C.V.; Utiamada, C.M., da Silva, L.H.C.; Siqueri, F.V.; Forcelini, C.A.; Jaccoud-Filho, D.D.S.; Miguel-Wruck, D.S.; Borges, E.P.; Juliatti, F.C. Meta-analytic modeling of the decline in performance of fungicides for managing soybean rust after a decade of use in Brazil. *Plant Dis* **2018**, 102, 807–817.
7. Ozkan, H.E.; Zhu, H.; Derksen, R.C.; Guler, H.; Krause, C. Evaluation of various spraying equipment for effective application of fungicides to control Asian soybean rust. *Asp. Appl. Biol.* **2006**, 77, 423–431.
8. Mueller, T. A.; Miles, M. R.; Morel, W.; Marois, J. J.; Wright, D. L.; Kemerait, R. C.; … & Hartman, G. L. Effect of fungicide and timing of application on soybean rust severity and yield. *Plant dis* **2009**, *93*, 243-248.
9. Cunha, J.P.A.R.; Juliatti, F.C.; Reis, E.F. Tecnologia de aplicação de fungicida no controle da ferrugem asiática da soja: resultados de oito anos de estudos em Minas Gerais e Goiás. *Biosc J* **2014**, 30, 950–957.
10. Hartman, G.L.; Miles, M.R.; Frederick, R.D. Breeding for resistance to soybean rust. *Plant dis* **2005**, *89*, 664-666.
11. Vittal, R.; Paul, C.; Hill, C.B.; Hartman, G.L. Characterization and quantification of fungal colonization of *Phakopsora pachyrhizi* in soybean genotypes. *Phytopathology* **2014**, 104, 86-94.

12. Twizeyimana, M.; Hartman, G.L. Effect of selected biopesticides in reducing soybean rust (*Phakopsora pachyrhizi*) development. *Plant dis* **2019**, *103*, 2460-2466.
13. Corley, C.D.; Pullum, L.L.; Hartley, D.M.; Benedum, C.; Noonan, C.; Rabinowitz, P.M.; Lancaster, M.J. Disease prediction models and operational readiness. *PloS one* **2014**, *9*, e91989.
14. Martinelli, F.; Scalenghe, R.; Davino, S.; Panno, S.; Scuderi, G.; Ruisi, P.; ...Dandekar, A.M. Advanced methods of plant disease detection. A review. *Agron Sustain Dev* **2015***,* 35(1), 1-25.
15. Zhang, J.; Huang, Y.; Pu, R.; Gonzalez-Moreno, P.; Yuan, L.; Wu, K.; Huang, W. Monitoring plant diseases and pests through remote sensing technology: A review. *Comput. Electron. Agric* **2019**, *165*, 104943.
16. Cui, D.; Zhang, Q.; Li, M.; Zhao, Y.; Hartman, G.L. Detection of soybean rust using a multispectral image sensor. *Sens Instrum Food Qual Saf* **2009**, *3*, 49-56.
17. Furlanetto, R.H.; Nanni, M.R.; Mizuno, M.S.; Crusciol, L.G.T.; da Silva, C.R. Identification and classification of Asian soybean rust using leaf-based hyperspectral reflectance. *Int. J. Remote Sens* **2021**, 42, 4177-4198.
18. Negrisoli, M. M.; Negrisoli, R. M.; da Silva, F. N.; Lopes, L. L.; Souza Júnior, F. S.; Velini, E. D.; Carbonari, C.A.; Rodrigues, S. A.; Raetano, C. G. Soybean rust detection and disease severity classification by remote sensing. *Agron J* **2022**. https://doi.org/10.1002/agj2.21152
19. Bajwa, S.G.; Rupe, J.C.; Mason, J. Soybean disease monitoring with leaf reflectance. *Remote Sens* **2017**, 9, 127.
20. Donatelli, M.; Magarey, R.D.; Bregaglio, S.; Willocquet, L.; Whish, J.P.; Savary, S. Modelling the impacts of pests and diseases on agricultural systems. *Agric. Syst* **2017**, *155*, 213-224.
21. Twizeyimana, M.; Hartman, G.L. Sensitivity of *Phakopsora pachyrhizi* isolates to fungicides and reduction of fungal infection based on fungicide and timing of application. *Plant Dis* **2017**, 101, 121–128.
22. Müller, M.; Rakocevic, M.; Caverzan, A.; Boller, W.; Chavarria, G. Architectural characteristics and heliotropism may improve spray droplet deposition in the middle and low canopy layers in soybean. *Crop Sci* **2018**, *58*, 2029-2041.

23. Tagliapietra, E.L.; Streck, N.A.; Da Rocha, T.S.M.; Richter, G.L.; Da Silva, M.R.; Cera, J.C.; Guedes, J.V.C.; Zanon, A.J. Optimum leaf area index to reach soybean yield potential in subtropical environment. *Agron J* **2018**, 10, 932–938.
24. Negrisoli, M.M.; Raetano, C.G.; de Souza, D.M.; Souza, F.M.S.; Bernardes, L.M.; Junior, L.D.B.; Rodrigues, D.M.; Sartori, M.M.P. Performance of new flat fan nozzle design in spray deposition, penetration and control of soybean rust. *Eur. J. Plant Pathol.* **2019**, 155, 755-767.
25. Brevant Sementes - Cultivares de soja: DS6217IPRO. Available online: https://www.brevant.com.br/produtos/soja/ds6217ipro.html. Accessed on 26 January 2022.
26. Tropical Melhoramento Genético (TMG) - Cultivares de soja: TMG 7063 IPRO. Available online: http://www.tmg.agr.br/ptbr/cultivar/tmg-7063-ipro. Accessed on 26 January 2022.
27. Abdel-Rahman, E.M.; Mutanga, O.; Odindi, J.; Adam, E.; Odindo, A.; Ismail, R. A comparison of partial least squares (PLS) and sparse PLS regressions for predicting yield of Swiss chard grown under different irrigation water sources using hyperspectral data. *Comput. Electron. Agric.* **2014**, *106*, 11-19.
28. Savitzky, A.; Golay, M.J. Smoothing and differentiation of data by simplified least squares procedures. *Analytical chemistry* **1964**, *36*, 1627-1639.
29. Bohnenkamp, D.; Behmann, J.; Mahlein, A.K. In-field detection of yellow rust in wheat on the ground canopy and UAV scale. *Remote Sens* **2019**, *11*, 2495.
30. Abdi, H.; Williams, L.J.; Valentin, D. Multiple factor analysis: principal component analysis for multitable and multiblock data sets. *Wiley Interdiscip. Rev. Comput. Stat.* **2013**, *5*, 149-179.
31. Qi, J.; Chehbouni, A.; Huete, A.R.; Kerr, Y.H.; Sorooshian, S. A modified soil adjusted vegetation index. *Remote Sens. Environ.* **1964**, 48, 119-126.
32. Rouse, J.W.; Hass, R.H.; Schell, J.A.; Deering, D.W.; Harlan, J.C. Monitoring the Vernal Advancement and Retrogradation (Green Wave Effect) of Natural Vegetation; Final Report, RSC 1978-4; Texas A&M University: College Station, TX, USA, 1974; pp. 1–120.

33. Richardson, A.J.; Wiegand, C.L. Distinguishing vegetation from soil background information. *Photogramm Eng Remote Sensing* **1977**, 43, 12, 1541-1552.
34. Pearson, R.L.; Miller, L.D. Remote mapping of standing crop biomass for estimation of the productivity of the shortgrass prairie. *Remote Sens. Environ* **1972**, 3, 1355.
35. Sripada, R.P.; Heiniger, R.W.; White, J.G.; Meijer, A.D. Aerial color infrared photography for determining early in-season nitrogen requirements in corn. *Agron J* **2006**, 98, 4, 968-977.
36. Penuelas, J.; Baret, F.; Filella, I. Semi-empirical indices to assess carotenoids/ chlorophyll a ratio from leaf spectral reflectance. *Photosynthetica* **1995**, 31, 221-230.
37. Gamon, J.; Serrano, L.; Surfus, J.S. The photochemical reflectance index: an optical indicator of photosynthetic radiation use efficiency across species, functional types, and nutrient levels. *Oecologia* **1997**, 112, 492-501.
38. Huete, A.R.; Liu, H.Q.; Batchily, K.V.; Van Leeuwen, W.J.D.A. A comparison of vegetation indices over a global set of TM images for EOS-MODIS. *Remote Sens. Environ.* **1997**, 59, 440-451.
39. Gamon, J.A.; Surfus, J.S. Assessing leaf pigment content and activity with a reflectometer. *New Phytol* **1999**, 143, 105-117.
40. Sims, D.A.; Gamon, J.A. Relationships between leaf pigment content and spectral reflectance across a wide range of species, leaf structures and developmental stages. *Remote Sens. Environ* **2002**, 81, 337-354.
41. Vogelmann, J.E.; Rock, B.N.; Moss, D.M. Red edge spectral measurements from sugar maple leaves. *Remote Sens* **1993**, 14, 1563-1575.
42. Merzlyak, M.N.; Gitelson, A.A.; Chivkunova, O.B.; Rakitin, V.Y. Non-destructive optical detection of pigment changes during leaf senescence and fruit ripening. *Physiol Plant* **1999**, 106, 135-141.
43. Gitelson, A.A.; Merzlyak, M.N.; Chivkunova, O.B. Optical properties and nondestructive estimation of anthocyanin content in plant leaves. *J. Photochem. Photobiol* **2001**, 74, 38-45.
44. Palladini, L.A.; Raetano, C.G.; Velini, E.D. Choice of tracers for the evaluation of spray deposits*. Sci Agric* **2005**, 62, 440–445.

45. Jonckheere, I.; Fleck, S.; Nackaerts, K.; Muys, B.; Coppin, P.; Weiss, M.; Baret, F. Review of methods for in situ leaf area index determination: Part I. Theories, sensors and hemispherical photography. *Agric For Meteorol* **2004**, *121*, 19-35.
46. Godoy, C.V.; Koga, L.J.; Canteri, M.G. Diagrammatic scale for assessment of soybean rust severity. *Fitopatol. Bras* **2006**, *31*, 63-68.
47. Campbell, C.L.; Madden, L.V. *Introduction to plant disease epidemiology*; John Wiley & Sons: New York, 1994, 532 pp.
48. Tan, C.W.; Zhang, P.P.; Zhou, X.X.; Wang, Z.X.; Xu, Z.Q.; Mao, W; …Yun, F. Quantitative monitoring of leaf area index in wheat of different plant types by integrating NDVI and Beer-Lambert law. *Sci. Rep* **2020**, *10*, 1-10.
49. Brasil. Ministério da Agricultura, Pecuária e Abastecimento. *Regras para Análise de Sementes*. Ministério da Agricultura, Pecuária e Abastecimento - Secretaria de Defesa Agropecuária: Brasília, DF, 395 pp.
50. R Core Team - R: A language and environment for statistical computing. R Foundation for Statistical Computing, Vienna, Austria.
51. Kelly, H.Y.; Dufault, N.S.; Walker, D.R.; Isard, S.A.; Schneider, R.W.; Giesler, L.J.; ... Hartman, G.L. From select agent to an established pathogen: the response to *Phakopsora pachyrhizi* (soybean rust) in North America. *Phytopathology* **2015**, *105*, 905-916.
52. Berger-Neto, A.; Jaccoud-Filho, D.S.; Wutzki, C.R.; Tullio, H.E.; Pierre, M.L.C.; Manfron, F.; Justino, A. Effect of spray droplet size, spray volume and fungicide on the control of white mold in soybeans. *Crop Prot* **2017**, 92, 190–197.
53. Balardin, R.; Madalosso, M.; Debortoli, M.; Lenz, G. Factors affecting fungicide efficacy in the tropics. In *Fungicides*, O. Carisse (Ed.); London: InTech Open, 2010, pp. 23-38.
54. Van Den Bosch, F.; Paveley, N.; Shaw, M.; Hobbelen, P.; Oliver, R. The dose rate debate: does the risk of fungicide resistance increase or decrease with dose?. *Plant Pathol* **2011**, 60, 597-606.
55. Ferguson, J.C.; Hewitt; A.J.; O'Donnell, C.C. Pressure, droplet size classification, and nozzle arrangement effects on coverage and droplet number density using air-inclusion dual fan nozzles for pesticide applications. *Crop Prot* **2016**, 89, 231-238.

56. Sharpe, S.M.; Boyd, N.S.; Dittmar, P.J.; Macdonald, G.E.; Darnell, R.L.; Ferrel, J.A. Spray penetration into a strawberry canopy as affected by canopy structure, nozzle type, and application volume. *Weed Technol* **2017**, 32, 80–84.
57. Childs, S.P.; Buck, J.W.; Li, Z. Breeding soybeans with resistance to soybean rust (*Phakopsora pachyrhizi*). *Plant Breed* **2018**,137, 250-261.
58. Hartman, G.L.; Hill, C.B.; Twizeyimana, M.; Miles, M.R.; Bandyopadhyay, R. Interaction of soybean and *Phakopsora pachyrhizi*, the cause of soybean rust. *CAB Rev.: Perspect. Agric. Vet. Sci. Nutr. Nat. Resour* **2011***,* 59.
59. Verreet, J.A.; Klink, H.; Hoffmann, G.M. Regional monitoring for disease prediction and optimization of plant protection measuares: The IPM wheat model. *Plant dis* **2000**, 84, 816-826.
60. Sapak, Z.; Salam, M.U.; Minchinton, E.J.; MacManus, G.P.V.; Joyce, D.C.; Galea, V.J. POMICS: A simulation disease model for timing fungicide applications in management of powdery mildew of cucurbits. *Phytopathology* **2017**, *107*, 1022-1031.
61. Gama, A.B.; Peres, N.A.; Singerman, A.; Dewdney, M.M. Evaluation of disease alert systems for postbloom fruit drop of citrus in Florida and economic impact of adopting the Citrus Advisory System. *Crop Prot* **2022**, 105906.
62. Yuan, H.; Yang, G.; Li, C.; Wang, Y.; Liu, J.; Yu, H.; ... Yang, X. Retrieving soybean leaf area index from unmanned aerial vehicle hyperspectral remote sensing: Analysis of RF, ANN, and SVM regression models. *Remote Sens* **2017**, 9, 309.
63. Kawuki, R.S.; Tukamuhabwa, P.; Adipala, E. Soybean rust severity, rate of rust development, and tolerance as influenced by maturity period and season. *Crop Prot* **2004**, 23, 447–455.
64. Kumudini, S.; Prior, E.; Omielan, J.; Tollenaar, M. Impact of *Phakopsora pachyrhizi* infection on soybean leaf photosynthesis and radiation absorption. *Crop Sci* **2008**, 48, 2343-2350.

3.6 APPENDICES

Figure A1. Experimental fields in Botucatu, SP, during trials conduction in the 2020/21 crop season.

Figure A2. Fungicide spraying at each treatment (A) and general pesticides application for trials maintenance during the 2020/21 crop season

Figure A2. Applications of the Brilliant Blue® dye marker in the quali-quantitative evaluations of the spraying and the positioning of the water-sensitive papers before and after the application.

Table S1. Vegetation indices (VIs) representative to the disease effect on the soybean crop used to assess to correlation of disease severity and spectral signatures.

Vegetation Indices (VI)	Description	Formula	Reference
C420	*C420*	$\frac{R_{420}}{R_{695}}$	[19]
MSAVI2	*Modified Chlorophyll Absorption Ratio Index Improved*	$\frac{1}{2}[\,2(R_{810}+1)-\sqrt{(2R_{810}+1)^2-8(R_{810}-R_{690})}$	[31]
NDVI	*Normalized Difference Vegetation Index*	$\frac{(R_{810}-R_{690})}{(R_{810}+R_{690})}$	[32]
DVI	*Difference vegetation Index*	$R_{755}-R_{698}$	[33]
RVI	*Ratio vegetation Index*	$\frac{R_{775}}{R_{698}}$	[34]
GRVI	*Green normalized Difference vegetation index*	$\frac{(R_{690}-R_{560})}{(R_{690}+R_{560})}$	[35]
SIPI	*Structure Independent Pigment Index*	$\frac{(R_{800}-R_{445})}{(R_{800}-R_{680})}$	[36]
PRI	*Photochemical reflectance Index*	$\frac{(R_{570}-R_{531})}{(R_{570}+R_{531})}$	[37]
SR	*Simple ratio index*	$\frac{R_{800}}{R_{670}}$	[32]

Continuation of Table S1. Summary of vegetation indices (VIs)

Vegetation Indices (VI)	Description	Formula	Reference
EVI	*Enhanced vegetation index*	$2{,}5 * \frac{(R_{800} - R_{670})}{(R_{800} + 6 * R_{670} - 7{,}5 * R_{490} + 1)}$	[38]
SG	*Sum green index*	$\frac{1}{n}\sum_{i=500}^{599} Ri$	[39]
RENDVI	*Red edge NDVI*	$\frac{(R_{750} - R_{705})}{(R_{750} + R_{705})}$	[40]
mRENDVI	*Modified red edge NVDI*	$\frac{(R_{750} - R_{705})}{(R_{750} + R_{705} - 2R_{445})}$	[40]
mRESR	*Modified red edge simple ratio index*	$\frac{(R_{750} - R_{445})}{(R_{705} - R_{445})}$	[40])
VOG1	*Vogelmann Red Edge Index 1*	$\frac{R_{740}}{R_{720}}$	[41]
RGRI	*Red green ratio index*	$\frac{mean(R_{500-600})}{mean(R_{600-700})}$	[39]
PSRI	*Plant senescence reflectance index*	$\frac{R_{680} - R_{500}}{R_{750}}$	[42]
ANTH1	*Anthocyanin reflectance index (1)*	$\frac{1}{R_{550}} - \frac{1}{R_{700}}$	[43]
ANTH2	*Anthocyanin reflectance index (2)*	$R_{800}\left[\frac{1}{R_{550}} - \frac{1}{R_{700}}\right]$	[41]

CONSIDERAÇÕES FINAIS

A utilização de cultivares com resistência parcial se mostrou eficaz na redução do impacto da doença e na produtividade, demonstrando diferentes comportamentos de acordo com o nível de resistência à *P. pachyrhizi*. Os resultados também possibilitaram explorar o efeito da doença sobre a capacidade fotossintética da planta. Foi possível a identificação de FAS e classificação de diferentes níveis de severidade com base na refletância dos folíolos, os quais foram essenciais para a criação do modelo de detecção da doença na cultura. A coleção de índices vegetativos foi a base de dados que proporcionou os melhores resultados e de forma mais prática para replicação do modelo à campo. O modelo foi eficaz na detecção da doença à campo e os diferentes momentos de aplicação avaliados influenciaram na qualidade da aplicação, tendo melhor distribuição em momentos de menor área foliar. O modelo de predição foi considerado um método eficaz para determinação dos momentos de aplicação. Portanto, a utilização do modelo de predição proposto e as técnicas de sensoriamento remoto foram considerados eficazes e promissores para ser integrados a programas de manejo da doença.

Com base nos trabalhos conduzidos à campo e laboratório, observa-se a relevância da integração de diferentes técnicas no manejo integrado da FAS, os quais demonstraram grande impacto em termos de eficácia de controle e otimização do monitoramento da doença. O monitoramento como limiar para decisão do momento de controle deve ser considerado na integração das diferentes técnicas do MID, tendo o sensoriamento remoto como uma das tecnologias com o maior potencial, especialmente considerando as inovações ligadas à agricultura de precisão. A tecnologia de aplicação de produtos fitossanitários também é de grande importância na sustentabilidade da produção da soja, tendo o momento de aplicação como um dos pilares para uma pulverização mais assertiva quanto à distribuição do produto no alvo, quantidade e local mais adequados.

REFERÊNCIAS

AHMED, M. R.; YASMIN, J.; MO, C.; LEE, H.; KIM, M. S.; HONG, S.J.; CHO, B.K. Outdoor applications of hyperspectral imaging technology for monitoring agricultural crops: a review. *Journal of Biosystems Engineering*, v. 41, n.4, p. 396-406, 2016.

BAJWA, S.G.; RUPE, J. C.; MASON, J. Soybean Disease Monitoring with Leaf Reflectance. *Remote Sensing*, v. 9, n. 127, p. 1-14, 2017.

CUI, D.; ZHANG, Q.; LI, M.; ZHAO, Y.; HARTMAN, G.L. Detection of soybean rust using a multispectral image sensor. *Sensing and instrumentation for food quality and safety*, v. 3, n. 49, p. 49-56, 2009.

CUNHA, J.P.A.R; JULIATTI, F.C.; REIS, E.F. Tecnologia de aplicação de fungicida no controle da ferrugem asiática da soja: resultados de oito anos de estudos em minas gerais e goiás. *Bioscience Journal,* v.30, n.4, p. 950-957, 2014.

DEISING, H.G.; REIMANN, S.; PASCHOLATI, S.F. Mechanisms and significance of fungicide resistance. *Brazilian Journal of Microbiology*, v. 286, p. 286-295, 2008.

FURLANETTO, R. H.; NANNI, M. R.; MIZUNO, M. S.; CRUSIOL, L. G. T.; DA SILVA, C. R. Identification and classification of Asian soybean rust using leaf-based hyperspectral reflectance*. International Journal of Remote Sensing*, v. 42, n. 11, 4177-4198, 2021.

GODOY, C.V., BUENO, A. F.; GAZZIERO, D. L. P. Brazilian soybean pest management and threats to its sustainability. *Outlooks in Pest Management*, v. 26, p. 113–117, 2015.

GODOY, C. V.; UTIAMADA, C. M.; MEYER, M. C.; CAMPOS, H. D.; LOPES, I.; DIAS, A. R.; MUHL; A. et al. Eficiência de fungicidas para o controle da ferrugem-asiática da soja, *Phakopsora pachyrhizi,* na safra 2019/2020: resultados sumarizados dos ensaios cooperativos. Embrapa Soja, 2020. 20 p. (Embrapa Soja, Circular Técnica, 120).

HATFIELD, P. L., & PINTER, P. J. Remote sensing for crop protection. *Crop Protection*, 12, 403-413, 1993.

HIKISHIMA, M.; CANTERI, M. G.; GODOY, C. V.; KOGA, L. J.; DA SILVA, A. J. Quantificação de danos e relações entre severidade, medidas de refletância e produtividade no patossistema ferrugem asiática da soja. *Tropical Plant Pathology*, v. 35, n. 2, p. 96-103, 2010.

IEAg/ABAG – Instituto de Estudos do Agronegócio/Associação Brasileira do Agronegócio (2015). O futuro da soja nacional. Acesso em: jan. 2017. Disponível em: http://www.abag.com.br/media/images/0-futuro-da-soja-nacional---ieag---abag.pdf.

INAMASU, R.Y.; BERNARDI, A.C.C. Agricultura de Precisão. IN: BERNARDI, A.C.C.; NAIME, J.M.; RESENDE, A.V.; BASSOI, L.H.; INAMASU, R.Y. *Agricultura de precisão: Resultados de um novo olhar. 2 ed. Brasília*: Embrapa, 2014. p. 21 -33.

KELLY, H. Y.; DUFAULT, N. S.; WALKER, D. R.; ISARD, S. A.; SCHNEIDER, R. W.; GIESLER, L. J.; WRIGHT, D. L.; MAROIS, J. J.; HARTMAN, G. L. From selected agent to an established pathogen: the response to *Phakopsora pachyrhizi* (soybean rust) in North America. *Phytopathology*, v. 105, n. 7, p. 905-916, 2015.

KHALED, A. Y.; ABD AZIZ, S.; BEJO, S. K.; NAWI, N. M.; SEMAN, I. A.; ONWUDE, D. I. Early detection of diseases in plant tissue using spectroscopy – applications and limitations. *Applied Spectroscopy Reviews*, v. 53, n.2, p. 36-64, 2018.

KUMUDINI, S; PRIOR, E.; OMIELAN, J.; TOLLENAAR, M. Impact of *Phakopsora pachyrhizi* infection on soybean leaf photosynthesis and radiation absorption. *Crop Science*, v. 49, p. 2343-2350, 2008.

MAHLEIN, A.-K.; RUMPF, T.; WELKE, P.; DEHNE, H.W.; PLUMER, L.; STEINER, U.; OERKE, E. C. Development of spectral indices for detecting and identifying plant diseases. *Remote Sensing of Environment*, v. 128, p. 21-30, 2013.

NEGRISOLI, M.M.; RAETANO, C.G.; DE SOUZA, D.M.; SOUZA, F.M.S.; BERNARDES, L.M.; JUNIOR, L.D.B.; RODRIGUES, D.M.; SARTORI, M.M.P. Performance of new flat fan nozzle design in spray deposition, penetration and control of soybean rust. *European Journal of Plant Pathology*, v. 155, 755-767, 2019.

SHIRATSUCHI, L.S.; BRANDÃO, Z.N.; VICENTE, L.N.; VICTORIA, D.C.; DUCATI, J.R.; OLIVEIRA, R.P.; VILELA, M.F. Sensoriamento Remoto: conceitos básicos e aplicações na Agricultura de Precisão. IN: BERNARDI, A.C.C.; NAIME, J.M.; RESENDE, A.V.; BASSOI, L.H.; INAMASU, R.Y. *Agricultura de precisão: Resultados de um novo olhar*. 2 ed. Brasília: Embrapa, 2014, p. 58-73.

TOLOI, M. N. V.; BONILLA, S. H.; TOLOI, R. C.; SILVA, H. R. O.; NÄÄS, I. D. A. Development Indicators and Soybean Production in Brazil. *Agriculture*, v. *11*, 1164, 2021.

WYLIE, F.R.; SPEIGHT, M.R. *Insect Pests in Tropical Forestry*. 2 ed. CABI, 2012. 365 p.